3차원 안면 Scan Data를 이용한 조종사 산소마스크 설계 방법 개발

Development of a Design Methodology of Pilot Oxygen Mask Using 3D Facial Scan Data

Development of a Design Methodology of Pilot Oxygen Mask Using 3D Facial Scan Data

by

Wonsup Lee
Department of Industrial and Management Engineering
(Human Factors and Ergonomics Program)
Pohang University of Science and Technology

A dissertation submitted to the faculty of the Pohang University of Science and Technology in partial fulfillment of the requirements for the degree of Doctor of Philosophy in the department of Industrial and Management Engineering
(Human Factors and Ergonomics Program)

Pohang, Korea
6. 26. 2013
Approved by
Heecheon You (Signature)
Academic Advisor

Development of a Design Methodology of Pilot Oxygen Mask Using 3D Facial Scan Data

Wonsup Lee

The undersigned have examined this dissertation and hereby certify that it is worthy of acceptance for a doctoral degree from POSTECH.

06/26/2013

Committee Chair	Heecheon You	(Seal)
Member	Soo Y. Chang	(Seal)
Member	Byung-In Kim	(Seal)
Member	Seikwon Park	(Seal)
Member	Kihyo Jung	(Seal)

DMIE 20062212
이원섭, Wonsup Lee, Development of a Design Methodology of Pilot Oxygen Mask Using 3D Facial Scan Data, 3차원 안면 Scan Data를 이용한 조종사 산소마스크 설계 방법 개발, Department of Industrial and Management Engineering (Human Factors and Ergonomics Program), 2013, 107P, Advisor: Heecheon You, Text in English.

ABSTRACT

An oxygen mask requires proper fit to the facial characteristics (e.g., shape and size of face) of a target population to prevent users from the harmful atmosphere. The MBU-20/P pilot oxygen mask, frequently used by the Korean Air Force (KAF) pilots, was originally designed using face anthropometric data of U.S. Air Force (USAF) personnel. Therefore, KAF pilots suffer from excessive pressure and/or oxygen leakage around the nasal root due to the lack of fit from the oxygen mask to the face, which is most likely caused by a significant difference in facial shape and size between KAF pilots and USAF personnel. Previous studies developed a respirator design method based on 3D face scan images; however, there is lack of systematic considerations about the characteristics of face, mask, and the interface between face and mask. Moreover, previous studies have limitations on ergonomic evaluation of a respirator which should be subjectively and objectively tested with respirator users. The present study designed the oxygen mask shape based on 3D facial characteristics of KAF pilots, and ergonomically evaluated the revised oxygen mask design with KAF pilots.

A face-mask interface (FMI) analysis was conducted to identify design problems of the existing oxygen mask and to determine design directions of the new oxygen mask for KAF pilots. First, high discomfort due to excessive pressure or oxygen leakage around the nasal root and nasal side were evident through a survey which was conducted to identify design problems of the MBU-20/P oxygen mask. Second, the design dimensions of the facepiece and hardshell of MBU-20/P were measured to examine design characteristics. Third, 22 facial dimensions (length dimensions: 9; depth dimensions: 2; width dimensions: 7; circumference/arc dimensions: 4) applicable to the design of an oxygen mask were selected, and the faces of the KAF pilots (278 males and 6 females) and 52 female cadets of KAF Academy were captured using a 3D scanner, and the facial dimensions were measured using 3D face scan data. The KAF male pilots' face measurements were found significantly larger (mean difference, $\bar{d}$ = 0.7 ~ 26.5 mm) and less varied (ratio of SDs = 0.29 ~ 0.82) than those of KAF male civilians. The average face length, lip width, and nasal root breadth of the KAF male pilots were significantly longer ($\bar{d}$ = 4.7 mm), narrower ($\bar{d}$ = -2.4 mm), and wider ($\bar{d}$ = 5.2 mm), respectively, than those of USAF male personnel. This can be the main cause of excessive pressure being experienced by most of KAF pilots wearing MBU-20/P masks. Lastly, the oxygen mask wearing characteristics (e.g., wearing position, wearing angle, fit, and clearance) were analyzed using photos of 85 KAF pilots' faces wearing the MBU-20/P mask taken by the present study.

Oxygen mask design revision strategies were established by analyzing relationships between FMI factors, and the oxygen mask shape was revised to fit the KAF pilots based on a virtual fit assessment (VFA) method. Correlations among the facial anthropometric characteristics such as oxygen mask design dimensions, oxygen mask wearing characteristics, and user preferences were analyzed to identify oxygen mask design problems and solutions. The VFA method, which virtually analyzes an oxygen mask fit using 3D face images and oxygen mask CADs, was developed and applied to redesign the oxygen mask shape for a better fit to KAF pilots. A VFA system was implemented for the automatic evaluation of the oxygen mask fit by virtually aligning various oxygen mask designs to the 3D face images and analyzing an infiltration of an oxygen mask design into the 3D face images to estimate contact pressure of the oxygen mask to the faces. Through the VFA method, the best oxygen mask design for the KAF pilots was identified, and the revised oxygen mask showed an increase of 27% in the satisfaction with the design by the KAF pilots compared to the existing oxygen mask.

An ergonomic usability evaluation was conducted to compare the existing oxygen masks and prototypes of the revised oxygen masks with the KAF pilots and the KAF Academy cadets. 83 KAF pilots (81 males and 2 females) who currently use the MBU-20/P oxygen mask and 58 KAF Academy cadets (32 males and 26 females) who were potential users of the oxygen mask. Prototypes of the revised oxygen masks were fabricated using similar materials as the MBU-20/P oxygen mask. The usability of the existing and revised oxygen masks was compared in terms of discomfort, pressure, and suitability for military equipment. The revised oxygen mask design had positive effect: 56% ~ 81% lower discomfort, 11% ~ 25% lower average pressure, 6% ~ 43% lower moderately pressed area, and 4% ~ 40% lower excessively pressed area than the existing oxygen mask for the KAF pilots. Also, the revised oxygen mask was found stable in PBG (pressure breathing for gravity) mode and a low pressure situation and any noticeable problem was not reported, and there was 31% ~ 83% lower oxygen mask slippage distance in the evaluation of oxygen mask suitability for military equipment. Lastly, 92% (120 out of 131 pilots and cadets) of the participants answered that they were more satisfied with the fit of the revised oxygen mask prototype to their face than the existing oxygen mask.

In the present study, a systematic and rational oxygen mask design methodology based on the face-mask interface analysis and the virtual fit assessment method was proposed. The revised oxygen mask showed better appropriateness to the KAF pilots, a decrease of excessive pressure and oxygen leakage, and an increase of satisfaction and wearability. The revised oxygen mask can support the safety and satisfaction of the KAF pilots and increase the military power of the KAF by reducing physical and mental workload due to discomforts caused from excessive pressure or oxygen leakage. Furthermore, the proposed methods including the FMI analysis, the VFA, and the usability evaluation can be applied to the mass-customized design and evaluation of wearable products which have importance in fit, comfort, performance, and safety.

TABLE OF CONTENTS

LIST OF FIGURES

LIST OF TABLES

Chapter 1. INTRODUCTION

1.1. Problem Statement

An oxygen mask (Figure 1.1) worn over the face of a fighter pilot supports a steady supply of oxygen and efficient communication for safe and effective mission accomplishment. The pilot oxygen mask is a half-face type mask covering the nasal area and mouth which is composed of facepiece, hardshell, and peripheral components. The facepiece, made of silicon rubber, fits to the pilot's face and prevents oxygen leakage, and the hardshell, made of nylon, keeps the shape of the facepiece and holds peripheral components such as a microphone, straps, and valves. The pilot oxygen mask encloses the pilot's nose and mouth for a stable supply of oxygen to the pilot while a mission is conducted at high altitude where oxygen is lacking. The pilot oxygen mask protects the pilot in adverse environments (e.g., decompression, fire, and fumes in the cockpit, windblast during ejection, and ditching) by continuously supplying oxygen to the pilot (Alexander, McConville, & Tebbetts, 1979). The pilot oxygen mask also houses the microphone for communication and is securely mounted to a helmet with adjustable straps, bayonet receivers, and connectors.

The MBU-20/P (Gentex Corporation, U.S.A.) pilot oxygen mask, originally designed for U.S. Air Force (USAF) personnel, has been causing excessive pressure and/or leakage of oxygen around the nasal root to a significant number of Korean Air Force (KAF) pilots. The MBU-20/P mask was initially designed using face anthropometric data of 2,420 USAF personnel collected by

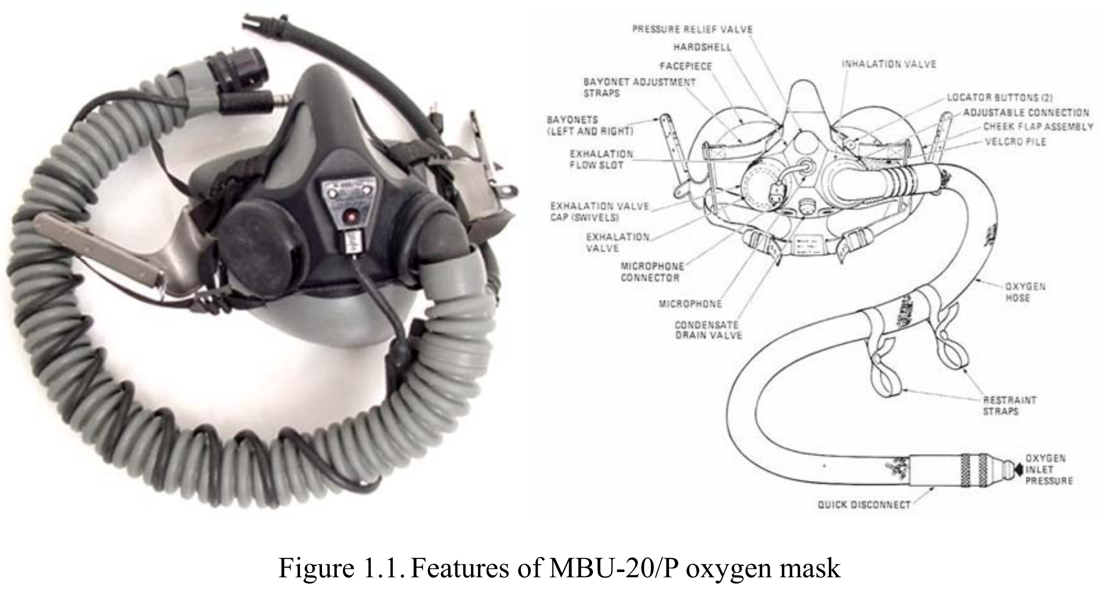

Figure 1.1. Features of MBU-20/P oxygen mask

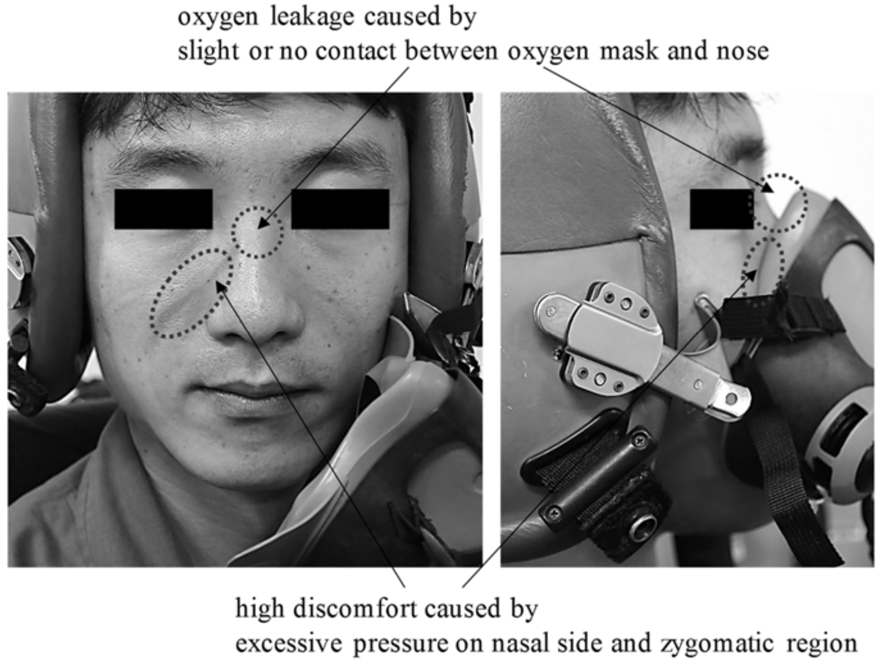

Figure 1.2. Discomfort of existing MBU-20/P mentioned by Korean Air Force pilots

Churchill, Kikta, and Churchill (1977) and has been improved by applying 3D face scan data of 60 (30 males and 30 females) pilots (M. E. Gross, Taylor, Mountjoy, & Hoffmeister, 1997). A survey conducted by KAF in 2006 on the usability of the MBU-20/P mask identified that a significant percentage of KAF pilots suffered from excessive pressure and/or oxygen leakage around the nasal root due to the lack of fit of the oxygen mask to the face (Figure 1.2), which is most likely caused by a significant difference in facial shape and size between KAF pilots and USAF personnel.

Facial measurements have been collected and applied for an ergonomic design of a half-face mask such as the pilot oxygen mask and an industrial dustproof mask. Previous research on the half-face mask design measured the dimensions of head (e.g., head height, head breadth, head length, and head circumference), face (e.g., face length, face width, and bitragion-subnasale arc), nose (e.g., nose length, nose width, and nose protrusion), lip (e.g., lip width), and chin (e.g., supramentale-to-menton length, chin width, and bizygomatic-menton arc). For example, Han, Rhi, and Lee (2004) measured 10 facial dimensions (face length, lower face length, nose length, nose protrusion, face width, chin width, nose width, lip width, bitragion-menton arc, and bitragion-subnasale arc) of 50 (26 males and 24 females) Korean civilians to develop a half-face industrial respirator for Koreans. M. E. Gross et al. (1997) measured 15 facial dimensions (head breadth, head length, head circumference, face length, lower face length, sellion-to-supramentale length, nose length, nose protrusion, face width, bi-inframalar breadth, bizygomatic breadth, lip width, nasal root breadth, nose width, and bitragion-subnasale arc) of 60 USAF pilots for the design of the MBU-20/P mask. Lastly, both Hack and McConville (1978)'s study on the design of an industrial respirator and Young (1966)'s study on the design of an oxygen mask for children measured detailed nose dimensions (e.g., nasal root breadth, maximum nasal bridge breadth, rhinion-to-menton length, and rhinion-to-promentale length), which are useful for the ergonomic design of the nasal part of a respirator.

The anthropometric information of KAF pilot faces is needed to develop the ergonomic design of the pilot oxygen mask. Facial data collected by a national anthropometric survey for Korean civilians (KATS, 2004) and a small scale study (50 civilians) by Han et al. (2004) for an industrial respirator design are available. However, the applicability of these facial anthropometric measurements of Korean civilians is quite limited for the design of the pilot oxygen mask because some nose-related measurements such as nasal root breadth, nasal bridge breadth, and rhinion-to-menton length, which are crucial for oxygen mask design, were not measured. Furthermore, anthropometric measurements often significantly differ between military personnel and civilians (W. Lee et al., 2013; Zhuang, Bradtmiller, & Shaffer, 2007). Jeon (2011) reported significant mean differences in various body dimensions between KAF pilots (1,238 males) and Korean civilians (1,741 males) – for example, the average leg length of KAF male pilots (101.1 ± 4.4 cm) was significantly shorter than that of Korean male civilians (105.8 ± 4.8 cm) at $\alpha = .01$. Moreover, the existing facial anthropometric data for Korean civilians do not include some facial dimensions (e.g., nasal root breadth, nasal bridge breadth, and rhinion-to-menton length) which can be used in oxygen mask design.

To design a respirator shape which is suitable for users' faces, previous studies have proposed respirator design and evaluation methods using 3D face images; however, those methods have limitations in terms of generalizability and validity. Some previous studies (M. E. Gross et al., 1997; Han & Choi, 2003; Song & Yang, 2010) proposed respirator design methods using 3D representative face models (RFMs) generated based on facial anthropometric data of user population. However, limitations include a lack of description of a detailed method for creating a respirator shape using 3D face images, and an empirical verification of their respirator designs was not considered. Conversely, Butler (2009), Dai, Yang, and Zhuang (2011), and Lei, Yang, and Zhuang (2012) introduced simulation methods to examine respirator fit based on the 3D face image and respirator CAD through a finite element modeling (FEM) system (e.g., LS-DYNA, Livermore Software Technology Corporation, U.S.A.) (Figure 1.3). Those studies tried to analyze a respirator fit, contact pressure, and discomfort using FEM systems; however, virtual respirator fit analysis methods are still at a preliminary stage, and still not applicable to the respirator design or evaluation.

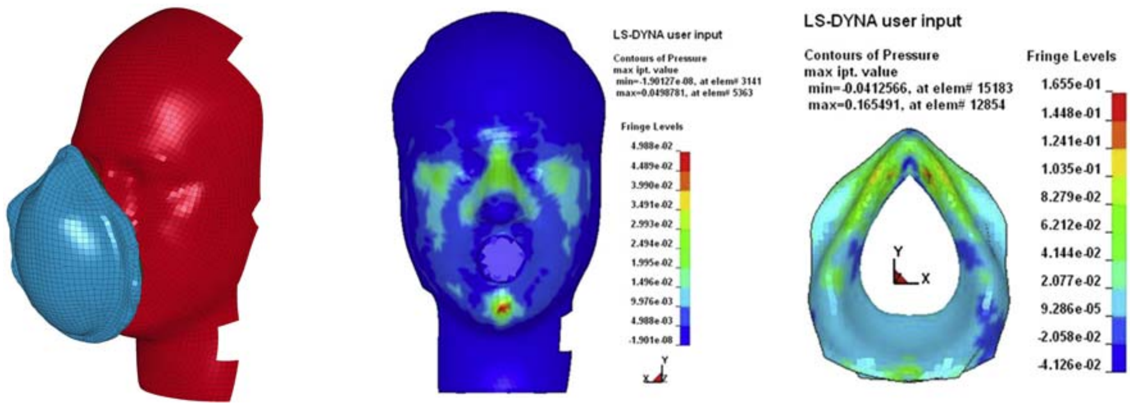

(a) 3D alignment of mask and face (b) Result of virtual fit evaluation

Figure 1.3. A quantitative mask fit evaluation conducted by LS-DYNA software (Dai et al., 2011)

1.2. Research Objectives

The present study collected anthropometric data and 3D images of KAF pilots' faces and analyzed their facial characteristics to apply to the pilot oxygen mask design in order to fit KAF pilots. Correlations among the facial anthropometric characteristics such as oxygen mask design dimensions, oxygen mask wearing characteristics, and user preferences were analyzed to identify design problems and solutions. A virtual fit assessment (VFA) method which virtually analyzes an oxygen mask fit using 3D face images and oxygen mask CADs was developed and applied to redesign the oxygen mask shape for a better fit to KAF pilots. Lastly, a prototype of the revised oxygen mask was manufactured, and an ergonomic usability evaluation of the existing and revised oxygen masks was conducted with KAF pilots. The design and evaluation methods developed by the present study (Figure 1.4) were applied to revise the shape of the MBU-20/P pilot oxygen mask.

First, in detail, the present study collected the facial measurements of KAF pilots in 3D to create the oxygen mask design and corresponding oxygen mask sizing system. Their characteristics were analyzed in comparison to Korean civilians and USAF personnel. Twenty-two facial dimensions were selected in the present study as those applicable to the design of an oxygen mask. The faces of KAF pilots (278 males and 58 females) were captured using a 3D scanner, and the facial dimensions were measured using 3D face scan data. Lastly, the facial measurements of KAF pilots were compared with those of Korean civilians and USAF personnel, and then were applied to generate an oxygen mask sizing system and RFMs, which was used in the oxygen mask design for KAF pilots.

Second, a face-mask interface (FMI) analysis was conducted to identify design problems of the existing oxygen mask and to determine design directions of the new oxygen mask for KAF pilots. The preferences of KAF pilots of the existing oxygen mask were surveyed in terms of discomfort,

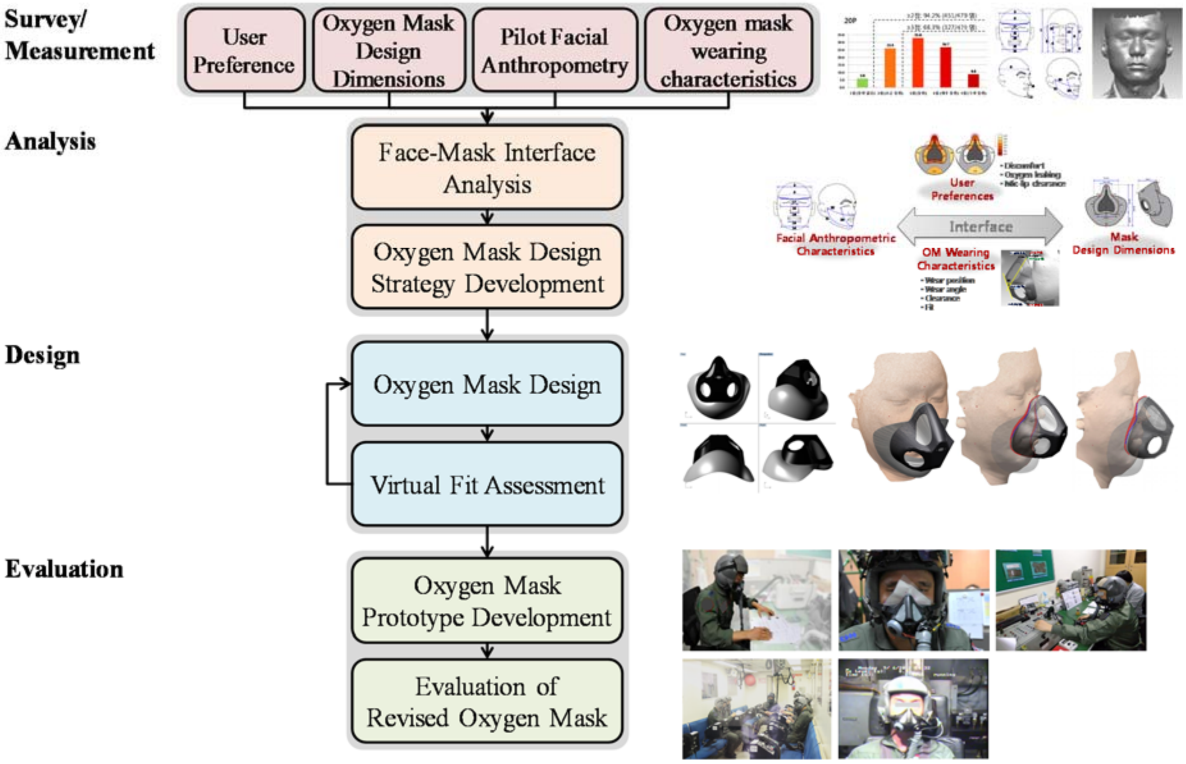

Figure 1.4. Framework of study

oxygen leakage, and slippage. The design dimensions of the facepiece and hardshell of the existing MBU-20/P pilot oxygen mask were measured to examine design characteristics. The oxygen mask wearing characteristics (e.g., wearing position, wearing angle, fit, and clearance) were analyzed using photos of KAF pilots taken by the present study. Finally, design revision strategies for the oxygen mask for KAF pilots were established by analyzing the correlation among four FMI factors (facial anthropometric characteristics, oxygen mask design dimensions, oxygen mask wearing characteristics, and user preferences).

Third, the present study designed the new oxygen mask shape for KAF pilots through the VFA method which can virtually analyze the oxygen mask fit, quantitatively and systematically. The new oxygen mask shape was initially designed based on the RFMs of KAF pilots, and then modified considering a variety of face shapes among KAF pilots. A VFA system was implemented for the automatic evaluation of the oxygen mask fit by virtually aligning various oxygen mask designs to the 3D face images and analyzing an infiltration of an oxygen mask design into the 3D face images to estimate contact pressure of the oxygen mask to the faces. The best oxygen mask design for KAF pilots was identified through an iterative design revision process conducted based on the VFA system.

Lastly, the present study manufactured the prototype of the revised oxygen mask design and conducted the ergonomic usability evaluation with KAF pilots in terms of discomfort, pressure, and suitability for military equipment. To compare the existing and revised oxygen masks under similar conditions, the present study used similar materials as the MBU-20/P oxygen mask in the manufacturing of the revised oxygen make prototype. The discomfort of the existing and revised oxygen masks was evaluated using a questionnaire developed by the present study. The pressure of the existing and revised oxygen masks was measured by pressure indicating film (Fujifilm, Japan) and analyzed by a pressure analysis system developed by the present study. Lastly, the revised mask's suitability for military equipment was evaluated in flight-like situations such as low atmospheric pressure and high gravity acceleration (high-G).

1.3. Significance of the Study

The present study on the oxygen mask design and evaluation has four areas of significance, theoretically and practically. First, the proposed product design method based on the FMI model can present quantitative design guidelines based on comprehensive understanding of a user, a product, and an interface between the user and product. In the present study, the facial anthropometric characteristics were surveyed to understand the users, the oxygen mask design dimensions were identified to comprehend the product, and the oxygen mask wearing characteristics and the preferences were analyzed to understand the interaction between the user and product. Finally, the design problems, design revision directions, and the design revision strategies could be quantitatively identified through the FMI analysis.

Second, the VFA method developed by the present study can be applied to the design of wearable products which require better fit and comfort to the body. The VFA method can quantitatively evaluate oxygen mask wearing characteristics such as fit, pressure, interference, clearance, and discomfort by using 3D body scan images and CAD of the product. By referring to results of the VFA, a manufacturer can find a better design for the users. The VFA method can be applied to the design of various types of respirators including an oxygen mask for medical patients, an industrial dust-proof mask, a military anti-gas mask, a firefighter mask, and a diving mask. Also, headwear, goggles, underwear, gloves, shoes, and special garments for disabled people can be designed by applying the VFA method and 3D body images of users.

Third, the oxygen mask evaluation methods proposed by the present study can be applied to the ergonomic usability testing for wearable products. The ergonomic usability evaluation method can include a survey of subjective preferences, measurement and analysis of fit and pressure of the product, and evaluation of suitability for their usage environment. In particular, previous research on respirator development did not measure pressure between the face and respirator; however, the present study proposed an empirical evaluation method for the pressure analysis using the pressure film. The proposed pressure evaluation method can be applied to the examination of the fit and comfort caused by contact between the product and the user. Additionally, the present study employed a suitability evaluation in specific usage situations (e.g., low atmospheric pressure and high-G) that is useful for identifying usability and functionality of the product.

Lastly, the proposed product design method based on 3D human body images will be useful in the design of a mass-customized product which considers a variety of sizes and shapes of human body parts. The mass-customized product can lead to the solution of some issues regarding mass-produced production which is that it is hard to simultaneously satisfy various user needs and a customized production, since the latter have limitations including inefficiency of production and high price. In particular, wearable products are more ideal for mass-customization due to their flexibility and simplicity of production procedure, in comparison with electronics, mechanical products, or home appliances. The oxygen mask design method proposed by the present study can be applicable to the mass-customization of wearable products. This method can systematically and efficiently determine sizes and corresponding shapes of a wearable product based on information surveyed from users (e.g., anthropometric characteristics, 3D human body shape, ways to use the product, and preferences); moreover, those designs can provide proper fit, comfort, and satisfaction to the users.

1.4. Organization of the Dissertation

The remainder of this dissertation is organized into six chapters and four appendices. Chapter 2 reviews literature that is relevant to the present study, including features of the pilot oxygen mask, facial anthropometric surveys and analyses, oxygen mask design methods based on a facial anthropometric data, and oxygen mask fit analysis methods. Chapter 3 introduces the FMI analysis and four FMI factors: the KAF pilots' preferences, oxygen mask design dimensions, facial anthropometric characteristics of KAF pilots, and oxygen mask wearing characteristics. Chapter 4 proposes an oxygen mask design process based on the FMI analysis and the VFA method. Chapter 5 describes methods and results of the ergonomic usability evaluation of the existing and revised oxygen masks. Chapter 6 discusses the effectiveness and limitations of the present study and suggests agendas for future studies. Chapter 7 presents concluding remarks about contributions of the present study and further research issues. Appendices include facial dimensions, a questionnaire for surveying the preferences of KAF pilots, oxygen mask wearing characteristics, and a questionnaire for the usability evaluation of the existing and revised oxygen masks.

Chapter 2. LITERATURE REVIEW

2.1. Pilot Oxygen Mask

The oxygen mask worn over the face of the fighter pilot is a functional mask developed to supply oxygen to the pilot at high altitudes where oxygen is lacking. Generally, masks can be classified into two main categories according to their purpose of use: functional and non-functional (Wikipedia, 2013). Masks used for ritual ceremonies or theatrical performances do not have practical functions. On the other hand, functional masks include industrial respirators (e.g., dust-proof mask and welding mask), protective masks (e.g., military anti-gas mask and helmet mask), medical masks (e.g., oxygen mask, anesthetic masks, face shields and C.P.R. masks), sport masks (e.g., fencing mask, baseball catcher's mask, and American football helmet mask), and diving masks, which are mainly used for health and safety. The pilot oxygen mask which is the focus of the present study is a military respirator which supports a steady supply of oxygen to the pilot. The pilot oxygen mask protects the pilot in adverse environments (e.g., decompression, fire, and fumes in the cockpit, windblast during ejection, and ditching) by continuously supplying oxygen to the pilot and houses a microphone for radio communication.

Respirators are categorized into full-face and a half-face type depending on the hazard of concern (Figure 2.1). The full-face respirator seals along the forehead, cheeks, and under the chin of a user to protect the face from hazardous environments as well as to provide oxygen or fresh air to the user. Examples of the full-face respirators include: a firefighting mask, a diving mask, and a military anti-gas mask. On the other hand, the half-face respirator covers the oral-nasal area of a user and supports oxygen supplying or air purifying. The pilot oxygen mask focused on in the present study is the half-face respirator which encloses the nose and mouth of the pilot.

(a) Full-face respirator (illustrated for firefighter's air purifying respirator)

(b) Half-face respirator (illustrated for protective filter mask worn by police officer)

Figure 2.1. Type of respirator shape: full-face respirator and half-face respirator

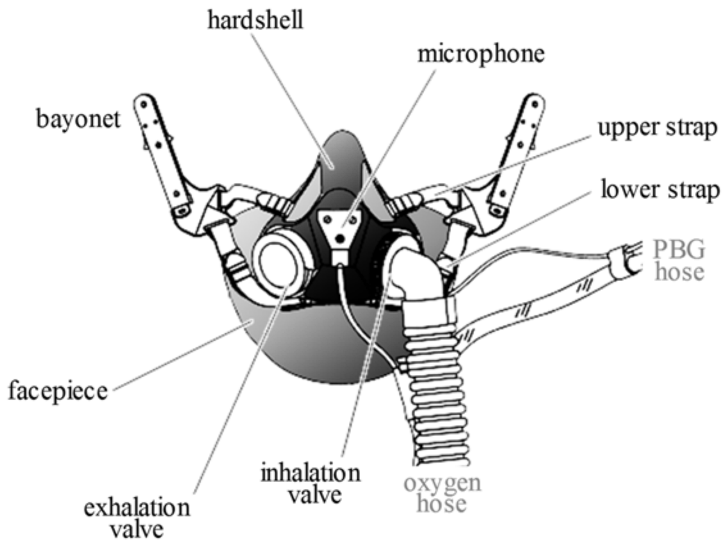

Figure 2.2. Components of MBU-20/P pilot oxygen mask (Gentex Corporation, U.S.A.)

The MBU-20/P pilot oxygen mask is composed of the facepiece, hardshell, microphone, valves, and straps (Figure 2.2). The facepiece, made of silicon rubber, encloses the pilot's face and prevents oxygen leakage. The hardshell, made of nylon, contains the facepiece to prevent deformation of the facepiece and holds peripheral components such as a microphone, straps, and valves. The MBU-20/P includes five sizes (extra small narrow, XSN; small narrow, SN; medium narrow, MN; medium wide, MW; large wide, LW) depending on length and width (M. E. Gross et al., 1997).

2.2. Facial Anthropometry

2.2.1. Facial Anthropometry Research

A large-scale survey of facial anthropometry has been conducted by military institutions for designing respirators or protective equipment; however, the data might not be acceptable to industrial product designs for civilians due to their differences in demographic factors. In the case of the USAF, in 1950, Hertzberg, Daniels, and Churchill (1954) measured 132 body dimensions including 40 head and facial dimensions of 4,063 USAF male personnel for designing military equipment (e.g., helmet, oxygen mask, and gas mask). Churchill et al. (1977) collected 182 body dimensions including 48 head and facial dimensions of 2,420 USAF male personnel during 1967 ~ 1968. The 1967-1968 USAF survey data were applied to the design of the MBU-20/P pilot oxygen mask by Alexander et al. (1979) and partially utilized to the design and evaluation of industrial respirators through the National Institute for Occupational Safety and Health (NIOSH) until early 2000s (Zhuang & Bradtmiller, 2005). In the case of the f U.S. Army, Gordon et al. (1988) surveyed 132 body dimensions including 16 head and facial dimensions of 8,997 U.S. Army personnel in 1987 ~ 1988, and Hotzman et al. (2011) measured 97 body dimensions including 14 head and facial dimensions and their 3D images of around 13,000 U.S. Army personnel during 2010 ~ 2011. However, the applicability to the design of industrial products may be limited because the anthropometric characteristics of military personnel can be significantly different from those of civilians due to factors such as occupation, age, and race (Roebuck, 1995; Sanders & McCormick, 1998; Zhuang et al., 2007).

Large-scale anthropometric investigations focused on the faces of civilians have occurred mostly since 2000 for the design of respirators and headwear for industrial or public use (Table 2.1). In one of the early surveys of facial anthropometric data, Young (1966) measured 18 facial dimensions of 978 U.S. children aged 1 month to 17 years for the design of a medical oxygen mask for infants and children. Additionally, Hughes and Lomaev (1972) collected 8 facial dimensions of 538 Australian male workers aged 15 to 80 years for the design of an industrial respirator. For practical purposes, respirator manufacturers in the U.S.A. have used respirator fit test panels from NIOSH which were based on the 1967-1968 USAF survey data by Hack et al. (1973). However, because of demographic differences between military personnel and civilians and demographic changes over the last 30 years, Zhuang and Bradtmiller (2005) of NIOSH collected 19 facial dimensions of 3,997 civilians (2,543 males and 1,454 females) aged 18 to 66 years including 3D face and head scan images of 1,013 participants in 2003 to design respirators for a better fit to U.S. civilians. Du et al. (2008) of China surveyed 19 head and facial dimensions of 3,000 Chinese civilian workers (2,026 males and 974 females) aged 18 to 66 years, and Research Institute of Human Engineering for Quality Life (HQL) (2008) of Japan investigated 17 facial dimensions of 6,842 Japanese civilians (3,530 males and 3,312 females) aged 19 to 80 years. In the case of South Korea, body dimensions of Korean civilians have been collected through the Size Korea project since 1979. The sixth Size Korea project (KATS, 2010) collected 139 body dimensions including 8 head and facial dimensions of 14,016 Korean civilians (7,532 males and 6,484 females) in 2010. Moreover, 45 head and facial dimensions of 848 participants (438 males and 410 females) aged 20 to 39 years were measured in 3D.

Table 2.1. Facial anthropometric surveys for civilian population

No.	Reference		Survey year	Nationality	Sample size	No. of facial dimension
1	Young (1966)		1966	U.S.A.	M & F: 978	18
2	Hughes and Lomaev (1972)		1972	Australia	M: 538	8
3	Zhuang and Bradtmiller (2005)		2003	U.S.A.	M: 2,543, F: 1,454	19
4	Du et al. (2008)		2006	China	M: 2,026, F: 974	19
5	HQL (2008)		2004 ~ 2006	Japan	M: 3,530, F: 3,312	17
6	KATS (2010)	Direct measurement	2010	Korea	M: 7,532, F: 6,484	8
		3Dmeasurement			M: 438, F: 410	45

2.2.2. Comparison of Facial Dimensions by Race

According to previous research, Korean and Chinese civilians have shorter and wider faces than Americans. H. Kim, Han, Roh, Kim, and Park (2003) compared Korean male civilians (KMC) data (Han, Willeke, & Colton, 1997; H. Kim et al., 2003; KATS, 1998) to U.S. male civilians (UMC) data (Brazile et al., 1998; S. F. Gross & Horstman, 1990; Liau, Bhattacharya, Ayer, & Miller, 1982; Oestenstad & Perkins, 1992) in some comparable dimensions (face length, face width, lip width, and nose width) and reported that the KMC have wider faces (KMC: 145.1 ~ 147.6 mm, UMC: 134.0 ~ 140.6 mm in face width) and noses (KMC: 36.7 ~ 38.3 mm, UMC: 29.0 ~ 36.0 mm) and narrower lips (KMC: 49.3 ~ 51.1 mm, UMC: 51.0 ~ 56.2 in lip width) than those of the UMC. However, the face length of the KMC (120.1 ~ 120.6 mm) was found to have no clear difference compared to the UMC (113.7 ~ 126.0 mm). L. Yang, Shen, and Wu (2007) measured 270 Chinese male civilians (CMC) aged 23 to 43 years and compared the CMC with the UMC (S. F. Gross & Horstman, 1990; Liau et al., 1982; Oestenstad & Perkins, 1992; Zhuang & Bradtmiller, 2005) in some dimensions (face length, face width, and lip width) which relate to respirator design (Hack et al., 1973; Zhuang et al., 2007). They found the CMC have shorter ($\bar{d}$ = -8.2 ~ -4.1 mm in face length) and wider ($\bar{d}$ = 3.7 ~ 11.5 mm in face width) faces, and wider lips ($\bar{d}$ = 2.1 ~ 5.4 mm in lip width) than those of the UMC. Du et al. (2008) also measured 2,026 CMC aged 18 to 66 years and compared their CMC data to the UMC measured by Zhuang and Bradtmiller (2005). They reported that the CMC have shorter ($\bar{d}$ = -5.4 mm in face width) and wider ($\bar{d}$ = 4.0 mm in face width) faces and slightly wider lips ($\bar{d}$ = 1.1 mm in lip width) than those of the UMC. Meanwhile, Ball et al. (2010) compared 3D head images between 600 CMC and 600 UMC which were randomly selected from the Size China data (Ball, 2009; Ball & Molenbroek, 2008) and the Civilian American and European Surface Anthropometry Resource (CAESAR®) data (Robinette et al., 2002). The CMC heads were found wider ($\bar{d}$ = 4.0 mm in head breadth) and horizontally shorter ($\bar{d}$ = -11.0 mm in head length) than those of the UMC (Figure 2.3). Table 2.2 presents some key facial dimensions collected from the large-scale anthropometric survey data of South Korea, China, and U.S.A. In summary, the KMC and CMC were found to have shorter and wider faces than the UMC in overall dimensions such as face length and face width, although the facial characteristics between populations are diverse in specific dimensions.

2.2.3. Development of Fit Test Panels based on Facial Dimensions

The fit test panels developed based on facial anthropometric data have been applied to design and evaluation of industrial respirators. Hack et al. (1973) of Los Alamos National Laboratory (LANL)

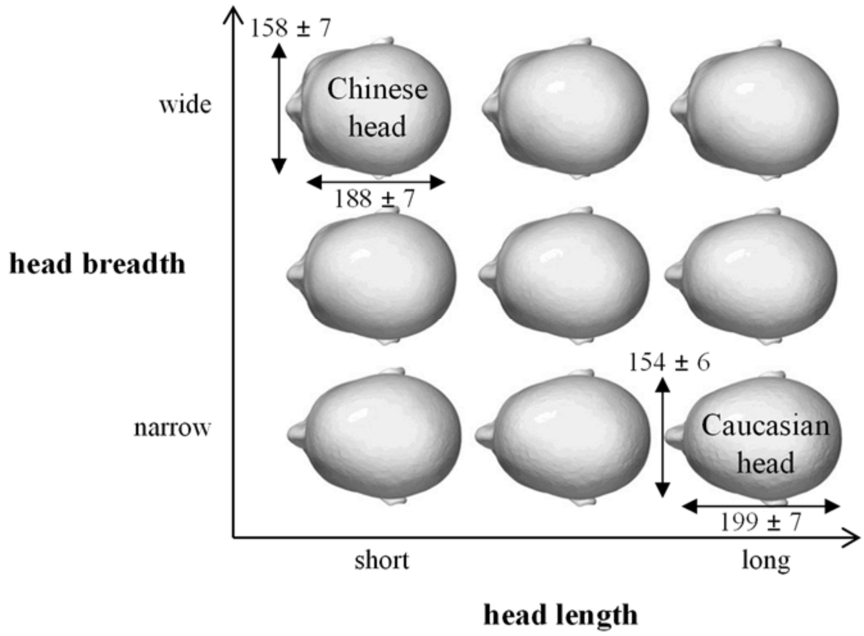

Figure 2.3. The demonstration of differences between Chinese and Caucasian head (Ball et al., 2010)

proposed fit test panels (LANL panels) by the request of the NIOSH (Figure 2.4a). The LANL panels were developed based on the 1967-1968 USAF survey data, because there were no facial measurements of U.S. civilians in the 1970s. Hack et al. (1973) measured some facial dimensions of 200 UMC, and by comparing the UMC data to the 1967-1968 USAF data, a significant similarity ($|\bar{d}|$ < 2.0 mm) was found between the UMC and USAF male personnel in terms of some important facial dimensions (face length, face width, and lip width) related to the respirator design. The LANL panels were used to design of the full-face and half-face industrial respirators until the 2000s.

Table 2.2. Comparison between facial anthropometric surveys (male; unit: mm)

Category / facial dimension	**Korean (Size Korea)**	**Chinese**	**American (NIOSH)**	**American (CAESAR)**
Reference	KATS (2004)	Du et al. (2008)	Zhuang and Bradtmiller (2005)	Harrison and Robinette (2002)
Survey year	2003 ~ 2004	2006	2003	2000
Sample size	1,819	2,026	2,543	1,119
Age	18 ~ 66	18 ~ 66	18 ~ 66	18 ~ 65
1 head length	177.0 ± 21.2	185.7 ± 5.8	197.3 ± 7.4	200.1 ± 10.4
2 head breadth	154.0 ± 18.5	157.2 ± 5.3	153.0 ± 6.0	154.5 ± 6.1
3 head circumference	572.0 ± 16.2	567.0 ± 13.6	575.7 ± 17.1	577.1 ± 18.1
4 face length*	111.3 ± 14.5	117.3 ± 5.6	122.7 ± 7.0	121.3 ± 8.0
5 face width*	-	147.5 ± 4.7	143.5 ± 6.9	142.7 ± 7.4
6 nose length	-	50.7 ± 2.9	52.0 ± 4.1	-
7 nose width	39.6 ± 3.6	39.2 ± 2.4	36.6 ± 4.1	-
8 nose protrusion	12.6 ± 2.4	18.9 ± 1.9	21.1 ± 2.7	-
9 lip width*	49.0 ± 5.6	52.2 ± 3.4	51.1 ± 4.2	-
10 bitragion-subnasale arc	-	302.5 ± 10.4	294.8 ± 13.2	-
11 bigonial breadth	-	119.0 ± 8.5	120.4 ± 10.4	123.7 ± 12.4
12 interpupillary distance	62.7 ± 5.4	64.2 ± 2.7	64.5 ± 3.6	67.7 ± 6.0

* Dimensions highly related to the respirator design

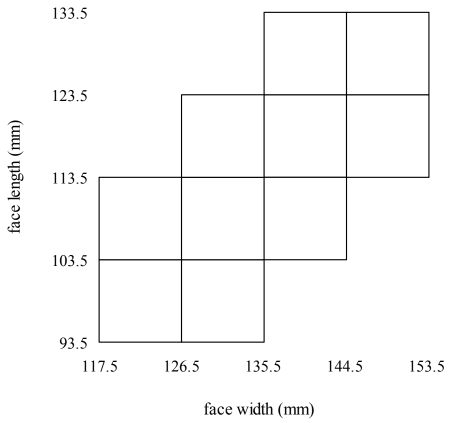

Fit test panel for the full-face respirator

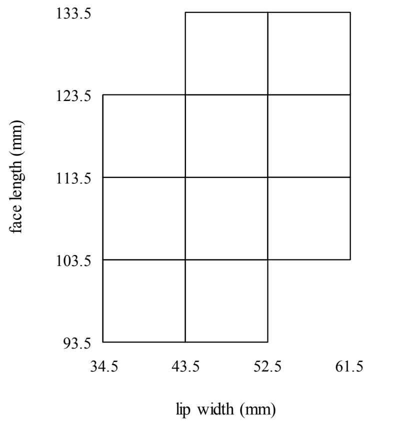

Fit test panel for the half-face respirator

(a) The LANL panels (Hack et al., 1973)

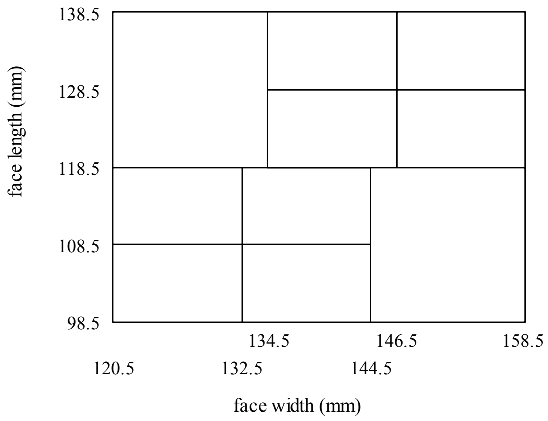

Fit test panel for both of the half-face and full-face respirator

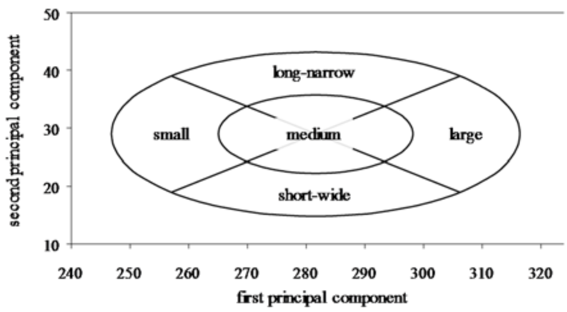

Fit test panel based on the principle component analysis

(b) The NIOSH panels (Zhuang et al., 2007)

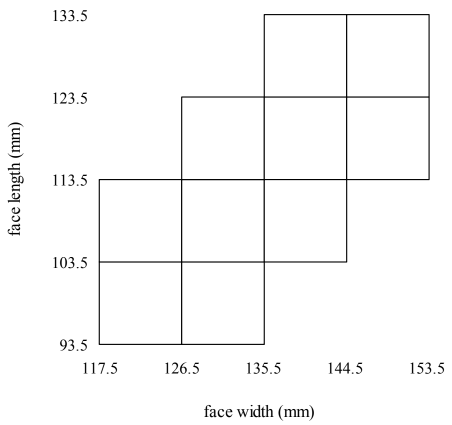

Fit test panels for the full-face respirator

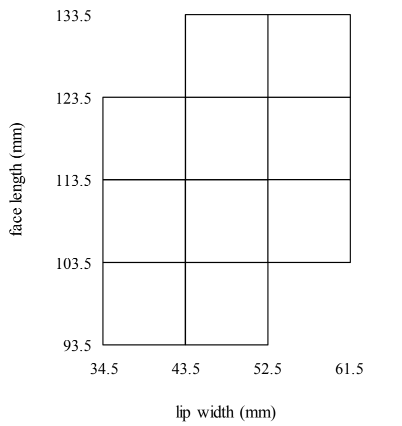

Fit test panels for the half-face respirator

(c) Korean panels developed based on the LANL panels (Han, 1999)

Figure 2.4. Proposed fit test panels for industry respiratory users

However, according to Zhuang, Guan, and Hsiao (2002) study, the LANL panels developed in the 1970s accommodate 84% of the CAESAR data (n = 2,391) collected in 2000. This is due to the fact that military personnel were younger and required strict physical criteria such as height, weight, and physical fitness compared to general civilians, and the demographics of the U.S. population have changed over the last 30 years (Zhuang & Bradtmiller, 2005). Therefore, the LANL panels needed to be revised to accommodate today's civilian workers. For this reason, Zhuang et al. (2007) of the NIOSH developed new fit test panels (NIOSH panels; Figure 2.4b) based on 3,996 UMC (2,543 males and 1,454 females) measured by Zhuang and Bradtmiller (2005) in 2003. A bivariate panel and a principal component analysis (PCA) panel were proposed. Both panels are more accurate the LANL panel in terms of accommodation percentage (> 95% of the UMC) and applicability to the full-face and half-face respirators; therefore, respirators designed based on the NIOSH panels may be more appropriate for the users. Meanwhile, the LANL panels have been applied to the other populations – for example, Han (1999) of South Korea measured 12 facial dimensions of 522 KMC (408 males and 114 females) and developed Korean fit test panels (Figure 2.4c) by following a development procedure of the LANL panels. The Korean panels were applied to the design of an industrial dust-proof mask for Korean civilian workers (Han et al., 2004).

2.2.4. 3D Facial Anthropometry and Representative Face Models

A 3D scan image of the head and face can be applicable to facial anthropometric measurement and respirator design. Most of anthropometric surveys since 2000s used not only a conventional direct measurement method, but also a 3D scan measurement method to collect both the size and shape information from a user population. Through 3D scanning of a human body part (e.g., whole body, face, foot, and hand) with landmarks, a 3D scan image and 3D location of landmarks can be found. Consequently, body dimensions including length, distance, thickness, width, circumference, and arc are measured based on the 3D scan image and the 3D landmark information. Regarding a 3D facial anthropometric survey, CAESAR (Harrison & Robinette, 2002) and Size Japan (HQL, 2008) collected 3D face images and corresponding measurements using a 3D full-body scanner. However, because those scanners were developed to scan the full-body, the face part was roughly captured and did not capture the small and complex features of face. Therefore, they could measure less than 20 conventional dimensions from the 3D images. On the other hand, the Size Korea survey (KATS, 2010) captured the head and face using a 3D head scanner and could specifically measure 45 facial dimensions using higher quality 3D images. The Size China survey also used a 3D head scanner to develop 10 headforms as illustrated in Figure 2.5, which can be useful for the design of headwear or facewear for Chinese (Ball, 2009; Ball & Molenbroek, 2008).

Figure 2.5. Ten headforms representing Chinese civilians (Ball, 2009)

The 3D head and face images and the landmarks have been applied to the generation of RFMs. Zhuang, Benson, and Viscusi (2010) proposed five RFMs (Figure 2.6) representing five size categories of the NIOSH's PCA fit test panel (Figure 2.4b). First, they selected five 3D heads whose facial measurements were closer to the average size of each size category. 3D head scan images of 1,013 UMC collected by Zhuang and Bradtmiller (2005) were used. Then, they manually conducted post-processing (e.g.., alignment and merging of 5 heads, patching and smoothing of the lip, eyes, and ears, and adjustment of dimensions) using Polyworks (InnovMETRIC™, Canada) software to form the RFMs. On the other hand, previous research introduced the RFMs generated through the PCA; for example, Zhuang, Slice, Benson, Lynch, and Viscusi (2010) proposed four RFMs (Figure 2.7a) based on the PCA using 3D location of 26 landmarks of 1,013 UMC collected by Zhuang and Bradtmiller (2005). Luximon, Ball, and Justice (2010) presented eight RFMs (Figure 2.7b) based on 3D location of 31 landmarks; furthermore, Luximon, Ball, and Justice (2012) proposed four RFMs (Figure 2.8) based on facial dimensions and 3D head images which were composed of more than 6,000 vertices. The Size China data (Ball & Molenbroek, 2008) were used for Luximon's studies. Compared to the RFMs based on the landmarks, Luximon et al. (2012)' RFMs based on 3D head and face images may be more useful for designing headwear or facewear due to more information about 3D head and facial shape.

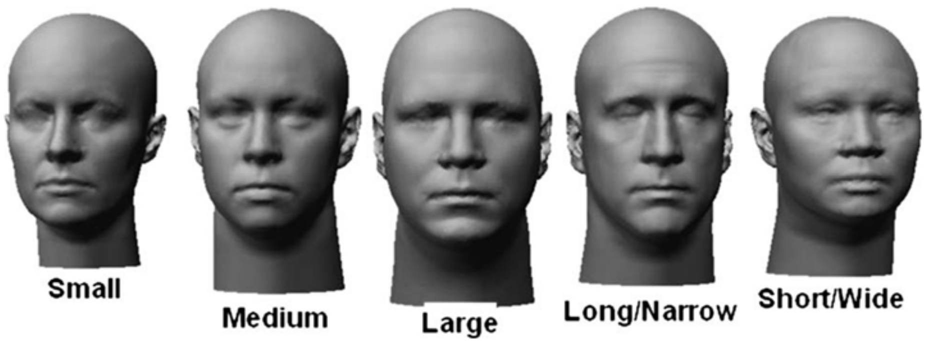

Figure 2.6. Five digital 3D headforms representing the five face size categories for the U.S. workforce: small, medium, large, long-narrow, short-wide (Zhuang, Benson, et al., 2010)

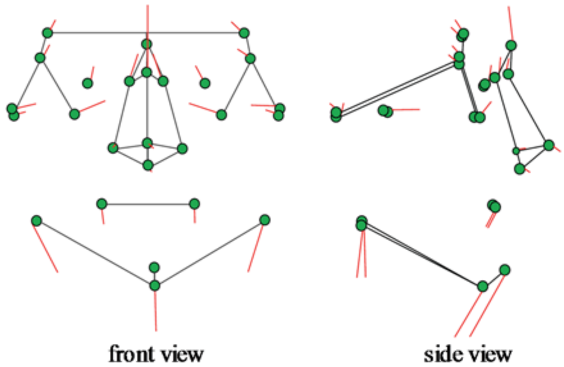

(a) The first principal component of Zhuang, Slice, et al. (2010)'s study (red lines present eigenvectors of xyz axis of each landmark and indicate the direction and relative magnitude of the landmarks)

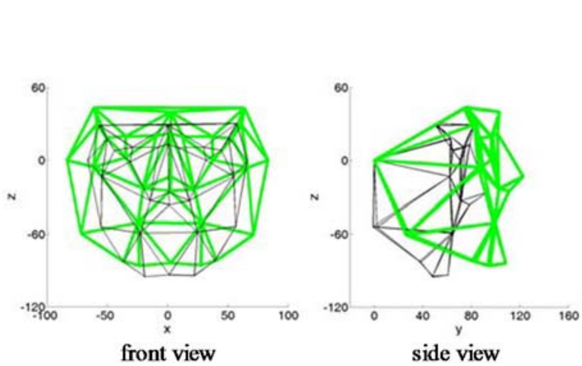

(b) The first principal component of Luximon et al. (2010)'s study (green and black lines present the variation of face shapes on this principal component)

Figure 2.7. Representative face models derived by principal component analysis using location of facial landmarks

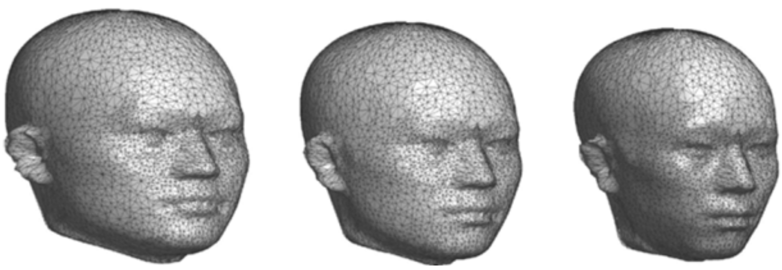

Figure 2.8. Representative 3D head shapes of male Chinese derived by principal component analysis (the face size presents the variation of the face shape of the first principal component)

2.3. Half-Face Respirator Design Methods

Early studies on the half-face respirator design had proposed some facial dimensions which might be related to the respirator design and more recent studies suggested that the 3D face scan images can be more appropriate. As shown in Table 2.3, previous research (Brazile et al., 1998; S. F. Gross & Horstman, 1990; Hack et al., 1973; Han & Choi, 2003; Liau et al., 1982; Oestenstad, Dillion, & Perkins, 1990; Oestenstad & Perkins, 1992; Zhuang, Coffey, & Ann, 2005) suggested some facial dimensions (e.g., face length, face width, nose length, and lip width) related to the respirator fit; however, the identified facial dimensions were different in each study. While some of early studies (S. F. Gross & Horstman, 1990; Hack et al., 1973; Liau et al., 1982) included lip width as importantly applicable to the respirator design, other studies conducted since 1990 indicated that nose-related width dimensions (e.g., nose width, nose protrusion, and nasal root breadth) are more precise for designing respirator size and shape. However, early respirator designs based on the facial anthropometric data needed to be improved in terms of fit and comfort; therefore, some previous

Table 2.3. Suggested facial dimensions related to respirator fit

No.	Reference	Facial dimension related to respirator fit
1	Hack et al. (1973)	face length, face width, lip width
2	Liau et al. (1982)	face width, lip width
3	S. F. Gross and Horstman (1990)	face length, nose length, lip width
4	Oestenstad et al. (1990)	lower-face length (subnasale to menton), biocular breadth, nasal root breadth
5	Oestenstad and Perkins (1992)	face length, lower-face length, biocular breadth, nasal root breadth
6	Brazile et al. (1998)	nose width, nose protrusion
7	Han and Choi (2003)	face width, nose protrusion, bitragion-menton arc
8	Zhuang et al. (2005)	face length, face width, bigonial breadth, nose protrusion

studies' (Cobb, 1972; Lovesey, 1974; Piccus, Smith, Standley, Volk, & Wildes, 1993; Seeler, 1961; Yatapanage & Post, 1992) facial anthropometric data alone would not be appropriately applicable to the respirator design due to the complex shape of the face. Since the 1990s, 3D scan technology has grown and been generalized to anthropometric research and more recent research (Butler, 2009; Dai et al., 2011; Godil, 2009; M. E. Gross et al., 1997; Han et al., 2004; K. Kim, Kim, Lee, Lee, & Kim, 2003; Luximon et al., 2012; Song & Yang, 2010; L. Yang & Shen, 2008; Zhuang, Benson, et al., 2010; Zhuang, Slice, et al., 2010) has tried to introduce respirator design or evaluation methods based on 3D face scan images.

One of the early studies on respirator design using 3D face images, Yatapanage and Post (1992), tried to design a respirator using the average shape of user faces. The 3D face images of 72 Anglo-Saxon males aged 21 to 63 years were scanned by GP-8-3D 3D sonic digitizer (Science Accessories Corp., U.S.A.). The 3D face images, composed of around 400 points in a grid-like pattern (Figure 2.9a), were aligned based on sellion landmarks, and an average and variance among the 3D face images were derived. Then, a fit contour was identified following minimum variance among participants at each facial grid as shown in Figure 2.9b. Finally, one size respirator shape as shown in Figure 2.9c was created based on the fit contour. However, the suggested respirator design was

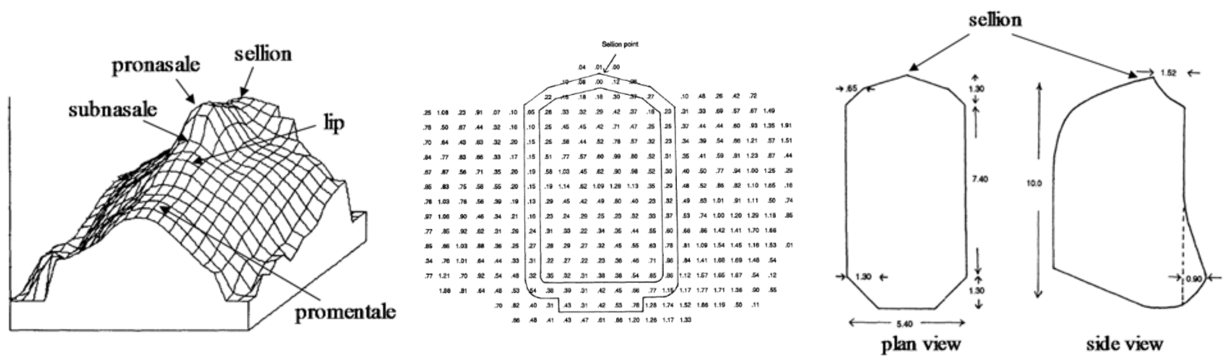

(a) Average shape of 3D face composed of 400 points in a grid-like pattern

(b) Variance values among participants at each facial area and the optimum fit contour.

(c) Shape of the optimum respirator designed to fit the participants (plan view)

Figure 2.9. Respirator design method based on average shape of participants

irrational in terms of their width (54 mm) due to less consideration about respirator design characteristics and respirator wearing characteristics.

M. E. Gross et al. (1997) redesigned an initial MBU-20/P oxygen mask based on 3D face images of the USAF pilots. The initial shape of the MBU-20/P was generated based on MBU-12/P, the previous version of the MBU-20/P, which was designed based on 1967-1968 USAF survey data. 3D face images (Figure 2.10a) of 60 randomly selected USAF pilots (30 males and 30 females) were used to the design revision. And, the 3D face images and 3D mask scan images were virtually aligned (Figure 2.10c) by referring 3D images of the face with the oxygen masks (Figure 2.10b). Then, an average fit contour of the oxygen mask (Figure 2.10d) was extracted by analyzing the virtually aligned images. Finally, eight mask design landmarks (Figure 2.10e) for drawing an oxygen mask seal shape were identified based on fit contour, and then the MBU-20/P design was improved based on those mask design landmarks. However, this research did not present a statistical consideration of sample size, a detailed process about the oxygen mask redesign, and a usability evaluation for the revised design.

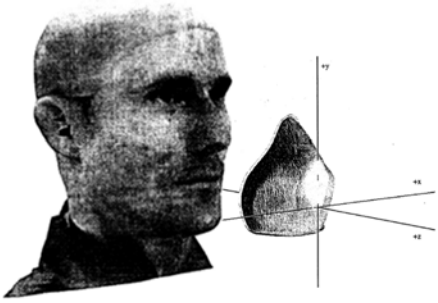

(a) 3D scan data of face and oxygen mask

(b) 3D scan data of face with the oxygen mask

(c) Virtual alignment of oxygen mask on the 3D face

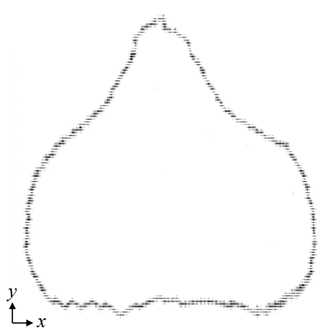

(d) Average fit contour extracted from 3D face scan images

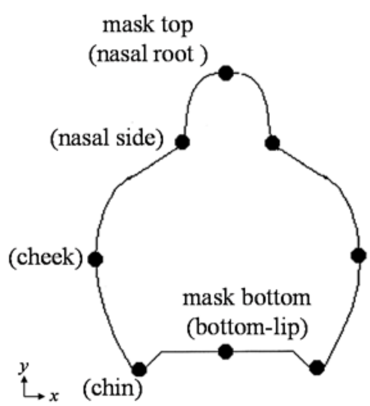

(e) Eight design landmarks to draw an oxygen mask shape

Figure 2.10. Pilot oxygen mask design method based on 3D face scan data and virtual fit analysis

Han et al. (2004) proposed an industrial respirator design process based on 3D face images of RMFs. Korean fit test panels (Han, 1999) as shown in Figure 2.4c were applied to select 50 Korean civilians (26 males and 24 females). Then, three RFMs who represented size groups (small, medium, large) were chosen based on their anthropometric measurements, and their faces were fabricated using clay (Figure 2.11a). Detailed dimensions of the clay faces were manually modified by referring to average values of facial dimensions. The clay faces were 3D scanned (Figure 2.11b) and applied to the respirator design (Figure 2.11c). Furthermore, Song and Yang (2010) fabricated an average size clay head (Figure 2.12a) based on 1,536 Korean male civilians aged 20 ~ 59 years measured in the 2004 Size Korea anthropometric survey (KATS, 2004). The clay head was scanned in 3D, and then the oral-nasal area of the 3D face (Figure 2.12b) was extracted to apply to the respirator design. Finally, the respirator prototype was manufactured as shown in Figure 2.12c. However, neither study explained the detailed processes of the design of a respirator faceseal shape, a usability testing with respirator users, and considerations about representativeness of RFMs used in their research.

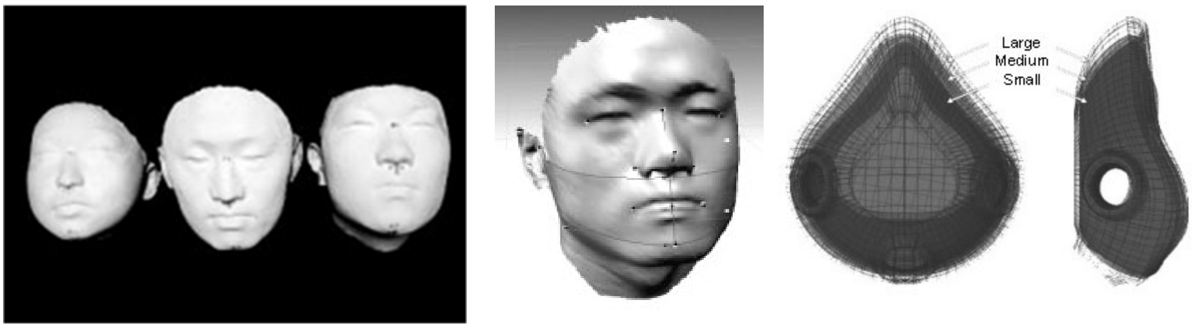

(a) Three size face models generated based on respirator fit test panel for Koreans

(b) 3D scan image of a clay model

(c) Respirator shapes designed based on 3D face model

Figure 2.11. Respirator design method based on three sizes of 3D face images

(a) Single size face model generated based on Size Korea facial measurements

(b) 3D scan image of a clay model

(c) Prototype of respirator

Figure 2.12. Respirator design method based on average size of 3D face image

2.4. Respirator Fit Test

2.4.1. Experimental Fit Evaluation

Several qualitative and quantitative respirator fit test methods were proposed to check infiltration of harmful air into the respirator, but they lack measurement of pressure caused from the respirator fit to the face. External air can be leaked into a respirator through a faceseal, an air-purifying element, an exhalation valve, or cracked part (Han & Lee, 2005; Kolear, Cosgrove, de la Barre, & Theis, 1982; Myers, 2000). Assuming there are no defects in the respirator parts, a faceseal fit performance is important to protect the user's health and life from a hazardous atmosphere (Han & Lee, 2005; NIOSH, 1987; J. Yang, Dai, & Zhuang, 2009). In the case of the U.S.A., therefore, American National Standards Institute (ANSI), Occupational Safety and Health Administration (OSHA), and the NIOSH present standards including the respirator fit test guidelines to the respirator manufacturing industries (Han et al., 1997). Previously, many studies proposed several qualitative and quantitative methods for the respirator fit test as illustrated in Figure 2.13 (Coffey, Lawrence, & Myers, 2002; Han et al., 1997; Kolear et al., 1982). Qualitative fit testing methods use aerosols (e.g., isoamyl acetate, sodium saccharin, and irritant fume) on a participant, and the participant subjectively evaluates whether the aerosol is detected by breathing. Quantitative fit testing methods use equipment to detect density of aerosol both inside and outside of a respirator (e.g., flame photometric aerosol measurement method, condensation nuclei count method, and particle penetration method) or to measure flow or pressure of leaked air (e.g., leak flow measurement method and leak and cartridge flow measurement method). The present research proposed respirator fit test methods to identify infiltration or leakage of air. An experimental fit testing method for the respirator pressure evaluation is required to design a respirator shape which can provide better fit and comfort to users.

(a) Qualitative fit testing based on aerosol

(b) Quantitative fit testing system, PORTACOUNT PRO+ Respirator Fit Tester 8038 (TSI Inc., U.S.A.)

Figure 2.13. Qualitative and quantitative respirator fit testing

2.4.2. Virtual Fit Evaluation

Recent studies have proposed virtual evaluation methods for respirator fit (e.g., fit, pressure, interference, and clearance) to the face. Through the virtual fit evaluation method, 3D images of the human body part and product can be virtually aligned to analyze their fit, pressure, and/or interference (Ashdown, Loker, Schoenfelder, & Lyman-Clarke, 2004; Bye & McKinney, 2010; Meunier, Tack, Ricci, Bossi, & Angel, 2000). The virtual fit evaluation method has been mostly applied to wearable products such as clothing, shoes, headwear, and respirators. Meanwhile, the FEM methods was used for respirator fit evaluation (Butler, 2009; Dai et al., 2011; Lei et al., 2012; J. Yang et al., 2009). Bitterman (1991) and Piccione and Moyer Jr. (1997) analyzed the MBU-20/P oxygen mask and a full-face gas filtering mask, respectively, through the FEM (Figure 2.14). The FEM can quantitatively visualize pressure or the interference of a respirator at the facial area by detecting a deformation of facial skin and mask.

Dye to technological advancement in 3D scanning, CAD, and FEMs, virtual respirator fit evaluation methods based on large amounts of 3D point cloud data and FEM systems were proposed for better analysis of a respirator fit; however, those results have not been applied to the respirator design yet. Butler (2009), Dai et al. (2011), and Lei et al. (2012) introduced virtual evaluation methods to identify respirator fit (e.g., fit, pressure, air leakage, and air flow) considering the material properties of a respirator and characteristics of facial skin by using commercial FEM simulation software. For example, Butler (2009) introduced the virtual fit evaluation cases for the full- and half-face respirator using CFD-ACE+ and CFD-GEOM (ESI Group, France) FEM software (Figure 2.15). Pressure of respirator to the face, pressure of exhalation air to the respirator, interior flow of air, and air leakage were identified by this simulation. J. Yang et al. (2009), Dai et al. (2011), and Lei et al. (2012) analyzed respirator fit characteristics depending on pressure of the respirator, location and

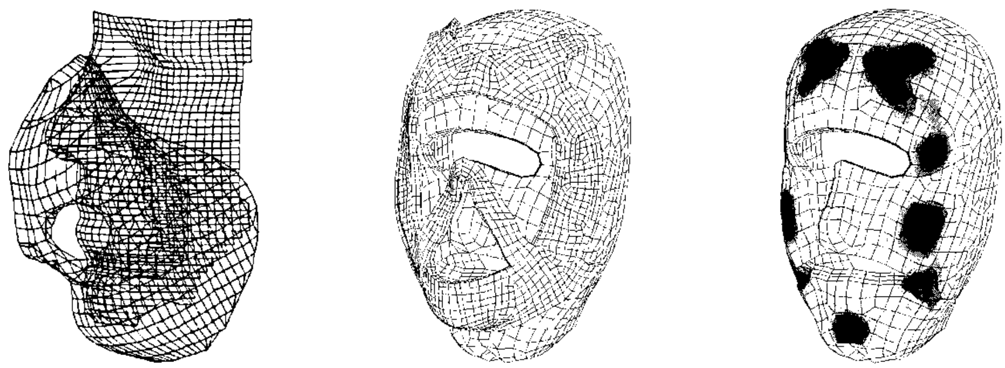

(a) 3D alignment between face and initial design of MBU-20/P pilot oxygen mask (Bitterman, 1991)

(b) 3D alignment between face and M40 full-face gas filtering mask considering mask and skin deformation (left) and a result of pressure analysis (right) (Piccione & Moyer Jr., 1997)

Figure 2.14. Early studies on virtual respirator fit evaluation based on finite element modeling (FEM)

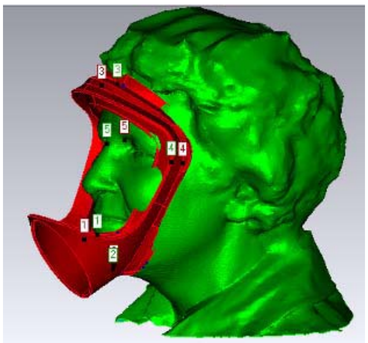

(a) 3D alignment between face and full-face mask

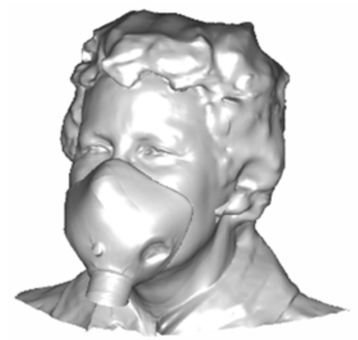

(b) 3D alignment between face and half-face mask

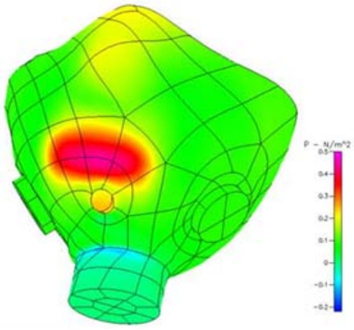

(c) Pressure of air during exhalation

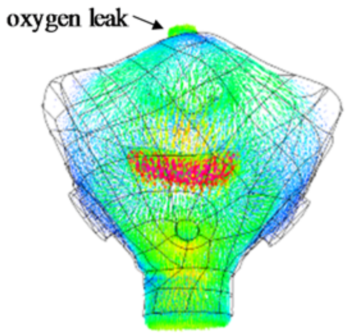

(d) Flow and pressure of air during oxygen leakage situation

Figure 2.15. Virtual respirator fit evaluation based on CFD-ACE+ and CFD-GEOM FEM system

tension direction of straps, and material properties and friction factors of the respirator by using LS-DYNA (Livermore Software Technology Corp., U.S.A.) FEM software (Figure 2.16). The proposed virtual fit evaluation methods based on the FEM can be applied to the evaluation of respirator design. However, the proposed methods are still on a trial, and further considerations are required in terms of respirator wearing characteristics (e.g., wearing position and wearing force), diversity of human face shapes, validity of FEM analysis, and applicability to the respirator design.

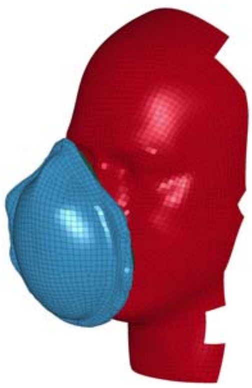

(a) Virtual alignment between mask and face

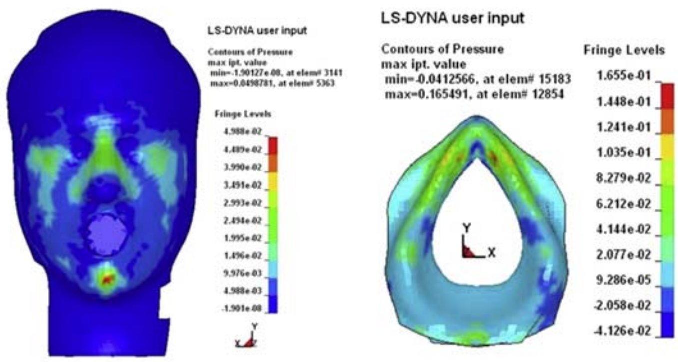

(b) Pressure analysis through virtual fit evaluation

Figure 2.16. Virtual respirator fit evaluation based on LS-DYNA FEM system

Chapter 3. FACE-MASK INTERFACE (FMI) ANALYSIS

3.1. Face-Mask Interface Model

The FMI model consists of four FMI factors: the facial anthropometric characteristics, oxygen mask design dimensions, oxygen mask wearing characteristics, and preferences of the pilots as shown in Figure 3.1. First, design problems of the pilot oxygen mask were identified through a survey of preferences collected from the KAF pilots. Then, the oxygen mask design dimensions related to the oxygen mask design problems were examined, and the facial anthropometric characteristics required for the oxygen mask design were analyzed. Lastly, the oxygen mask wearing characteristics were investigated to identify how the oxygen mask fit to a pilot's face.

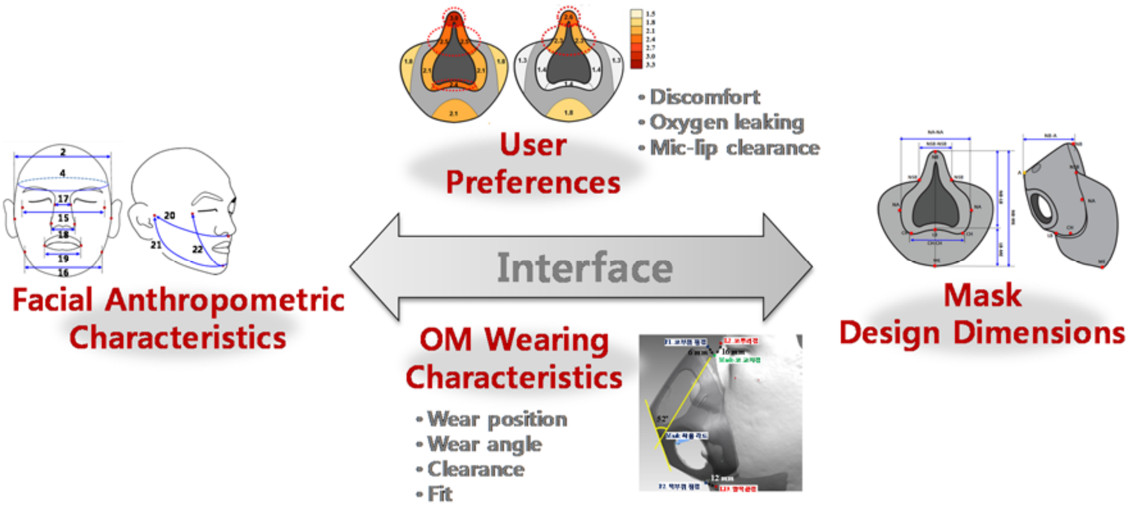

Figure 3.1. Face-mask interface model

3.2. Oxygen Mask User Preferences

3.2.1. Survey Method of User Preferences

The preferences for the MBU-20/P pilot oxygen mask were surveyed by the KAF pilots in terms of discomfort, oxygen leakage, slippage, and contact between the microphone and lip. A questionnaire (Figure 3.2, Appendix A) was prepared by referring to the *combat edge fit assessment questionnaire* proposed by M. E. Gross et al. (1997). Six facial areas (nasal root, nasal side, zygomatic bone, cheek, bottom lip, and chin) were evaluated, respectively, in terms of discomfort (1 = no discomfort,

MBU-20/P 산소 Mask의 설계 적합성 평가 설문지

- 본 설문 평가는 **MBU-20/P 산소 mask 개선 설계**를 위한 기초자료로 사용될 예정입니다.
- 설문 평가 예상 **소요 시간은 약 5분** 입니다.
- 본 설문에 기재된 신상 정보 및 설문 결과는 본 연구의 분석을 위해서만 사용될 것입니다.
- 연구 수행 기관: 포항공과대학교 산업경영공학과
  공군사관학교 시스템공학과/기계공학과
  경북대학교 의류학과

Ⅰ. 기본 정보

1. 이름: ______________ 2. 생년월일: ________ 년 ____ 월 ____ 일

3. 본인 착용 산소 mask size (mask 하단부 표기 사항 참고)

☐ Extra Small Narrow ☐ Small Narrow ☐ Medium Narrow ☐ Medium Wide ☐ Large Wide

4. 현재 MBU-20/P 수령 이후 비행시간: _______ 시간

Ⅱ. 산소 Mask 적합성 평가

Ⅱ-1. 착용 안락감 (comfort)

1. 아래 그림을 참고하여 산소 mask 각 부위별 압박에 따른 불편감에 대해 표시해 주세요.

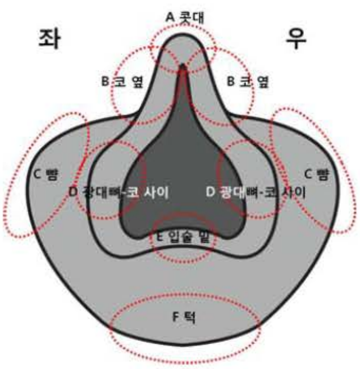

부 위	불편 없음 (comfortable)	조금 불편 (slightly uncomfortable)	불편 (moderately uncomfortable)	매우 불편 (very uncomfortable)	극히 불편 (hot spot)
A: 콧대	☐	☐	☐	☐	☐
B: 코 옆	☐	☐	☐	☐	☐
C: 뺨	☐	☐	☐	☐	☐
D: 광대뼈-코 사이	☐	☐	☐	☐	☐
E: 입술 밑	☐	☐	☐	☐	☐
F: 턱	☐	☐	☐	☐	☐

Figure 3.2. Questionnaire for surveying user preferences

5 = extreme discomfort) caused by pressure of the oxygen mask and oxygen leakage (1 = no leakage, 4 = excessive leakage) due to lack of fit of the oxygen mask to the face. Also, a slippage of oxygen mask (1 = no slippage, 4 = excessive slippage), contact between the microphone and lip (contacted or not contacted), and subjective opinions about the MBU-20/P pilot oxygen mask were surveyed. 490 KAF pilots (483 males and 7 females) who currently wear the MBU-20/P participated in the survey. Their age was 29.9 ± 4.1 (24 to 47 years old), and the size of oxygen mask was distributed as XSN = 0.5%, SN = 14.4%, MN = 52.0%, MW = 18.1%, and LW = 15%. The survey was conducted from December 2010 to January 2011.

3.2.2. Results

In terms of the discomfort, 68% of the KAF pilots answered with a discomfort score ≥ 3 at least one facial area, and higher discomfort particularly occurred at the nasal root, nasal side, and bottom lip. Regardless of the facial areas, the highest discomfort scores were distributed as no discomfort = 5.8%, slight discomfort = 25.9%, moderate discomfort = 32.8%, very discomfort = 26.7%, and extreme discomfort = 8.8% as shown in Figure 3.3a. The pilots had relatively higher discomfort at the nasal root (score = 3.0), nasal side (score = 2.5), and bottom lip (score = 2.4) as shown in Figure 3.3b. The discomfort at the nasal root and nasal side was caused by an excessive fit of the oxygen mask to the face; however, the discomfort at the bottom lip might have occurred by the lip coming into contact with a reflective seal on the facepiece.

In terms of the oxygen leakage, 41% of the KAF pilots replied that the oxygen leakage ≥ 3 at least one facial area, and much oxygen leakage was caused at the nasal root and nasal side in particular. Regardless of the facial areas, the highest scores for the oxygen leakage were distributed as

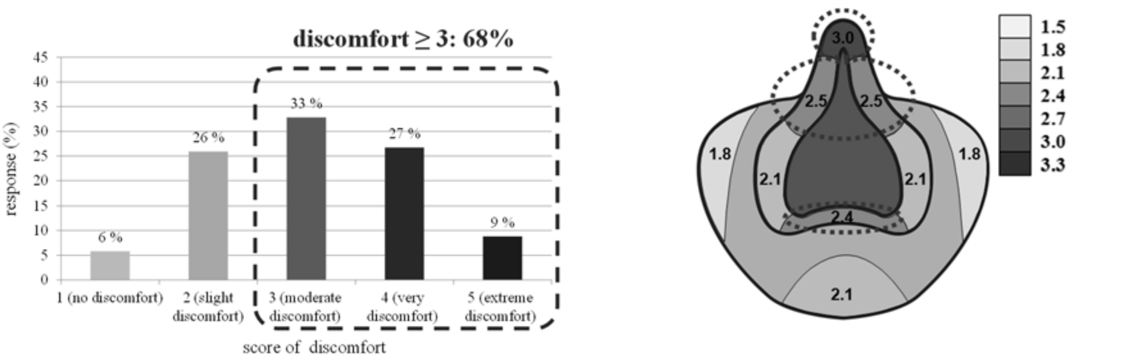

(a) Distribution of the highest score (b) Average discomfort score by facial area

Figure 3.3. User preference about discomfort

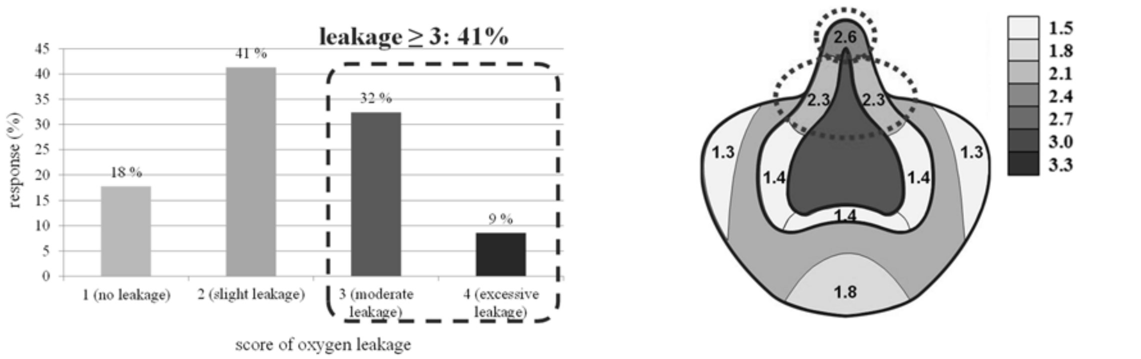

(a) Distribution of the highest score (b) Average oxygen leakage score by facial area

Figure 3.4. User preference about oxygen leakage

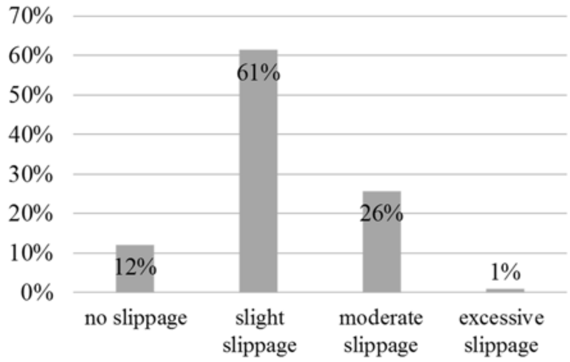

(a) Result of slippage

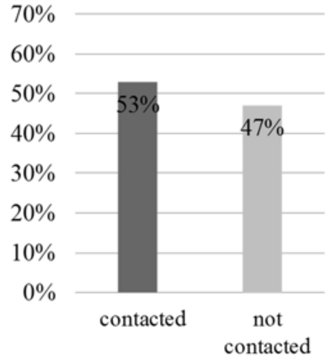

(b) Result of microphone-lip contact

Figure 3.5. User preference about slippage and microphone-lip contact

no leakage = 17.7%, slight leakage = 41.3%, moderate leakage = 32.4%, and excessive leakage = 8.6% as shown in Figure 3.4a. The pilots felt the greatest amount of leakage at the nasal root (score = 2.6) and nasal side (discomfort = 2.3) as shown in Figure 3.4b.

The oxygen mask slippage due to the lack of fit and the contact between the microphone and lip was identified as shown in Figure 3.5. The scores for the oxygen mask slippage were distributed as no slippage = 12%, slight slippage = 61%, moderate slippage = 26%, and excessive slippage = 1%. 53% of the KAF pilots answered that the microphone in the oxygen mask contacted their lip.

3.3. Pilot Oxygen Mask Design Dimensions

3.3.1. Measurement Method of Mask Design Dimensions

The design dimensions of the facepiece and hardshell were identified using a 3D digitizer based on the oxygen mask design landmarks identified by M. E. Gross et al. (1997) who proposed sizes of the MBU-20/P pilot oxygen mask. The Immersion MicroScribe® 3D Digitizer (Revware Inc., U.S.A.) as shown in Figure 3.6 was used to measure the design dimensions of the facepiece and hardshell. Nose-to-chin length, nose width, chin width, and maximum width were selected for the oxygen mask design dimensions (Figure 3.7). Among four dimensions, the nose-to-chin length and maximum width are related to the oxygen mask sizes (e.g., SN, MN, MW, and LW). The hardshell was measured based on the eight MBU-20/P design landmarks proposed by M. E. Gross et al. (1997), and the facepiece was measured based on the eight corresponding design landmarks defined by referring to the hardshell landmarks in the present study.

Figure 3.6. Immersion MicroScribe® 3D Digitizer

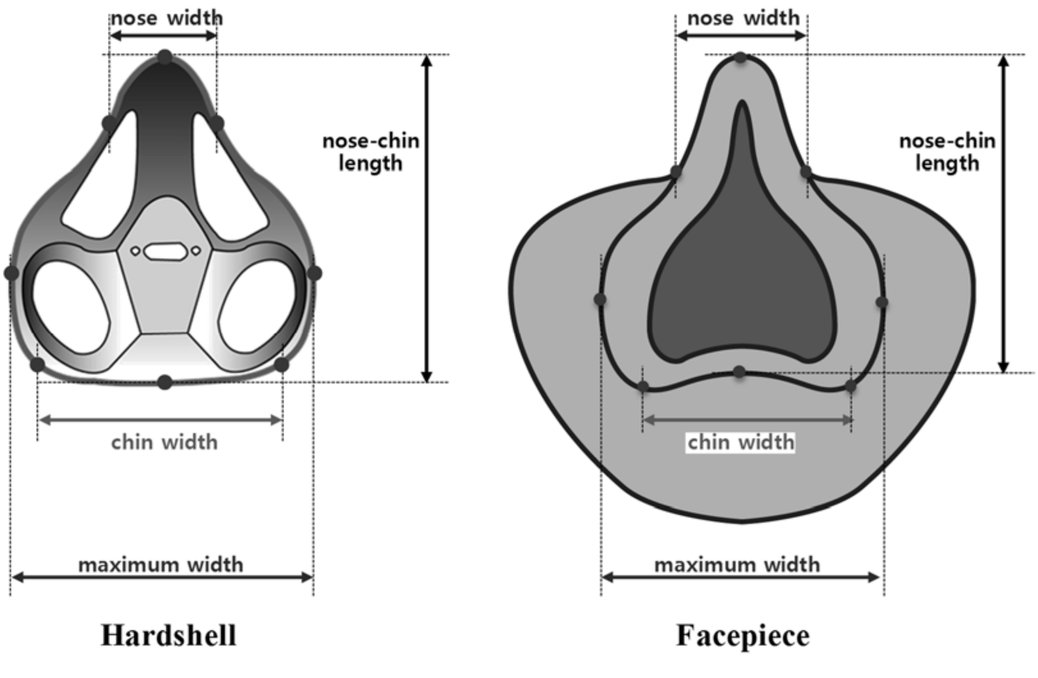

Figure 3.7. Design dimensions of facepiece and hardshell based on design landmarks

3.3.2. Results

The existing oxygen mask was found to have low design rationality due to inconsistent intervals between sizes. Nose-to-chin length of the facepiece were categorized as small (SN) = 94 mm, medium (MN & MW) = 100 mm, and large (LW) = 114 mm. However, corresponding intervals between sizes (medium – small = 6 mm, but large – medium = 14 mm) was inconsistent (Figure 3.8a). Nose-to-chin length of the hardshell also showed similar results with those of the facepiece. Width dimensions of the facepiece and hardshell were similar between wide sizes (MW and LW); however, the dimensions of the SN were wider than the MN and even similar to the wide sizes as shown in Figure 3.8b and c. Therefore, the existing oxygen mask can be described as having less consistency and low design rationality in terms of intervals between sizes.

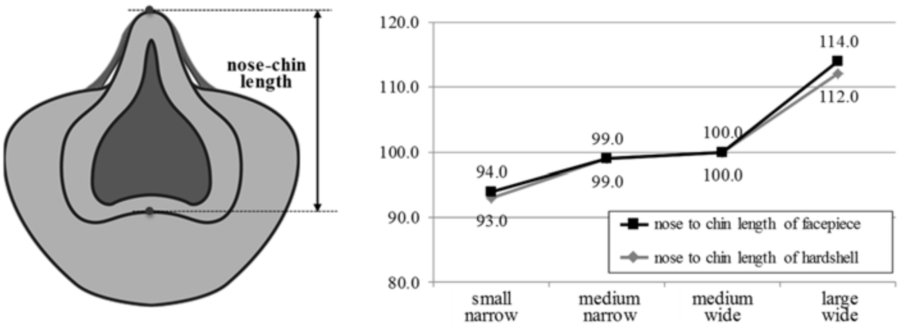

(a) Nose-to-chin length of facepiece and hardshell

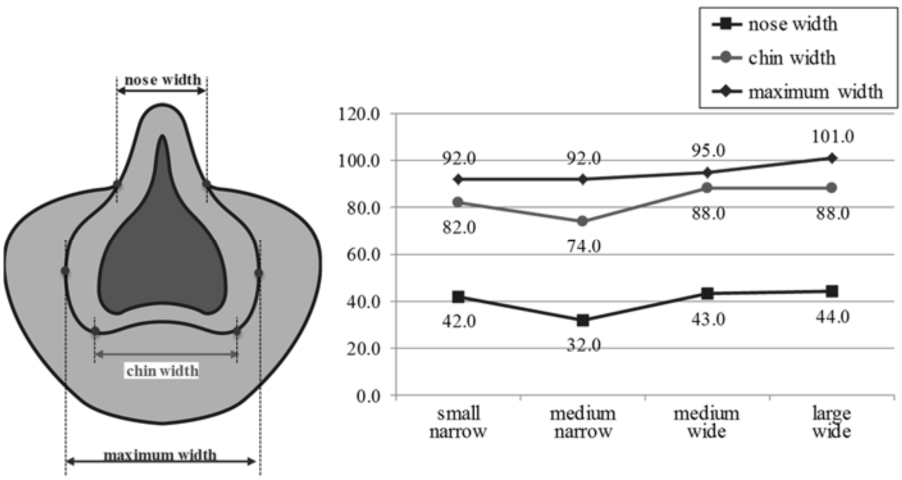

(b) Width dimensions of facepiece

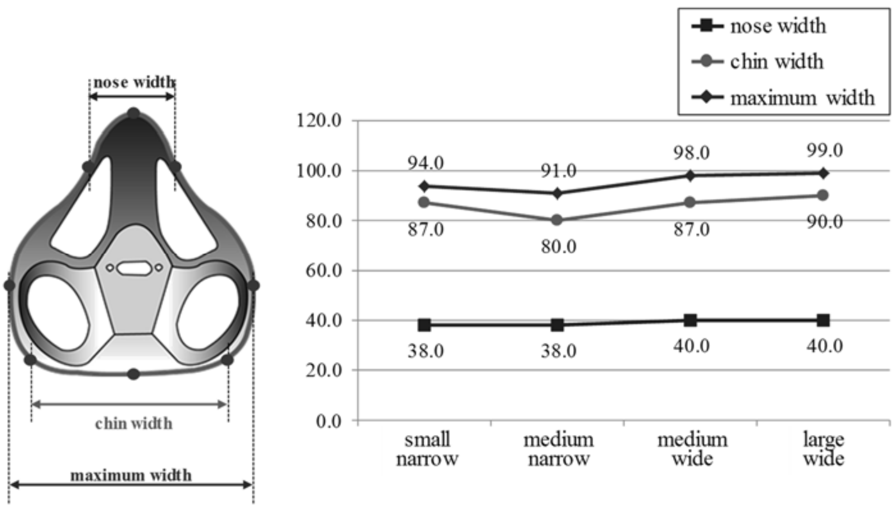

(c) Width dimensions of hardshell

Figure 3.8. Measurements of design dimensions for 4 sizes

3.4. Pilot’s Anthropometric Facial Characteristics

3.4.1. Measurement Method of Face

Selection of Facial Dimensions

For the design of an oxygen mask, 22 facial dimensions were selected through a review of literature and the recommendation of a panel of experts. Fifteen journal papers (Ahn & Suh, 2004; Alexander et al., 1979; Clauser, Tebbetts, Bradtmiller, McConville, & Gordon, 1988; Hack & McConville, 1978; Han & Choi, 2003; Hughes & Lomaev, 1972; S. Kim, 2004, 2005; S. Kim, Lee, & Choi, 2004; KATS, 2004; Oestenstad et al., 1990; Oh & Park, 2010; Yokota, 2005; Zhuang & Bradtmiller, 2005) were reviewed which measured facial dimensions for the design of a half-face mask (Table 3.1). Through the literature review, 107 facial dimensions (length dimensions: 45; depth dimensions: 24; width dimensions: 17; circumference/arc dimensions: 21) were identified (Appendix B.1). Of these facial dimensions, 22 dimensions (length dimensions: 9; depth dimensions: 2; width dimensions: 7; circumference/arc dimensions: 4) were selected by a panel of three ergonomists and three clothing experts as those applicable to the design of an oxygen mask and their importance in designing an oxygen mask was classified into one of three categories (low, medium, and high) as shown in Figure

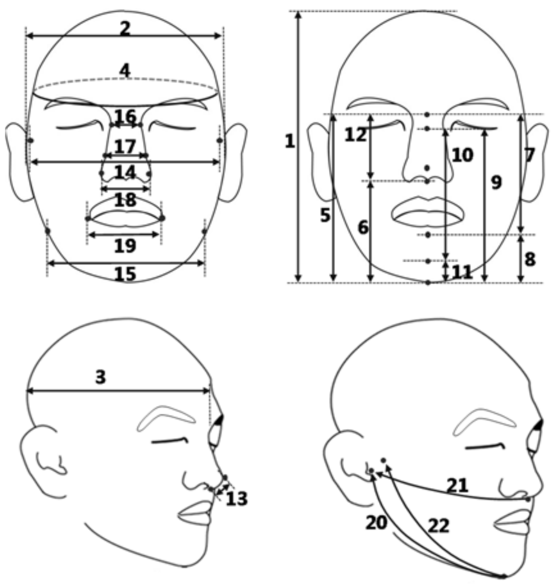

	Face dimensions	Importance (L: low; M: medium; H: high)
1	head height	L
2	head breadth	L
3	head length	L
4	head circumference	L
5	face length	H
6	lower-face length	M
7	sellion-to-supramentale length	M
8	supramentale-to-menton length	L
9	rhinion-to-menton length	M
10	rhinion-to-promentale length	H
11	promentale-to-menton length	L
12	nose length	M
13	nose protrusion	M
14	face width	M
15	chin width	L
16	nasal root breadth	H
17	maximum nasal bridge breadth	H
18	nose width	H
19	lip width	H
20	bitragion-menton arc	L
21	bitragion-subnasale arc	L
22	bizygomatic-menton arc	L

Figure 3.9. Facial dimensions and their importance for design of a pilot oxygen mask

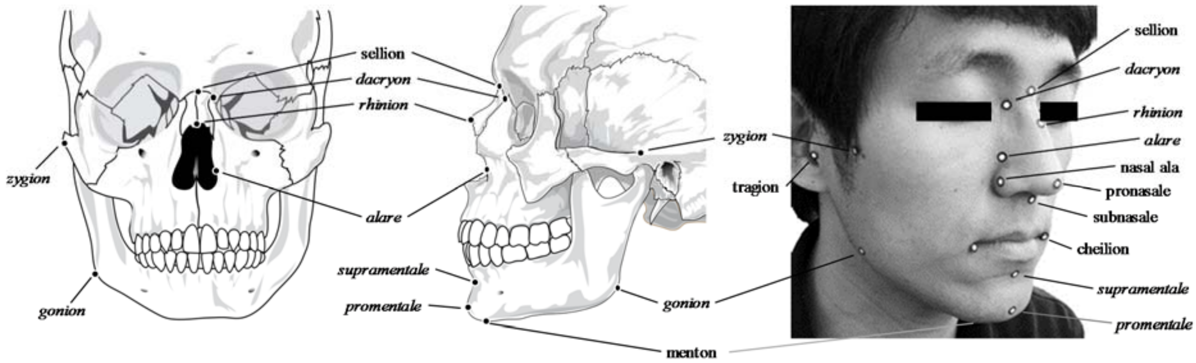

Figure 3.10. Facial landmarks for measurement of facial dimensions

3.9 and appendix B.2. For measurement of the selected facial dimensions, 14 landmarks (Figure 3.10 and appendix B.3) were identified by referring to Alexander et al. (1979), Buikstra and Ubelaker (1994), Clauser et al. (1988), Hack and McConville (1978), and Young (1966).

Participants

336 KAF male pilots (KMP) and KAF female pilots and cadets (KFP) were measured in the present survey. The minimum sample size requirement of each facial dimension was identified by considering the age distribution of KAF pilots and applying the Korean civilian data (KATS, 2004) to Equation 1 (ISO, 2006):

$$n = (1.96 \times \frac{CV}{k})^2 \times 1.534^2 \qquad \text{(Equation 1)}$$

where: CV = coefficient of variation,
k = precision level

The sample mean and sample standard deviation (SD) of a facial dimension of the KAF pilot population mixed in gender and age were estimated by applying corresponding Korean citizen data to Equations 2 and 3, respectively:

$$\overline{X} = \frac{\sum_{i=1}^{j} \overline{X}_i \times n_i}{\sum_{i=1}^{j} n_i} \qquad \text{(Equation 2)}$$

where: $\overline{X}$ = sample mean of a composite population,
$\overline{X}_i$ = sample mean of population i,
n_i = sample size of population i,
j = the number of population

Table 3.1. Reviewed references for oxygen mask design in this study

No.	Reference (A to Z)	Population	Survey year	Sample size	Age	No. of dimensions	Purpose of survey	Measurement method
1	Ahn and Suh (2004)	Korean civilians	2003	F: 285	18 ~ 35	67	application to develop tightly fitted headwear for Korean woman	DM
2	Alexander et al. (1979)	U.S. Air Force	1967 ~ 1968	M: 2,420	21 ~ 50	48 out of 182 whole body dimensions	application to development of face forms for the sizing and design of half-face oxygen masks	DM
3	Clauser et al. (1988)	U.S. Army	1987 ~ 1988	M: 8,997	25 ~ 40	16 out of 132 whole body dimensions	application to guide the design and sizing of clothing and personal protective equipment and the design and layout of military workstations	DM
4	Hack and McConville (1978)	U.S. workers	1970s	M: 200	n.s.	21	development of the respirator test panels representing a major of the U.S. working population	DM
5	Han and Choi (2003)	Korean civilians	n.s.	M: 26 F: 24	20 ~ 50	10	analysis of the relationship between facial dimensions and the fit factors of half-face respirators for designing respirators for Korean workers	DM
6	Hughes and Lomaev (1972)	Australian civilians	n.s.	M: 538	15 ~ 80	8	application to design respirator for an industrial or a general population of Australia	DM
7	S. Kim (2004)	Korean children	2004	F: 269	9 ~ 12	28	obtaining the fundamental measurement data of the head and face for Korean children and shape classification for the headwear sizing systems	DM
8	S. Kim (2005)	Korean children	2004	F: 419	9 ~ 12	19		DM
9	S. Kim et al. (2004)	Korean children	2004	M: 241	9 ~ 12	31		DM
10	KATS (2004)	Korean civilians	2003 ~ 2004	M: 7,050 F: 7,150	0 ~ 70s	40 out of 206 whole body dimensions	obtaining high-quality anthropometric data including 3D body scan data of Koreans to establish the anthropometric database to design products and systems which appropriate to Koreans	DM & SM
11	Oestenstad et al. (1990)	U.S. civilians	n.s.	M: 73	21 ~ 50	12	analysis of characteristics of the facial dimensions which affect faceseal leaks	DM
12	Oh and Park (2010)	Korean Army	n.s.	F: 93 M: 408	25±3.3	10	application to design gas filtering mask for Korean Army personnel	SM
13	Yokota (2005)	U.S. Army	n.s.	M: 2,043	18 ~ 35	13	analysis of multivariate craniofacial anthropometric distributions between biologically admixed populations or single racial populations of U.S. Army males	DM
14	Young (1993)	U.S. civilians	1960s ~ 1990s	F: 195 M: 172	17 ~ 69	22	application to develop protective equipment for the head and face	DM
15	Zhuang and Bradtmiller (2005)	U.S. workers	2003	M: 2,543 F: 1,454	18 ~ 66	19	development of an anthropometric database of respirator users and use the database to establish fit test panels to be incorporated into the NIOSH's respirator certification and international standards	DM & SM

DM: direct measurement, SM: 3D scan measurement
n.s.: not specified on the reviewed material

$$s = \sqrt{\frac{n_1 \times \overline{X}_1^2 + (n_1 - 1) \times s_1^2 + n_2 \times \overline{X}_2^2 + (n_2 - 1) \times s_2^2 - (n_1 + n_2) \times \overline{X}^2}{n_1 + n_2 - 1}}$$

$$\cong \sqrt{p_1 \times \left(\overline{X}_1^2 + s_1^2\right) + p_2 \times \left(\overline{X}_2^2 + s_2^2\right) - \overline{X}^2} \qquad \text{(Equation 3)}$$

where: s = sample SD of a composite population,
$\overline{X}$ = sample mean of composite population,
$\overline{X}_i$ = sample mean of population i,
s_i = sample SD of population i,
n_i = sample size of population i,
p_i = proportion of population i,
j = the number of population

Of the 22 facial dimensions, 10 dimensions (head height, head breadth, head length, head circumference, face length, lower face length, nose length, nose protrusion, nose width, and lip width) were measured in the 2004 Size Korea anthropometric survey (KATS, 2004). The minimum sample size requirements of the facial dimensions were calculated for two levels of precision (k = sampling error/sample mean = 3% and 4%) as shown in Figure 3.11. Lastly, the sample size for the facial anthropometric survey on KAF pilots in the present study was determined by the prioritized facial dimensions, sample size requirement analysis results, and sampling errors (SEs). The SEs of the four high-importance facial dimensions (face length, rhinion-to-promentale length, nose width, and lip width) measured in the Korean national anthropometric survey were further calculated as shown in Table 3.2 for k = 3% and 4%. It was agreed upon by the expert panel in the present study that k = 3%

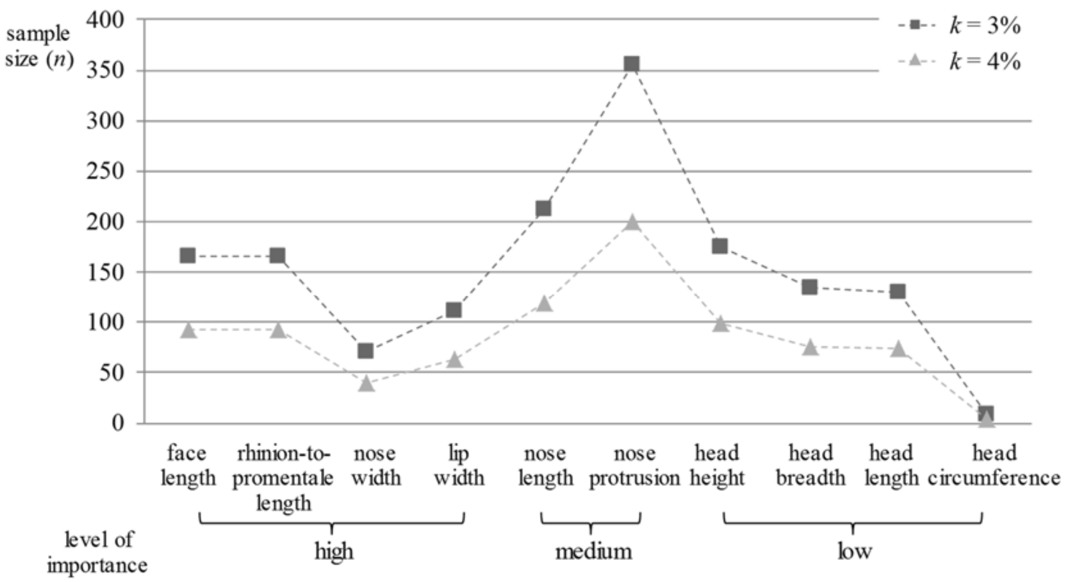

Figure 3.11. Minimum sample size requirements by precision (k) for face anthropometric survey

Table 3.2. Maximum sampling error (SE; unit: mm) and minimum sample size (n) according to the level of precision (k) for the 4 facial dimensions highly relevant to designing oxygen masks

Precision (*k*)	Category	Face length	Rhinion to promentale length	Nose width	Lip width	Max.
3%	SE	3.4	1.9	1.2	1.5	3.4
	min. *n*	166	165	72	122	166
4%	SE	4.5	2.5	1.6	1.9	4.5
	min. *n*	93	93	40	63	93

(maximum SE = 3.4 mm in face length) is acceptable in oxygen mask design, resulting in n = 166 as the minimum sample size of the facial anthropometric survey. However, 278 KMPs and 58 KFPs were measured during the available study period to apply facial data to various applications and accommodate a change in the gender composition of the KAF pilot population in the future.

Measurement Protocol

Direct and 3D measurement methods were used to measure the facial dimensions. The face measurement process consisted of four phases: (1) orientation of the study purpose and measurement process; (2) attachment of stickers to the designated landmark locations on the face; (3) direct measurement using a Martin-type anthropometer; and (4) 3D measurement using a 3D scanner. In the orientation phase, the purpose and process of face measurement were explained to the participant. In the landmarking phase, the landmarks (Figure 3.10) were marked using stickers. In the direct measurement phase, four facial dimensions (head height, head breadth, head length, and head circumference) were measured using a Martin-type anthropometer. Lastly, in the 3D measurement phase, the face was captured using a Rexcan 560 (Solutionix Co., South Korea) 3D scanner and then the face scan was processed using the ezScan (Solutionix Co., South Korea) image processing program. The face was captured in a darkroom tent (150 cm × 150 cm × 200 cm, Figure 3.12) for a proper contrast to obtain 3D scan images with high quality. The face was scanned at five different positions (front, 30° and 60° degrees to the left and to the right).

Figure 3.12. Face capturing in a darkroom

After 3D facial scans were post-processed in five phases (alignment, merging, editing, landmark refinement, and measurement extraction; Figure 3.13) using the ezScan software, the facial dimensions were measured using a program developed in the present study. In the alignment and merging phases, the five facial images of the participant scanned at different angles were aligned and merged. In the editing phase, the merged 3D facial image was edited by applying hole-filling, smoothing, and abnormal surface cleaning functions provided by the image processing software. In the landmark refinement phase, landmarks which were not captured during 3D scanning or lost in the alignment and merging phases were marked manually. After the image post-processing was completed, a program developed with Matlab 2008a (MathWorks, Inc., U.S.A.) in the study was used to automatically measure the facial dimensions that were not measured by the direct measurement method. Of the facial dimensions, length and width dimensions were measured by calculating Euclidian distances between corresponding landmarks, and arc dimensions were measured by creating a virtual plane passing corresponding three landmarks and forming the arc which intersects the plane and the facial image. Figure 3.14 illustrates that the lip width is measured by calculating the Euclidian distance between the left and right cheilions and the bitragion-menton arc by measuring the length of the arc intersecting the facial image and the cross-sectional plane passing the left tragion, menton, and right tragion.

The integrity of facial measurements using 3D facial scans was assured by an outlier checking process. Measurements of each facial dimension exceeding the range of mean $\pm$ 3SD were examined and repeated measurement was made for accuracy.

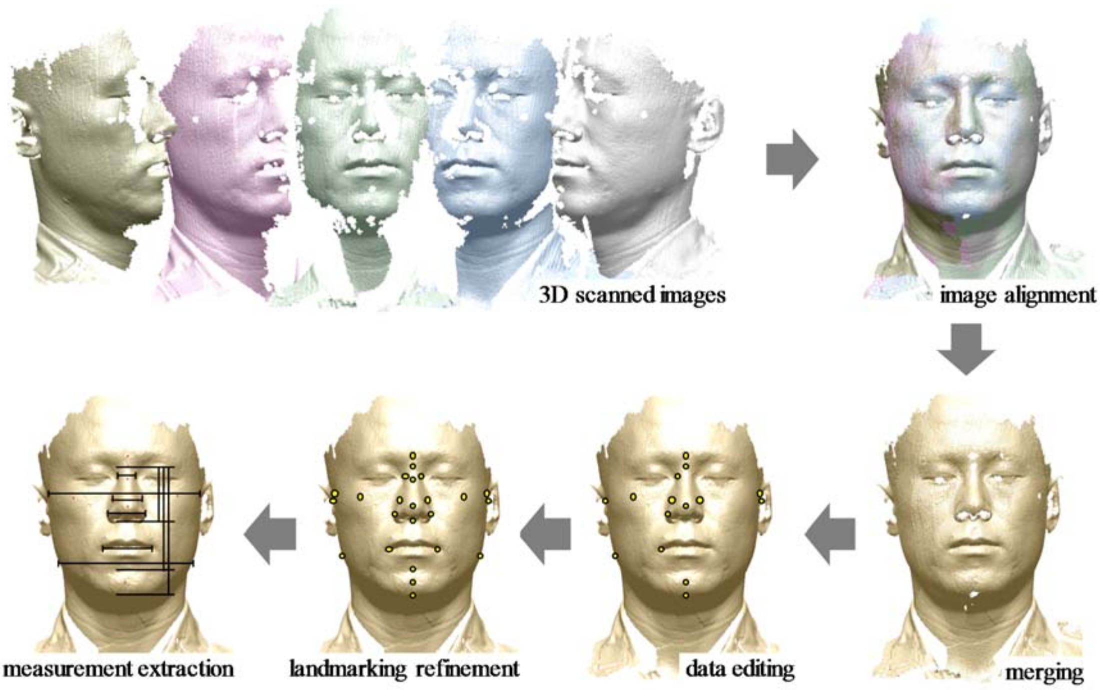

Figure 3.13. Post-processing of 3D face scan images

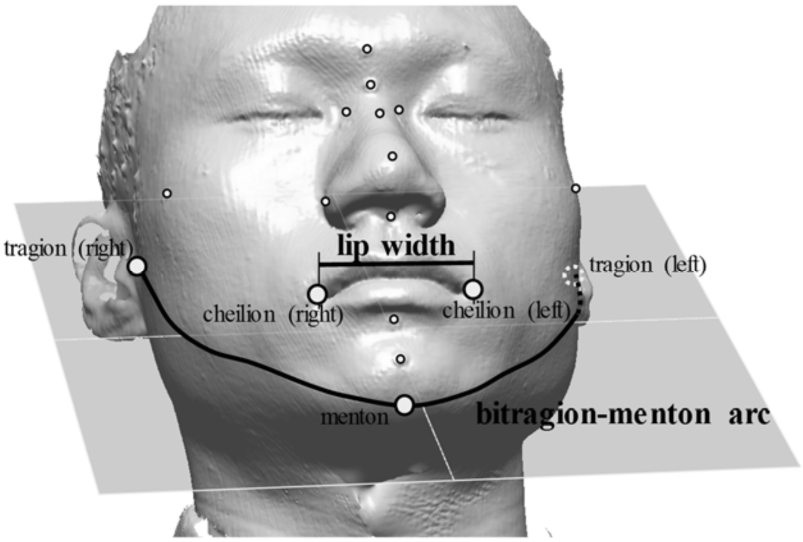

Figure 3.14. Illustration of face dimension measurement: lip width and bitragion-menton arc

The facial measurements of KAF pilots were compared with those of Korean civilians (KATS, 2004) and USAF personnel (Churchill et al., 1977) as shown in Table 3.3. Of the 22 facial dimensions, 10 dimensions were comparable with the Korean civilian anthropometric study and 13 with the USAF personnel anthropometric study. Note that nose length (sellion-to-pronasale length) in the Korean civilian anthropometric study was measured differently from that (sellion to subnasale length) of the USAF personnel anthropometric study. Also note that, of the USAF facial measurements, those of nasal root breadth and maximum nasal bridge breadth were collected by the LANL survey data (Hack et al., 1973). *t*-test and *F*-test were conducted using MINITAB v. 14 (Minitab Inc., U.S.A.) to examine the statistical significance of the differences in mean and SD, respectively, between the KAF pilots, Korean civilians, and USAF personnel.

Table 3.3. Facial anthropometric studies compared in the present study

Category	**Korean Air Force**		**Korean male civilian**	**U.S. Air Force male personnel**
	Male	**Female**		
Reference	The present study		KATS (2004)	Churchill et al. (1977)
Survey year	2010 ~ 2011		2003 ~ 2004	1967 ~ 1068
Sample size	278	58	1,034 (2,568*)	2,420
Age	25 ~ 43	20 ~ 28	25 ~ 49 (8 ~ 75*)	21 ~ 50
Facial dimensions	22		10 (40*)	13 (48*)
Remarks	- - 278 pilots	- 6 pilots - 52 cadets		- 1187 pilots - 505 navigators - 505 student pilots - 118 student navigators

* The information of original data; face measurements matching in age with the present study and facial dimensions corresponding to the present study were used for comparison.

3.4.2. Analysis of Face Measurements

Facial Measurements of KAF Male Pilots and KAF Female Pilots and Cadets

The descriptive statistics (mean, SD, min, max, and percentiles) of the KMP facial measurements and that of the KFP facial measurements are presented in Table 3.4 and 3.5, respectively. For example, the descriptive statistics of KMP face width (unit: mm) in Table 4 shows mean ± SD = 156.4 ± 5.2, min = 143.4, max = 171.5, $p_{.01}$ = 145.0 mm, $p_{.05}$ = 148.3 mm, $p_{.95}$ = 164.7, $p_{.99}$ = 168.8.

Table 3.4. Descriptive statistics of Korean Air Force (KAF) male pilot anthropometric data (unit: mm)

No.	face dimensions	*n*	mean	SD	min	max	percentile			
							1st	5th	95th	99th
1	head height	277	241.0	8.2	221.5	263.0	223.4	227.5	255.6	259.0
2	head breadth	277	161.8	6.4	123.5	180.5	145.4	151.9	171.5	175.6
3	head length	277	188.3	6.5	162.0	204.0	171.8	178.0	199.0	202.5
4	head circumference	277	566.0	13.4	516.5	604.5	532.1	545.4	589.1	596.6
5	face length	278	125.0	5.2	110.5	140.4	112.9	116.3	133.4	136.8
6	lower face length	278	70.0	4.2	59.2	83.6	60.8	63.0	76.9	79.9
7	sellion-to-supramentale length	278	98.3	4.6	85.8	114.1	88.0	90.4	104.8	109.7
8	supramentale-to-menton length	278	26.7	2.9	18.9	36.2	20.6	21.9	31.2	34.7
9	rhinion-to-menton length	278	110.4	4.8	94.2	124.3	99.1	102.8	118.0	121.2
10	rhinion-to-promentale length	278	97.2	4.7	82.0	108.9	86.8	89.7	105.7	108.1
11	promentale-to-menton length	278	13.1	2.4	4.9	19.4	7.9	9.4	17.6	18.9
12	nose length									
	- sellion-to-subnasale	278	55.0	3.1	46.7	62.2	47.3	50.2	60.5	61.9
	- sellion-to-pronasale	278	43.5	3.2	32.9	52.3	35.8	38.2	48.2	51.0
13	nose protrusion	278	14.4	1.6	9.8	18.2	10.4	11.9	17.1	17.8
14	face width	278	156.4	5.2	143.4	171.5	145.0	148.3	164.7	168.8
15	chin width	278	132.0	8.1	110.1	156.7	114.2	119.7	145.5	151.3
16	nasal root breadth	278	20.6	2.5	14.0	27.7	14.9	16.6	24.9	27.0
17	maximum nasal bridge breadth	278	31.3	2.4	25.1	37.7	25.9	27.3	35.4	36.9
18	nose width	278	38.1	2.5	31.7	45.8	32.6	34.1	42.5	43.9
19	lip width	278	49.9	3.4	38.8	58.2	41.8	44.4	56.1	57.5
20	bitragion-menton arc	278	318.2	13.0	285.6	361.1	289.0	297.5	339.4	348.5
21	bitragion-subnasale arc	278	285.8	11.1	251.9	319.6	259.0	268.9	304.8	312.1
22	bizygomatic-menton arc	278	309.0	11.0	283.1	349.3	289.5	291.9	328.9	337.7

Table 3.5. Descriptive statistics of Korean Air Force (KAF) female pilot and cadet anthropometric data (unit: mm)

No.	face dimensions	*n*	mean	SD	min	max	percentile			
							1st	5th	95th	99th
1	head height	57	227.5	7.2	212.5	240.0	213.3	214.5	237.7	240.0
2	head breadth	58	157.1	5.0	148.5	173.0	148.5	150.4	165.6	170.4
3	head length	58	181.1	5.7	168.0	192.5	168.3	170.4	189.6	192.2
4	head circumference	58	557.0	11.7	535.0	582.5	535.9	539.8	578.7	581.1
5	face length	58	116.1	4.6	106.7	125.6	106.9	107.9	123.3	125.0
6	lower face length	58	65.0	3.5	57.5	71.3	58.0	58.5	70.1	70.9
7	sellion-to-supramentale length	58	91.3	4.0	80.7	98.1	82.9	85.1	97.4	97.9
8	supramentale-to-menton length	58	24.9	3.0	18.6	30.7	18.8	20.4	30.4	30.7
9	rhinion-to-menton length	58	102.9	4.4	93.2	112.8	93.9	96.0	109.8	112.7
10	rhinion-to-promentale length	58	88.8	3.7	78.2	97.6	79.9	83.8	95.9	97.3
11	promentale-to-menton length	58	14.1	2.6	7.9	20.6	8.8	10.1	18.5	19.5
12	nose length									
	- sellion-to-subnasale	58	51.1	3.0	43.2	56.9	43.5	46.5	55.5	56.5
	- sellion-to-pronasale	58	38.4	3.3	30.4	44.8	31.4	32.7	43.1	44.1
13	nose protrusion	58	12.4	1.5	9.6	17.1	9.6	10.0	14.7	15.9
14	face width	58	147.0	6.0	132.4	162.7	133.7	137.9	157.8	161.2
15	chin width	58	122.2	6.1	105.4	137.8	105.8	113.6	130.6	135.5
16	nasal root breadth	58	17.2	2.2	12.3	23.5	12.9	14.0	20.9	22.9
17	maximum nasal bridge breadth	58	27.0	1.9	22.3	31.7	23.2	24.2	29.8	30.7
18	nose width	58	35.0	2.0	30.3	40.2	30.4	31.9	37.9	39.4
19	lip width	58	45.4	3.2	38.5	53.4	38.5	41.2	51.8	52.7
20	bitragion-menton arc	58	292.1	12.1	269.0	317.3	270.4	272.8	311.4	317.2
21	bitragion-subnasale arc	58	269.8	12.4	234.9	301.2	238.8	251.9	290.9	298.8
22	bizygomatic-menton arc	58	315.7	17.7	275.6	347.8	277.1	283.0	343.7	347.7

Comparison of KAF Male Pilots and Korean Male Civilians

A comparison in mean and SD between the KMP and Korean male civilians (KMC) presented in Table 3.6 and Figure 3.15 reveals that the KMP had a significantly lager head and a more protruded nose (ratio of means > 1.05) and was less varied in all the facial dimensions than the KMC. The KMP was found significantly larger than the KMC in all the head-related dimensions (head height, head breadth, head length, face length, and lower face length; $\bar{d}$ = 6.6 ~ 26.5, ratio of means = 1.05 to 1.12) except head circumference ($\bar{d}$ = -6.5; ratio of means = 0.99). Next, the KMP was found having a longer, higher, but slightly narrower nose ($\bar{d}$ = 1.2 in nose length, 1.8 in nose protrusion, and -1.4 in nose width) and a slightly wider lip ($\bar{d}$ = 0.7 in lip width). The SD ratio analysis results indicate that the facial measurements of the KMP were significantly less dispersed than those of the KMC in all the facial dimensions (ratio of SDs = 0.29 to 0.82). This means that the design of the pilot oxygen mask for the KAF pilots requires the KAF facial anthropometric data.

Table 3.6. Comparison of KAF male pilots (KMP) and Korean male civilians (KMC) (unit: mm)

No.	Anthropometric dimensions	KMP (n = 278)		KMC (n = 1034)		KMP vs. KMC		
		M_{KMP}	SD_{KMP}	M_{KMC}	SD_{KMC}	$M_{KMP-KMC}$	M_{KMP}/M_{KMC}	SD_{KMP}/SD_{KMC}
1	head height	241.0	8.2	214.6	28.9	26.5 **	1.12	0.29 **
2	head breadth	161.8	6.4	154.3	18.3	7.5 **	1.05	0.35 **
3	head length	188.3	6.5	176.8	20.7	11.5 **	1.07	0.31 **
4	head circumference	566.0	13.4	572.5	16.3	-6.5 **	0.99	0.82 **
5	face length	125.0	5.2	111.3	14.6	13.7 **	1.12	0.36 **
6	lower face length	70.0	4.2	63.4	8.4	6.6 **	1.10	0.50 **
7	sellion-to-supramentale length	98.3	4.6	-	-	-	-	-
8	supramentale-to-menton length	26.7	2.9	-	-	-	-	-
9	rhinion-to-menton length	110.4	4.8	-	-	-	-	-
10	rhinion-to-promentale length	97.2	4.7	-	-	-	-	-
11	promentale-to-menton length	13.1	2.4	-	-	-	-	-
12	nose length (sellion-to-pronasale)	43.5	3.2	42.3	6.1	1.2 **	1.04	0.52 **
13	nose protrusion	14.4	1.6	12.6	2.4	1.8 **	1.14	0.66 **
14	face width	156.4	5.2	-	-	-	-	-
15	chin width	132.0	8.1	-	-	-	-	-
16	nasal root breadth	20.6	2.5	-	-	-	-	-
17	maximum nasal bridge breadth	31.3	2.4	-	-	-	-	-
18	nose width	38.1	2.5	39.6	3.7	-1.4 **	0.96	0.68 **
19	lip width	49.9	3.4	49.2	5.6	0.7 **	1.01	0.61 **
20	bitragion-menton arc	318.2	13.0	-	-	-	-	-
21	bitragion-subnasale arc	285.8	11.1	-	-	-	-	-
22	bizygomatic-menton arc	309.0	11.0	-	-	-	-	-

* $p < .05$; ** $p < .01$

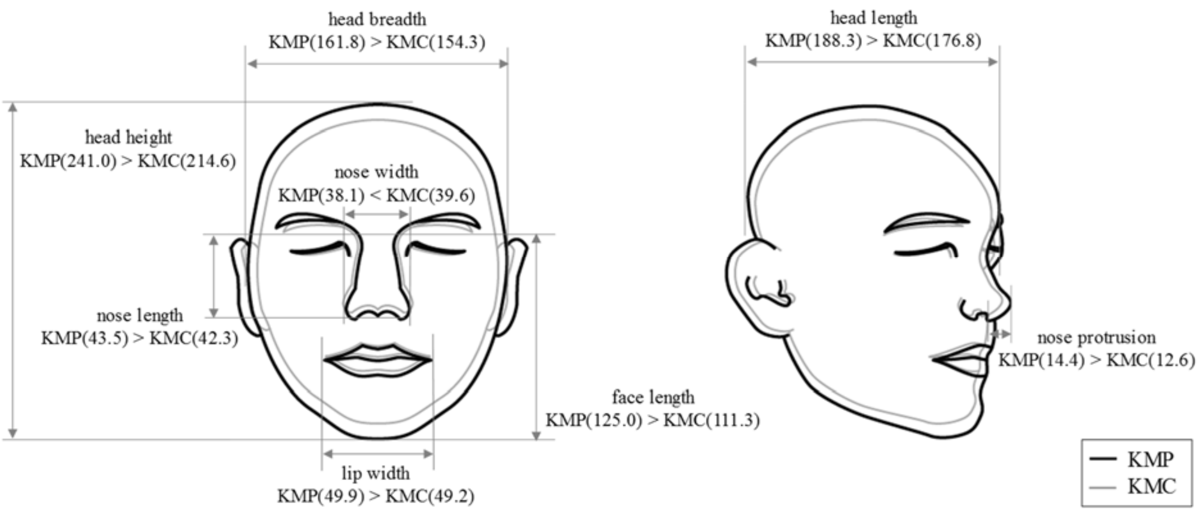

Figure 3.15. The mean differences of facial measurements between Korean Air Force male pilots (KMP) and Korean male civilians (KMC) (unit: mm)

Comparison of KAF Male Pilots and USAF Male Personnel

A comparison in mean and SD between the KMP and USAF male personnel (UMP) presented in Table 3.7 and Figure 3.16 indicates that the KMP had a significantly longer, wider, but flatter head and a longer and wider nose, and was less varied in the length and width dimensions of the head, nose, and lip, but more varied in chin width, nasal root breadth, bitragion-menton arc, and bitragion-subnasale arc than the UMP. The mean length differences between the KMP and UMP decreased in the following order for the head ($\bar{d}$ = 13.3; ratio of means = 1.06), face ($\bar{d}$ = 4.7; ratio of means = 1.04), and lower face ($\bar{d}$ = 1.0; ratio of means = 1.01). The KMP width measurements of the face, chin, nasal root, and nose were found significantly larger than the corresponding UMP measurements (ratio of means = 1.09 to 1.34), but the opposite was found in maximum nasal bridge breadth (ratio of means = 0.90) and lip width (ratio of means = 0.95). The mean head length of the KMP was found

Table 3.7. Comparison of KAF male pilots (KMP) and U.S. Air Force male personnel (UMP) (unit: mm)

No.	Anthropometric dimensions	KMP (n = 278)		UMP (n = 2420)		KMP vs. UMP		
		M_{KMP}	SD_{KMP}	M_{UMP}	SD_{UMP}	$M_{KMP-UMP}$	M_{KMP}/M_{UMP}	SD_{KMP}/SD_{UMP}
1	head height	241.0	8.2	227.7	10.2	13.3 **	1.06	0.81 **
2	head breadth	161.8	6.4	-	-	-	-	-
3	head length	188.3	6.5	198.7	6.7	-10.4 **	0.95	0.97 **
4	head circumference	566.0	13.4	-	-	-	-	-
5	face length	125.0	5.2	120.3	6.1	4.7 **	1.04	0.85
6	lower face length	70.0	4.2	69.0	5.3	1.0 **	1.01	0.79 **
7	sellion-to-supramentale length	98.3	4.6	-	-	-	-	-
8	supramentale-to-menton length	26.7	2.9	-	-	-	-	-
9	rhinion-to-menton length	110.4	4.8	-	-	-	-	-
10	rhinion-to-promentale length	97.2	4.7	-	-	-	-	-
11	promentale-to-menton length	13.1	2.4	-	-	-	-	-
12	nose length (sellion-to-subnasale)	55.0	3.1	51.3	3.7	3.7 **	1.07	0.83 **
13	nose protrusion	14.4	1.6	-	-	-	-	-
14	face width	156.4	5.2	142.3	5.2	14.1 **	1.10	1.00
15	chin width	132.0	8.1	117.3	6.9	14.7 **	1.13	1.18 **
16	nasal root breadth	20.6	2.5	15.4	1.9	5.2 **	1.34	1.33 **
17	maximum nasal bridge breadth	31.3	2.4	34.7	3.2	-3.4 **	0.90	0.75 **
18	nose width	38.1	2.5	35.0	2.9	3.1 **	1.09	0.86 **
19	lip width	49.9	3.4	52.3	3.7	-2.4 **	0.95	0.94
20	bitragion-menton arc	318.2	13.0	327.0	12.4	-8.8 **	0.97	1.05
21	bitragion-subnasale arc	285.8	11.1	293.0	10.2	-7.2 **	0.98	1.09 *
22	bizygomatic-menton arc	309.0	11.0	-	-	-	-	-

* $p < .05$; ** $p < .01$

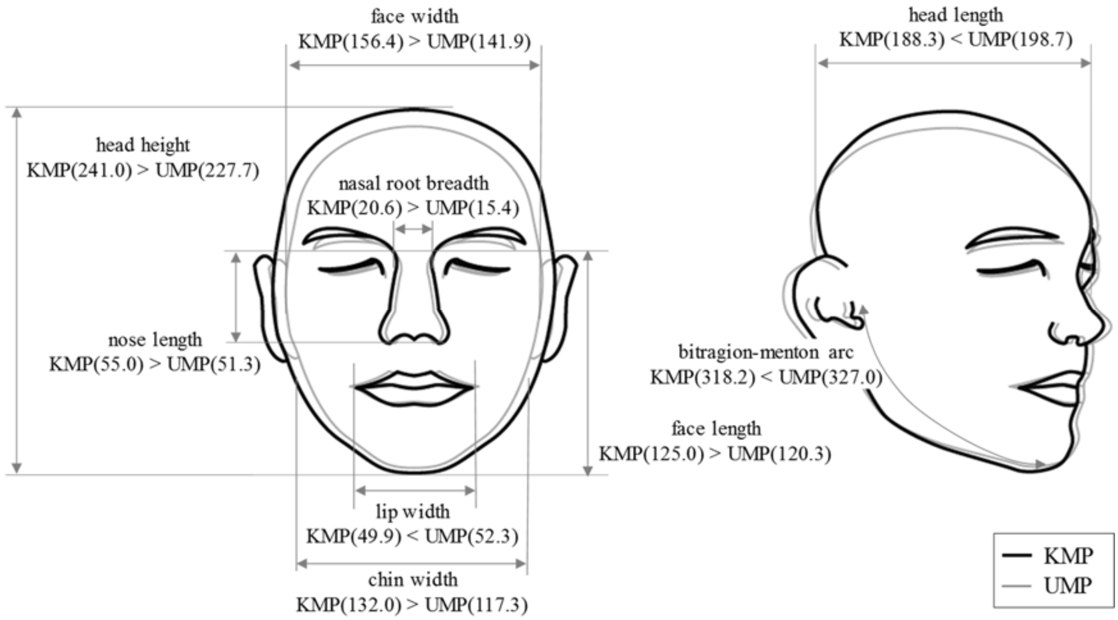

Figure 3.16. The mean differences of facial measurements between Korean Air Force male pilots (KMP) and U.S. Air Force male personnel (UMP) (unit: mm)

significantly smaller than that of the UMP (ratio in mean = 0.95), indicating the KMP had a flatter head than the UMP. The mean nose length of the KMP was found significantly longer than that of the UMP ($\bar{d}$ = 3.7; ratio in mean = 1.07). The largest mean difference at the nasal root area between the KMP and UMP was found in nasal root breadth ($\bar{d}$ = 5.2, ratio of means = 1.34), which can be the main cause of excessive pressure being experienced by most of KAF pilots wearing MBU-20/P masks. Lastly, the SD ratio analysis results indicate that the facial measurements of the KMP were less varied in the length and width dimensions of the head, nose, and lip (ratio of SDs = 0.75 to 0.97), but more varied in chin width, nasal root breadth, bitragion-menton arc, and bitragion-subnasale arc (ratio of SDs = 1.05 to 1.33) than those of the UMP.

Comparison of KAF Male Pilots and KAF Female Pilots and Cadets

A comparison in mean and SD between the KMP and KFP presented in Table 3.8 and Figure 3.17 shows that the KMP was larger in all the facial dimensions (ratio of means = 1.02 ~ 1.20) except promentale-to-menton length (ratio of means = 0.93) and more varied in all the facial dimensions (ratio of SDs = 1.03 ~ 1.33) except face width, bitragion-subnasale arc, and chin-related dimensions (supramentale-to-menton length, promentale-to-menton length, bizygomatic-menton arc) than the KFP. Of the facial dimensions, relatively large mean differences ($\bar{d}$ > 10. 0 mm or ratio of means > 1.10) between the KMP and KFP were found in head height, bitragion-menton arc, bitragion-subnasale arc, bizygomatic-menton arc, nasal root breadth, and maximum nasal bridge breadth.

Table 3.8. Comparison of KAF male pilots (KMP) and KAF female pilots and cadets (KFP) (unit: mm)

No.	Anthropometric dimensions	KMP (n = 278)		KFP (n = 58)		KMP vs. KFP		
		M_{KMP}	SD_{KMP}	M_{KFP}	SD_{KFP}	$M_{KMP-KFP}$	M_{KMP}/M_{KFP}	SD_{KMP}/SD_{KFP}
1	head height	241.0	8.2	227.5	7.2	13.6 **	1.06	1.14
2	head breadth	161.8	6.4	157.1	5.0	4.7 **	1.03	1.28 *
3	head length	188.3	6.5	181.1	5.7	7.2 **	1.04	1.14
4	head circumference	566.0	13.4	557.0	11.7	9.0 **	1.02	1.14
5	face length	125.0	5.2	116.1	4.6	8.8 **	1.08	1.14
6	lower face length	70.0	4.2	65.0	3.5	5.0 **	1.08	1.18
7	sellion-to-supramentale length	98.3	4.6	91.3	4.0	7.0 **	1.08	1.17
8	supramentale-to-menton length	26.7	2.9	24.9	3.0	1.8 **	1.07	0.95
9	rhinion-to-menton length	110.4	4.8	102.9	4.4	7.4 **	1.07	1.10
10	rhinion-to-promentale length	97.2	4.7	88.8	3.7	8.4 **	1.09	1.29 *
11	promentale-to-menton length	13.1	2.4	14.1	2.6	-1.0 **	0.93	0.93
12	nose length (sellion-to-subnasale)	55.0	3.1	51.1	3.0	3.8 **	1.08	1.03
13	nose protrusion	14.4	1.6	12.4	1.5	2.0 **	1.16	1.05
14	face width	156.4	5.2	147.0	6.0	9.4 **	1.06	0.88
15	chin width	132.0	8.1	122.2	6.1	9.8 **	1.08	1.33 *
16	nasal root breadth	20.6	2.5	17.2	2.2	3.4 **	1.20	1.13
17	maximum nasal bridge breadth	31.3	2.4	27.0	1.9	4.3 **	1.16	1.28 *
18	nose width	38.1	2.5	35.0	2.0	3.2 **	1.09	1.25 *
19	lip width	49.9	3.4	45.4	3.2	4.4 **	1.10	1.05
20	bitragion-menton arc	318.2	13.0	292.1	12.1	26.1 **	1.09	1.08
21	bitragion-subnasale arc	285.8	11.1	269.8	12.4	16.0 **	1.06	0.90
22	bizygomatic-menton arc	309.0	11.0	284.6	12.1	24.5 **	1.09	0.93

* $p < .05$; ** $p < .01$

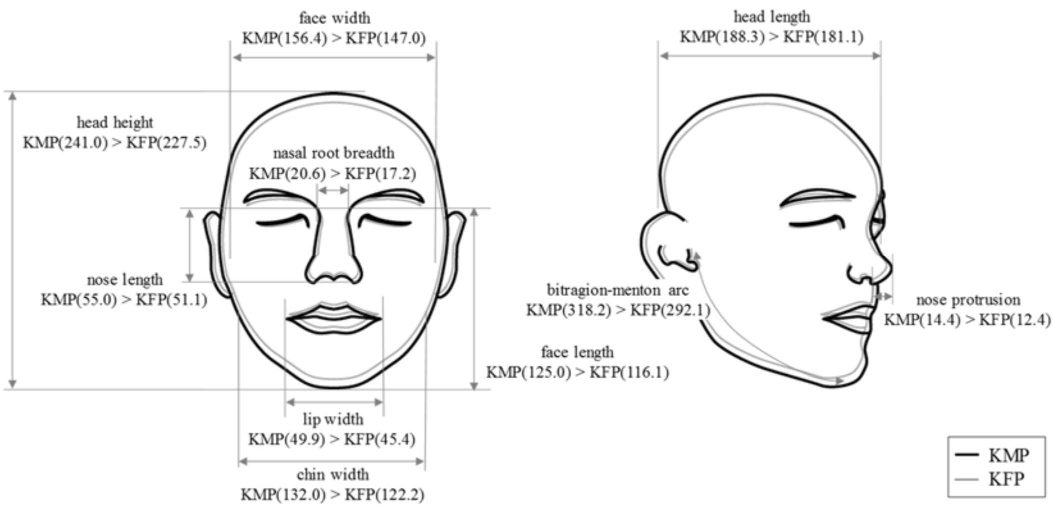

Figure 3.17. The mean differences of facial measurements between Korean Air Force male pilots (KMP) and Korean Air Force female pilots and cadets (KFP) (unit: mm)

Lastly, significant SD differences (ratio of SDs > 1.2) between the KMP and KFP were found mainly in the width-related dimensions (head breadth, rhinion-to-promentale length, chin width, maximum nasal bridge breadth, and nose width). The faces of the KFP were found significantly smaller than the KMP (e.g., at nasal root breath $\bar{d}$ = 3.4 and ratio of means = 1.20) and less dispersed. This means that a composite population (e.g., male: female = 9: 1) of KAF pilots needs to be formed for oxygen mask design to reflect an increasing rate of the KFP in the future.

3.4.3. Oxygen Mask Sizing System Development

Analysis of the Existing Sizing System

A sizing system of the MBU-20/P proposed by M. E. Gross et al. (1997) consists of the XSN, SN, MN, MW, and LW depending on their length and width (Figure 3.18). The length sizes (small, medium and large) are categorized by sellion-to-supramentale length which corresponds to the oxygen mask length. The width sizes (narrow and wide) are classified by lip width which corresponds to the oxygen mask width. A size interval of length is 13 mm and that of width is 15 mm. Based on M. E. Gross et al. (1997)'s sizing system, the XSN size was added to the sizing system to accommodate female pilots who have relatively smaller head and face.

Due to the significant differences in mean and SD between the KMP and UMP, a customized sizing system needs to be developed for the KAF pilots. Because there are no sellion-to-supramentale length dimension in the 1967-1968 USAF data, face length was used for comparison between the KMP and UMP. Face length of the KMP (125.0 ± 5.2 mm) is 4.7 mm longer on average than that of the UMP (120.3 ± 6.1 mm), and lip width of the KMP (49.9 ± 3.4 mm) is 2.4 mm

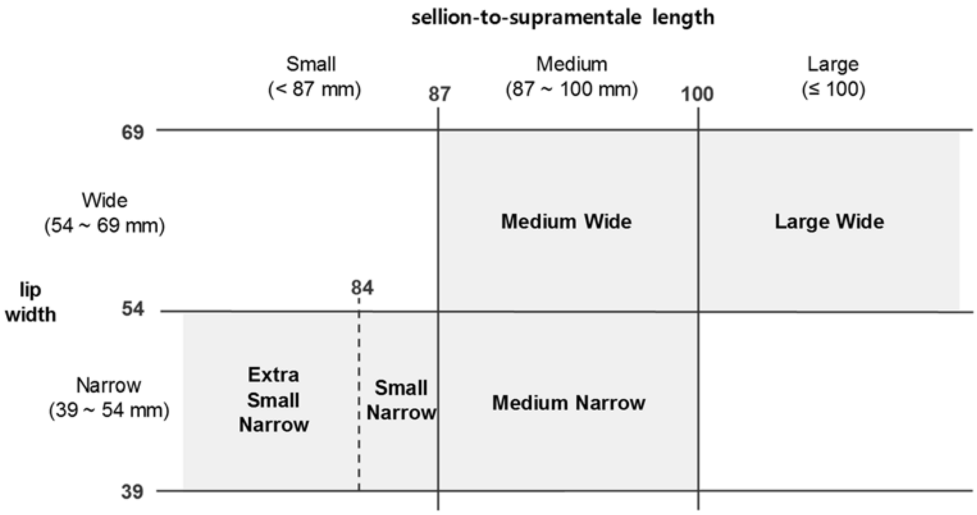

Figure 3.18. The sizing system of the MBU-20/P pilot oxygen mask

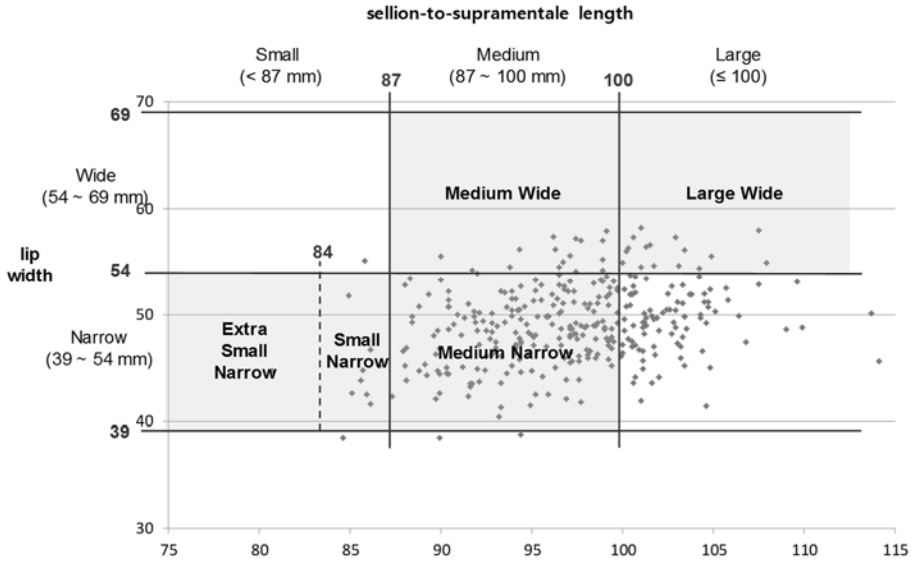

Figure 3.19. Scatter plot of the KAF pilots to the MBU-20/P sizing system

narrower on average than that of the UMP (52.3 ± 3.7 mm). Differences on the face size between the Korean and U.S. Air Force personnel are visualized in Figure 3.19 which presents a scatter plot of the KAF pilots (n = 336) to the existing MBU-20/P sizing system. According to the analysis, the oxygen mask sizing system for the KAF needs to be modified as longer (e.g., 5.0 mm) and narrower (e.g., 2.5 mm) than the existing sizing system.

KAF Pilots' Oxygen Mask Sizing System Development

A grid method was practically applied to the custom design of the oxygen mask sizing system for the KAF pilots. The present study used the grid method (Robinette & Annis, 1986) which was properly applied to the sizing system design (Jung, Kwon, & You, 2010; B. Lee, Jung, & You, 2011). A revised sizing system created through the grid method accommodated 98% of the KAF pilots including small wide (SW) and large narrow (LN) sizes (Figure 3.20a), but it excluded 12% of the SW and LN sizes (Figure 3.20b) which are not included in the existing sizing system. Considering an accommodation percentage and an applicability to the oxygen mask design, the revised sizing system was adjusted by a panel of ergonomist as shown in Figure 3.20c. A range of length of the SN size was changed from 80 ~ 90 mm to 85 ~ 90 mm by considering the length distribution of the KAF pilots. Additionally, a range of width of the LW size was modified from 50 ~ 60 mm to 45 ~ 55 mm to accommodate some pilots classified into the LN size. By adjusting the SN and LW, the accommodation percentage was increased to 93%. However, considering an elasticity of the material (silicon rubber) of the facepiece, an actual accommodation percentage can be higher than 93%. The USAF added the XSN size to include female pilots, but the present study did not need the XSN size due to consideration of sufficient amount of female participants (male: female = 83: 17).

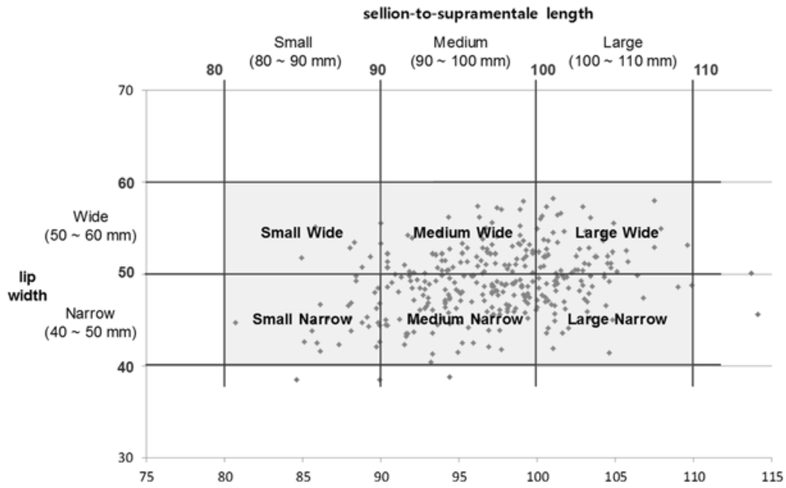

(a) Proposed size categories for KAF pilots (accommodation percentage: 98%)

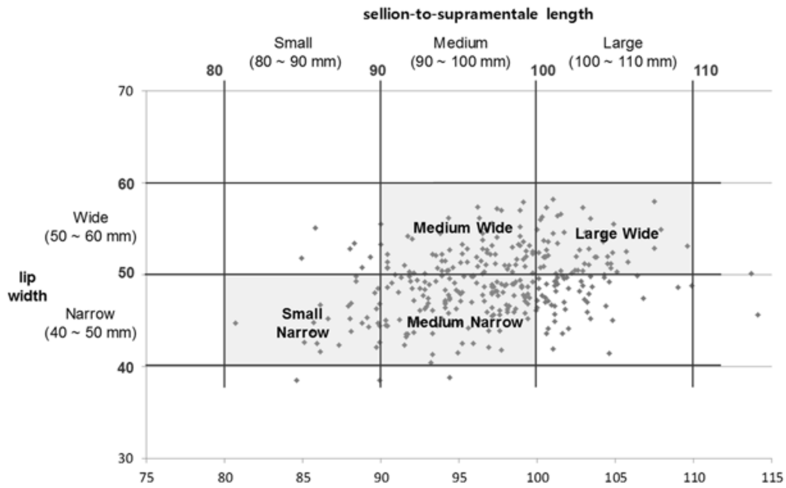

(b) Modified sizing criteria and the number of size categories (accommodation percentage: 88%)

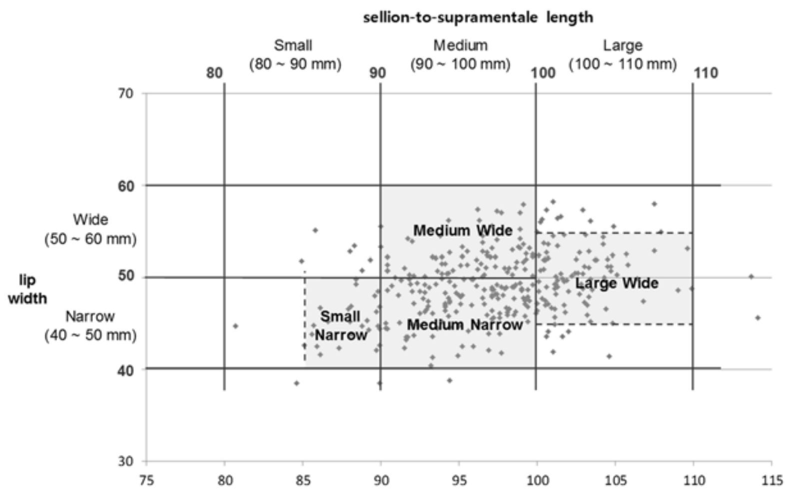

(c) Revised sizing system considering suitability and accommodation percentage (93%)

Figure 3.20. The revised sizing system of MBU-20/P for KAF pilots

Representative Face Model Generation

The RFMs of the KAF pilots were generated to apply to the oxygen mask design and evaluation. Four KAF pilots were selected as the RFMs whose face sizes were closer to a centroid of the size categories. The facial dimensions of the centroid were defined as mode values of sellion-to-supramentale length and lip width, and average values of the other 16 facial measured by the present study. Among the KAF pilots, the RFMs were selected who have the shortest Euclidian distance from the centroid. For the calculation of Euclidian distance, weights (L = 1, M = 2, H = 3) were considered according to the importance of facial dimensions shown in Figure 3.9. Figure 3.21 presents locations of the RFMs depending on the sellion-to-supramentale length and lip width, and the face shape of the RFMs is like Figure 3.22. The RFMs were applied to the oxygen mask design in the next step of the present study.

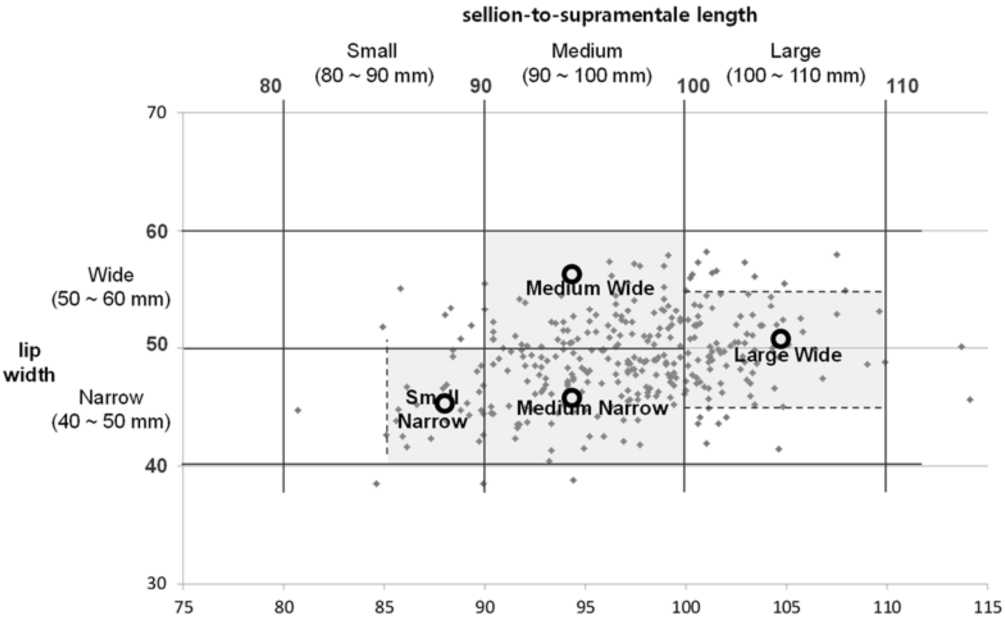

Figure 3.21. Representative face models of the revised sizing system

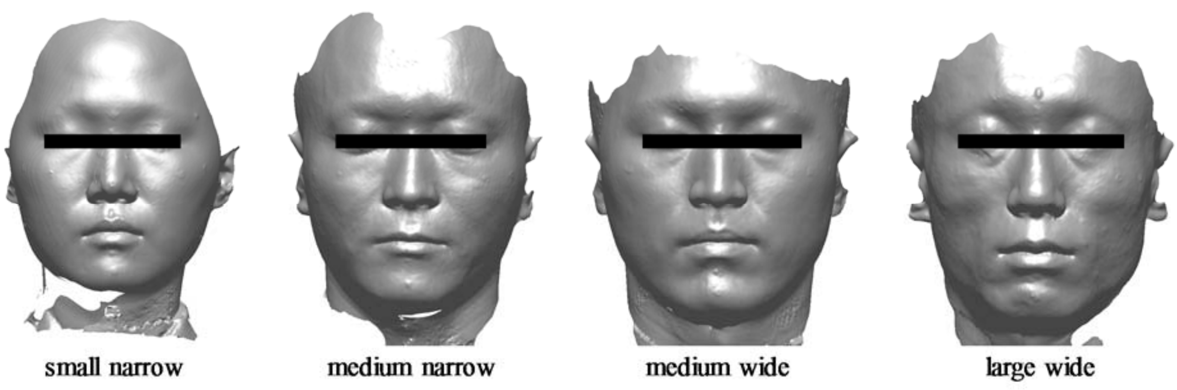

Figure 3.22. Representative face models of KAF pilots

3.5. Oxygen Mask Wearing Characteristics

The oxygen mask wearing characteristics were identified by analyzing photos of pilots wearing the MBU-20/P oxygen mask, followed by four-step process (Figure 3.23). First, a photo of a pilot wearing the oxygen mask was taken. Second, the photo was printed on a transparent film (e.g., OHP film) and features of the face and the oxygen mask were marked on the film. Third, the film was attached to a PC monitor, and the 3D face and oxygen mask images were virtually aligned using RapidForm™ 2006 (Inus Technology, Inc., South Korea) software by referring to the features marked on the film. Lastly, the oxygen mask wearing characteristics (e.g., wearing position at nose and chin, angle between the oxygen mask and nasal bridge, fit, and clearance) were identified by analyzing the virtually aligned 3D images of the face and oxygen mask.

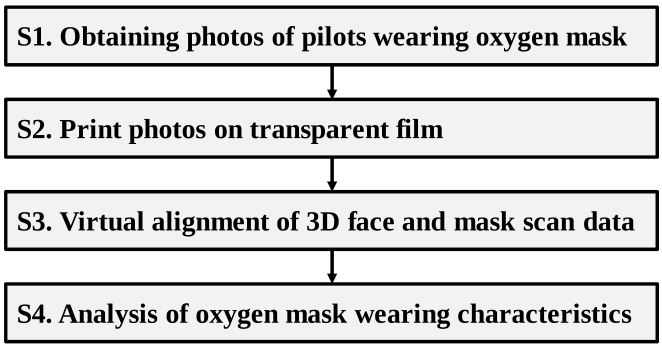

Figure 3.23. Process for the oxygen mask wearing characteristics analysis

3.5.1. Analysis Method of Wearing Characteristics

Obtaining Photos of Pilots Wearing Oxygen Mask

The photos of pilots wearing the oxygen mask were taken of 85 KAF pilots (SN: 21, MN: 23, MW: 19, and LW: 22) who attended the facial anthropometric survey portion of the present study. To take the photo, the pilots wore their own helmets and oxygen masks and looked straight ahead, sitting in a chair (Figure 3.24). The experimenter took the photo at eye height from the side of the pilot.

Virtual Alignment of Oxygen Mask to 3D Face

The OHP film which contained the features of the face and oxygen mask was attached to a PC monitor, and the 3D face and oxygen mask images were virtually aligned using the CAD software by referring the features marked on the film. The features of the face (e.g., nose, eye, eyebrow) and oxygen mask (e.g., facepiece, hardshell, valsalva hole, and valve) were marked onto the printed film as illustrated in Figure 3.25. Then, the film was attached to the PC monitor as shown in Figure 3.26a.

Figure 3.24. A guideline for taking photo of pilots who wear their own oxygen mask

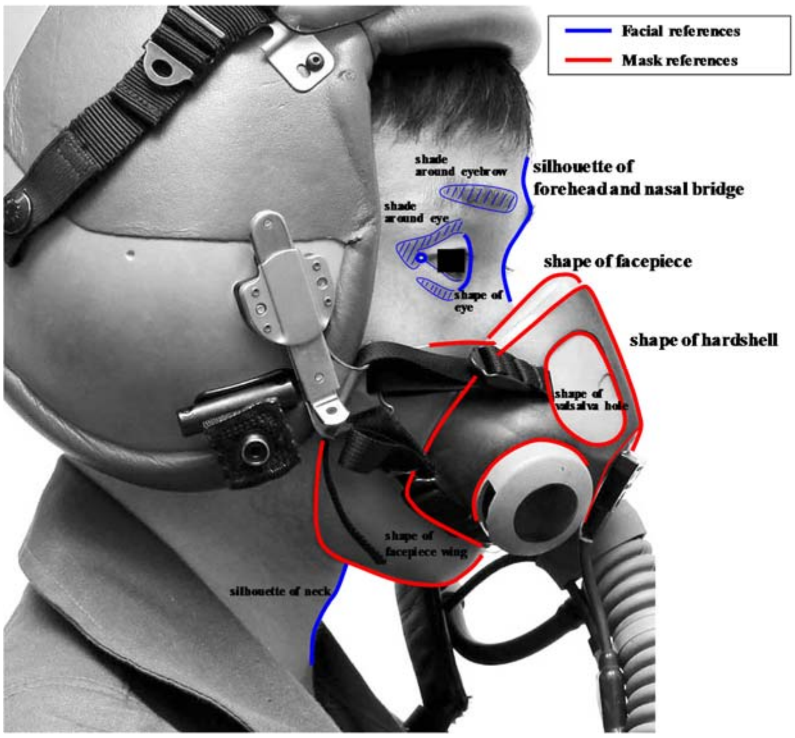

Figure 3.25. Reference features on face and mask

The 3D scan images of the face and the oxygen mask were loaded onto the RapidForm™ 2006 software, and then those images were virtually aligned (Figure 3.26b and c) by a four-step process: (1) zooming the screen of CAD software to match the size of the oxygen mask between the film and 3D image, (2) panning the view point of CAD software to match the features of the face between the film and 3D images by referring the features of face marked on the film, (3) transferring and rotating the 3D oxygen mask image toward the 3D face image by referring the features of face and oxygen mask marked on the film, and (4) finishing the virtual alignment, and then measuring the oxygen mask wearing characteristics.

(a) Attaching a film on the monitor

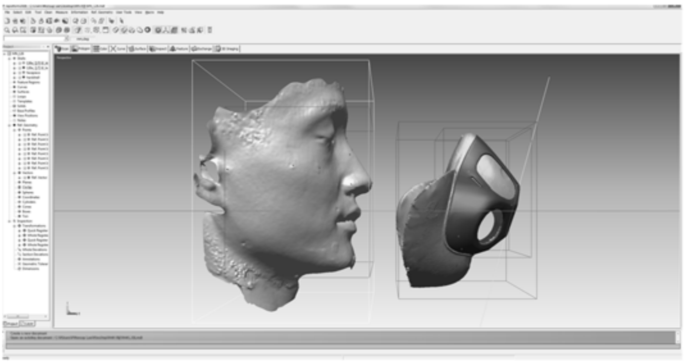

(b) Loading 3D face and mask scan data

(c) Result of virtual alignment

Figure 3.26. Virtual alignment process

Analysis of Oxygen Mask Wearing Characteristics

The oxygen mask wearing characteristics were identified in terms of the wearing position, wearing angle, fit, and clearance. The wearing position was defined by measuring four distances (mask-top-to-sellion vertical distance, mask-top-to-sellion horizontal distance, mask-bottom-to-supramentale vertical distance, and mask-bottom-to-supramentale horizontal distance) between the facial landmarks (sellion and supramentale) and oxygen mask design landmarks (mask top point and mask bottom point) explained in Chapter 3.3 (Figure 3.27a). The wearing angle between a frontal shape of the oxygen mask and nasal bridge was analyzed as shown in Figure 3.27b.

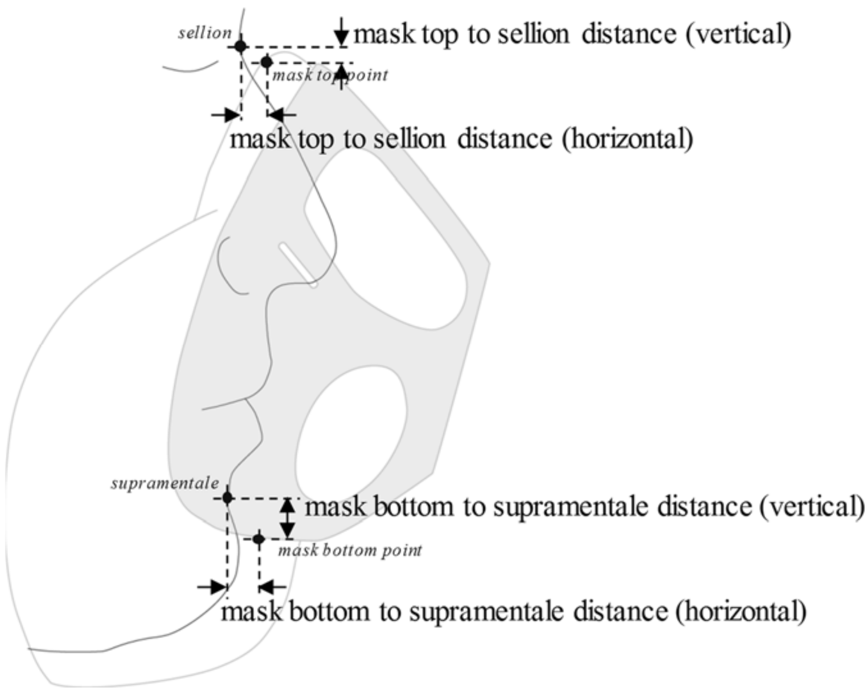

(a) Mask wear position

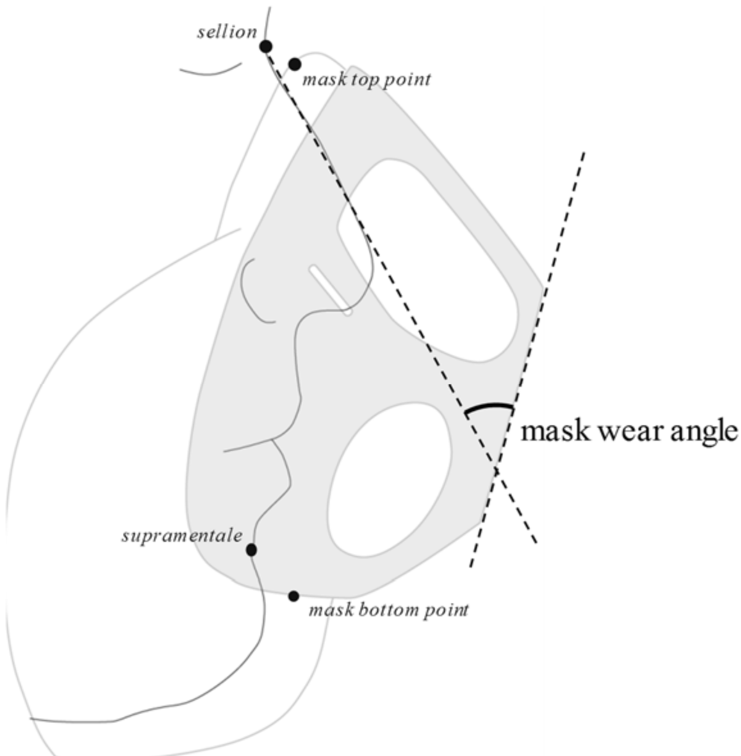

(b) Mask wear angle

Figure 3.27. Mask wearing characteristics: wear position and wear angle

The fit of the oxygen mask to the face was identified as an infiltration distance of the oxygen mask CAD from the 3D face image. The actual oxygen mask made of silicone rubber is deformed when a pilot wears the mask; however, the oxygen mask CAD infiltrates into the 3D face during virtual fitting as highlighted in red in Figure 3.28. Therefore, the present study identified the fit as the infiltration distance between the oxygen mask CAD and 3D face image. Deep infiltration (e.g., infiltration distance > 10 mm) means an excessive pressure, while no infiltration (infiltration distance < 0 mm) can be explained as an oxygen leakage. The fit was analyzed by 1 mm according to the vertical location of the face as shown in Figure 3.29 (e.g., vertical location of nasal root area: 0 ~ 10 mm). For instance, the oxygen mask is slightly fitted (infiltration distance < 5 mm) or not fitted (infiltration distance < 0 mm) at the nasal root area (vertical location = 0 ~ 10 mm), while it is deeply fitted (maximum infiltration distance = 20 mm) at the nasal side and zygomatic bone areas (vertical location = 10 ~ 60 mm).

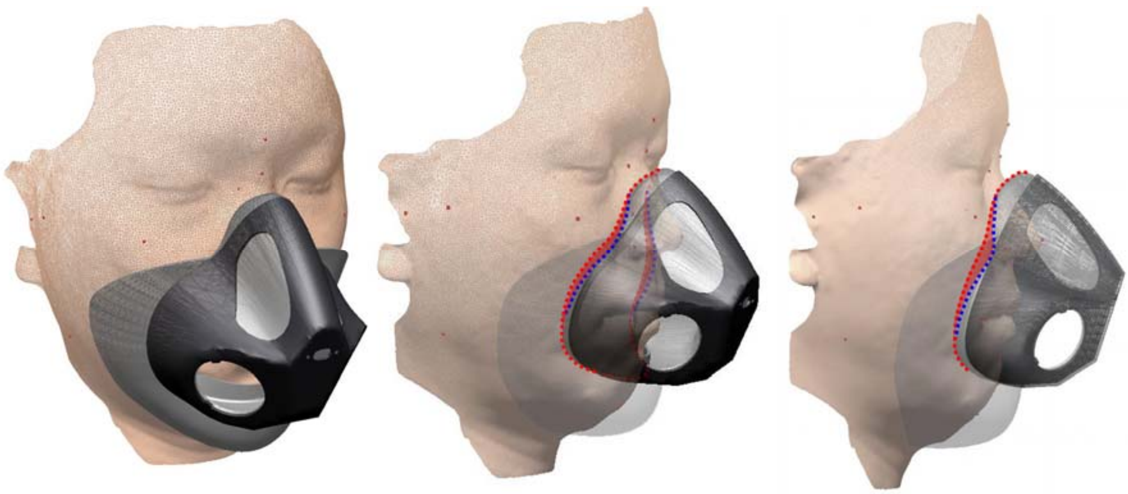

Figure 3.28. Illustration of oxygen mask fit (red area: infiltration of facepiece into face)

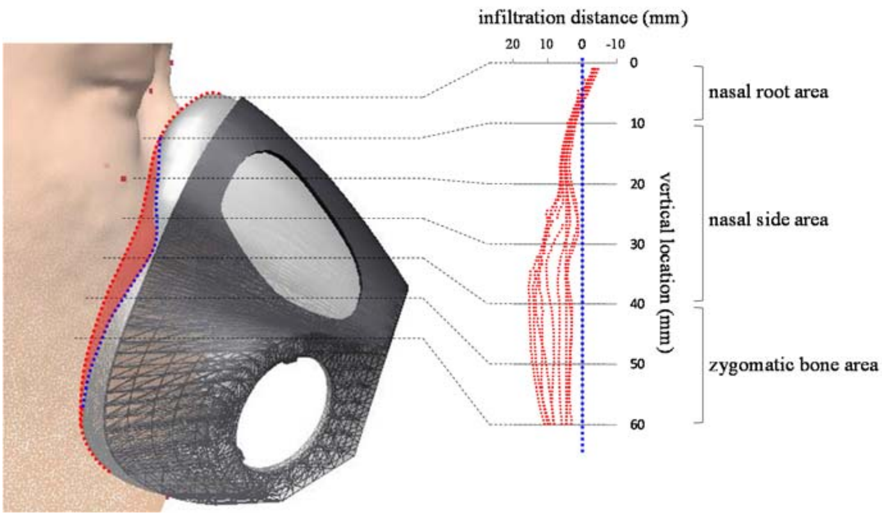

Figure 3.29. Fit of the oxygen mask according to the vertical location

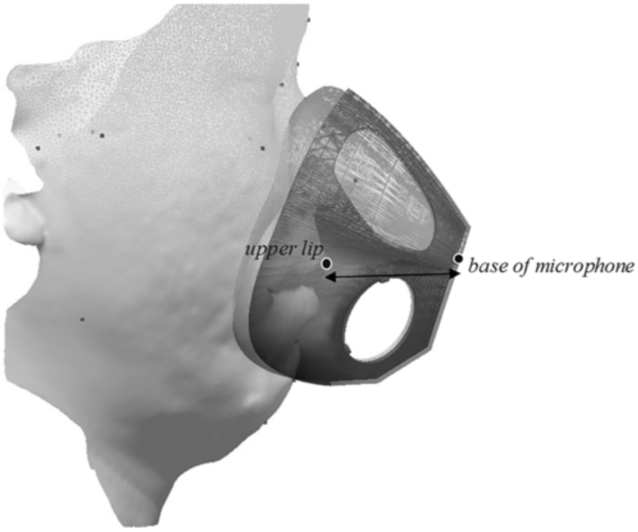

Figure 3.30. Microphone to upper-lip clearance

Lastly, the clearances between a facial landmark and an oxygen mask design landmark were analyzed. For example, the clearance between the microphone and lip was identified by calculating a distance between a base of the microphone and a center of upper-lip (Figure 3.30).

Evaluation of Reliability of Mask Wearing Characteristics Analysis

The reliability of the proposed method for analysis of oxygen mask wearing characteristics was evaluated in terms of an intra-experimenter variability. The analysis of oxygen mask wearing characteristics was conducted through a manual alignment by the experimenter based on the photo and 3D scan images. Because results of the analysis can be arguable in terms of reliability, the present study evaluated the repeatability of the analysis tasks. One experimenter conducted the analysis twice for five pilots' photos, respectively. Then the intra-experimenter variability was analyzed for the mask wearing position and angle.

3.5.2. Results and Application

The analysis method of oxygen mask wearing characteristics was reliable, because the intra-experimenter variability was satisfied in terms of SD ≤ 2 mm (Table 3.9). The variability in SD was evaluated as the satisfactory reliability criteria (SD = 2 mm) described in previous research (W. Lee, Yoon, & You, 2010; Ozsoy, Demirel, Yildirim, Tosun, & Sarikcioglu, 2009; Weinberg, Scott, Neiswanger, Brandon, & Marazita, 2004). The intra-variability of five pilots in five wearing characteristics (4 wearing positions and wearing angle) were satisfied in terms of SD ≤ 2 mm except one case. Therefore, the present study applied this method to the other pilots without repetition.

Table 3.9. Intra-experimenter variability of virtual alignment (gray: SD > 2 mm)

No.		Wearing characteristics	Pilot 1	Pilot 2	Pilot 3	Pilot 4	Pilot 5
1	wear position	mask-top-to-sellion distance (v)	0.8	0.5	1.0	0.7	0.2
2		mask-top-to-sellion distance (h)	0.8	0.1	1.1	1.3	0.3
3		mask-bottom-to-supramentale distance (v)	0.6	0.2	0.7	0.7	0.3
4		mask-bottom-to-supramentale distance (h)	0.1	1.6	0.1	2.8	0.2
5	wear angle		1.0	1.1	0.4	0.6	0.3

Additionally, the mask-bottom-to-supramentale distance (h) of one pilot appeared to be SD = 2.8. This occurred due to a difficulty of virtual alignment for the chin area, because the features (e.g., silhouette of chin area, silhouette of the oxygen mask) at the chin area were hidden by a wing shape of the facepiece. Therefore, the present study checked the mask-bottom-to-supramentale distance (h) after finishing the virtual alignment; and if the mask-bottom-to-supramentale distance (h) ≥ 2 mm, the experimenter slightly adjusted the wearing position at the chin for a realistic alignment between the 3D images.

The oxygen mask wearing characteristics were identified for each size of the oxygen mask, respectively. For example for the MN size oxygen mask (n = 23) as illustrated in Table 3.10, the mask-top-to-sellion horizontal distance was 5.8 ± 2.3 mm (range: 1.9 ~ 10.6 mm) and the wearing angle was 52.5 ± 5.6° (range: 43.3 ~ 61.7°). Those of the other oxygen mask sizes are shown in Appendix C. The oxygen mask wearing characteristics were applied to the VFA method in the next step of the present study. The fit was analyzed by focusing on the nasal root, nasal side, and zygomatic bone area which is where high discomfort occurs due to the excessive pressure.

Table 3.10. Oxygen mask wearing characteristics (illustrated for MN size; n = 23; unit: ˚, mm)

No.		Wearing characteristics	Average	SD	Min	Max
1	wear position	mask-top-to-sellion distance (v)	16.4	6.3	5.2	29.7
2		mask-top-to-sellion distance (h)	5.8	2.3	1.9	10.6
3		mask-bottom-to-supramentale distance (v)	9.9	5.1	0.5	19.5
4		mask-bottom-to-supramentale distance (h)	-0.3	2.0	-2.9	2.9
5	wear angle		52.5	5.6	43.3	61.7
6	microphone to upper-lip clearance		36.0	2.4	32.5	41.5
7	fit	nasal root area (0 ~ 10 mm)	-1.3	1.0	-4.8	3.2
8		nasal side area (11 ~ 40 mm)	4.2	1.2	-0.7	10.2
9		zygomatic bone area (41 ~ 60 mm)	8.5	2.7	0.5	15.3

Chapter 4. OXYGEN MASK DESIGN IMPROVEMENT

This chapter introduces an improvement strategies based on correlation analysis within and between FMI factors. Design problems of the MBU-20/P were identified based on the user preferences of the KAF pilots and the oxygen mask wearing characteristics. The oxygen mask was revised by four design improvement strategies: (1) changing of sizes of the oxygen mask according to the revised oxygen mask sizing system, (2) widening of nose area of the oxygen mask by applying the difference between the KMP and UMP, (3) adjustment of the microphone base to avoid contact between the microphone and lip, and (4) design of oxygen mask shape to fit to the KAF pilots through the VFA method. This chapter presents the oxygen mask improvement by giving an example of the MN size.

4.1. Correlation Analysis Within and Between FMI Factors

Correlations between and within the FMI factors were analyzed to identify strategies for the oxygen mask design improvement. The correlation analysis was conducted based on 18 facial dimensions, 9 oxygen mask wearing characteristics, and 15 user preferences by sizes of the oxygen mask. Correlation coefficients (r) and p-values were found for 861 items, and a correlation criteria was determined by applying a conventional understanding ($r \geq 0.7$: high correlation, $0.4 \leq r < 0.7$: moderate correlation) at $\alpha = 0.05$. In the case of the MN size ($n = 23$), 56 items highly correlated to the oxygen mask design were examined by correlation analysis. Then, those items were interpreted by experimenters and some items less correlated to the oxygen mask design were screened. Additionally, the present study reviewed correlation plots of all the 861 items to visually examine items which could be correlated even if those correlation were low ($r < 0.4$). Finally, 26 items were chosen for the MN size. For example, among correlated items, the discomfort at nasal side was positively correlated to nasal root breadth (Figure 4.1). This means that wider nasal root breadth caused higher discomfort

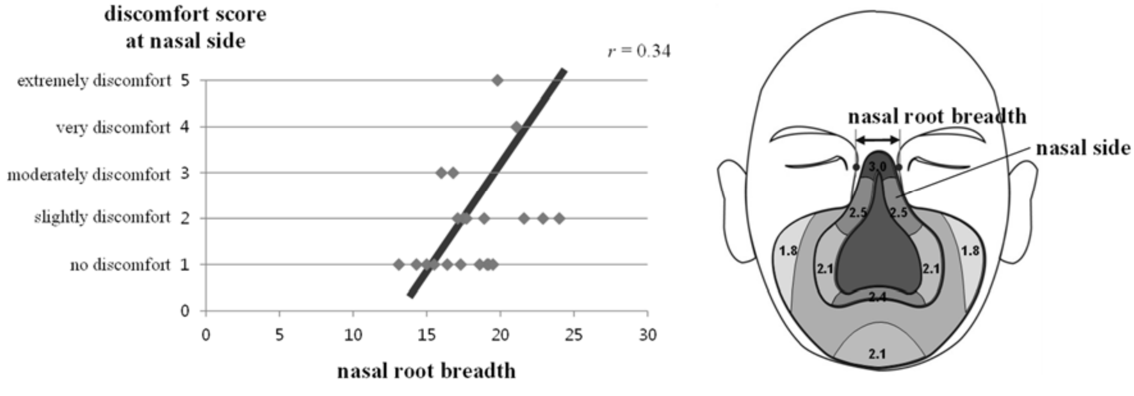

Figure 4.1. Correlation between discomfort at nasal side and nasal root breadth

due to higher pressure of the oxygen mask to the nasal side area. The results of the correlation analysis were applied to identify design solutions quantitatively.

4.2. Development of Design Improvement Strategies

4.2.1. Oxygen Mask Design Dimensions

The oxygen mask size was determined based on the revised sizing system (Figure 3.20), and an oxygen mask design rationality was increased in terms of a size interval. The oxygen mask lengths (nose-to-chin length) and widths (maximum width) were chosen by following steps: (1) determination of the medium size, and then (2) application of size intervals. First, the medium sizes of the existing sizing system (sizing criteria = 87 and 100 mm) and the revised sizing system (sizing criteria = 90 and 100 mm) are similar (Figure 4.2). Therefore, the oxygen mask length of the medium size was

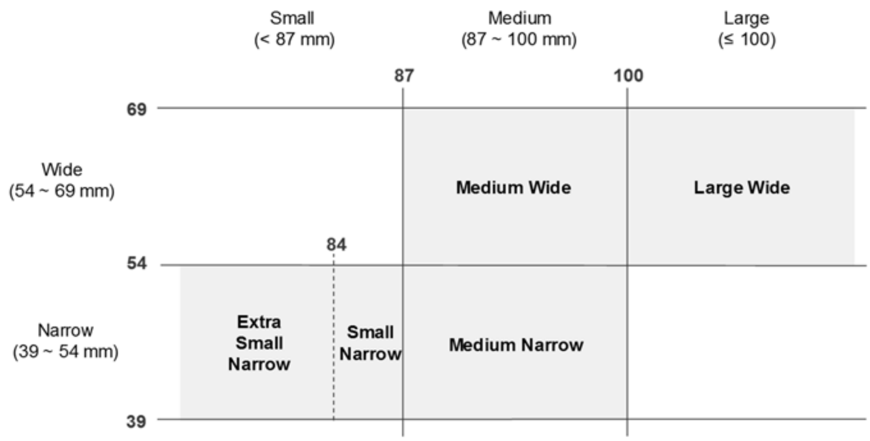

(a) Existing sizing system of the MBU-20/P based on USAF facial anthropometric data

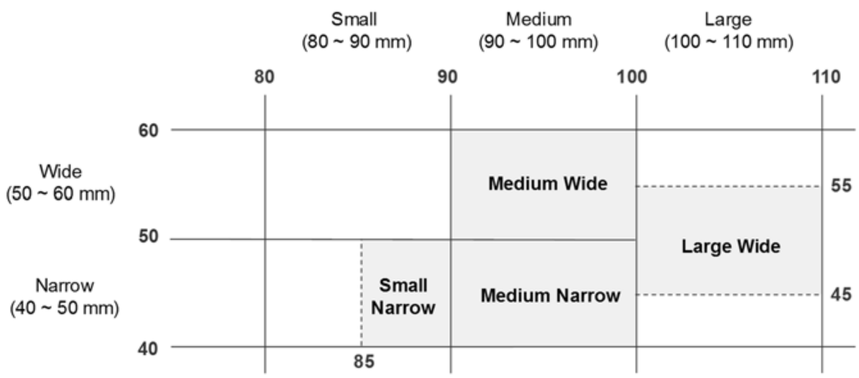

(b) Revised sizing system based on facial anthropometric data of the KAF pilots

Figure 4.2. The existing and revised sizing system of the MBU-20/P

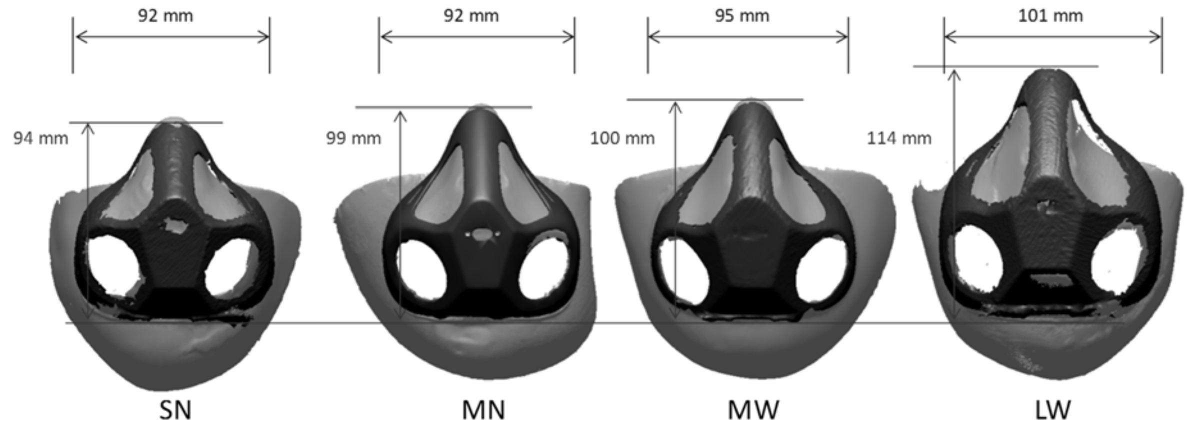

(a) Sizes of the existing MBU-20/P

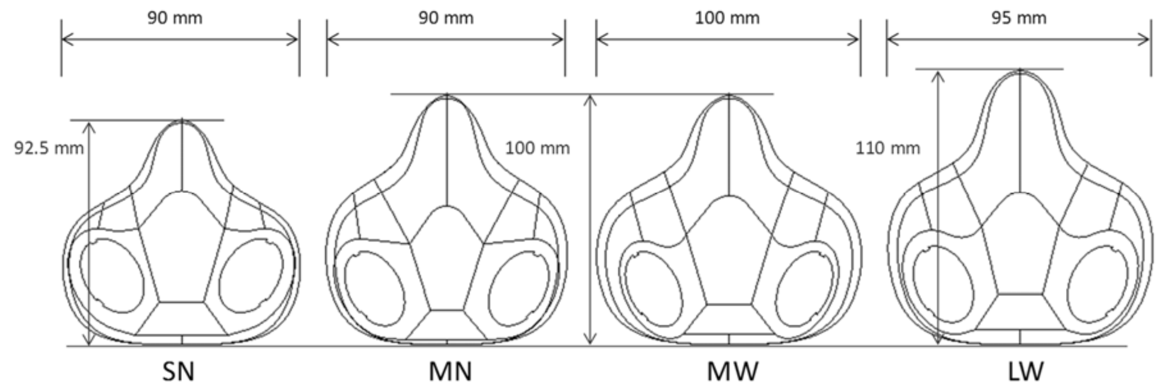

(b) Sizes of the revised oxygen mask (illustrated without facepiece)

Figure 4.3. Comparison of sizes of the existing and revised oxygen mask

determined as 100 mm, which is same as that of the existing oxygen mask. Then, lengths of the other sizes (small and large) were chosen as SN = 92.5 mm and LW = 110 mm based on size intervals (medium – small = 7.5 mm, large – medium = 10 mm) of the revised sizing system as shown in Figure 4.3. In addition, widths of the revised oxygen mask were also determined based on the facial anthropometric data and the revised sizing system. In terms of lip width which determines the width of the oxygen mask sizing system, the KMP (49.9 ± 3.4 mm) is 2.4 mm narrower on average than that of the UMP (52.3 ± 3.7 mm). The sizing criteria of the revised sizing system (sizing criteria = 50 mm) is also 4 mm narrower than that of the existing sizing system (sizing criteria = 54 mm). Therefore, width of the narrow sizes (SN and MN) was determined as 90 mm which is 2 mm narrower than the existing narrow sizes (width = 92 mm). Then, width of wide sizes (MW and LW) was chosen as 100 mm based on the size interval (wide – narrow = 10 mm) of the revised sizing system. However, the present study adjusted the length of LW to increase the accommodation percentage, therefore, the length of LW was decided as 95 mm. In summary, the revised oxygen mask showed consistency in size intervals (Figure 4.4) and this means that the design rationality might be increased. The sizes of

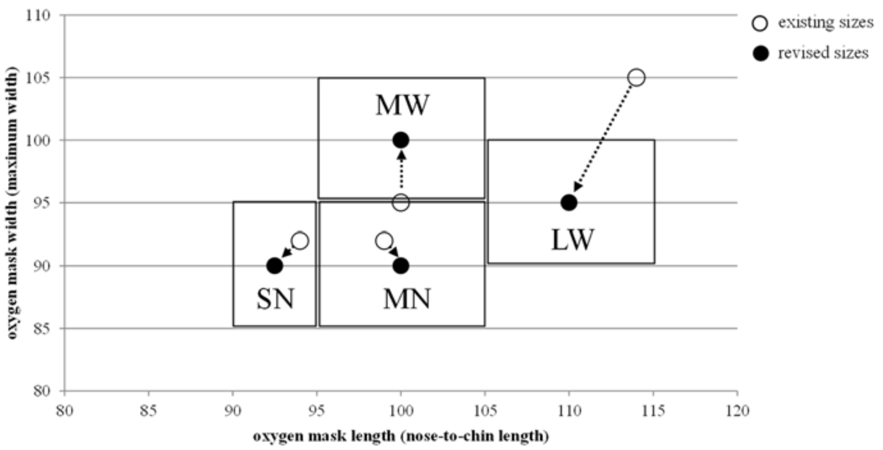

Figure 4.4. Sizes of the existing and revised oxygen masks (blue box presents the revised size categories)

the SN, MN, and MW of the existing oxygen mask (marked as ○ in Figure 4.4) are gathered between 94 ~ 100 mm in length and 92 ~ 95 mm in width, but that of the LW is quite distant from those sizes. Consequently, the sizes of the revised oxygen mask (marked as ● in Figure 4.4) rationally designed by determining the centroids of the revised sizing system can accommodate the KAF pilots effectively.

4.2.2. Size of Nose of Oxygen Mask

Considering the excessive pressure of the existing oxygen mask to the face, nose area of the oxygen mask was widened based on facial measurements. The width of nose area was widened about 5 mm by determining a difference of nasal root breadth between the KMP (20.6 ± 2.5 mm) and the UMP (15.4 ± 1.9 mm) as shown in Figure 4.5.

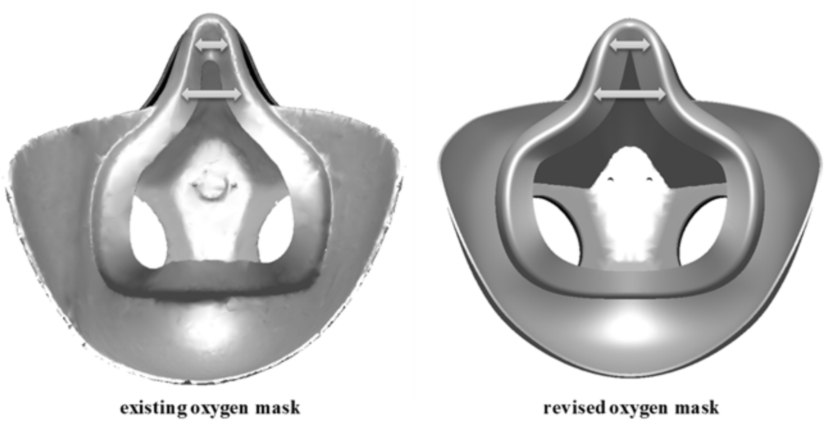

Figure 4.5. Comparison between existing and revised mask designs

4.2.3. Location of Microphone Base

The microphone was transferred to the upper side to avoid contact with pilot's lip. The microphone of the current oxygen mask contacted to 53% of the KAF pilots, because the microphone is located in front of valves in the facepiece as shown in Figure 4.6a and positioned closer to the lip. The present study transferred a location of microphone base to the upper side (2 ~ 3 mm depend on the size), and the microphone could be located to the between valves as shown in Figure 4.6b where it is further back than the current location.

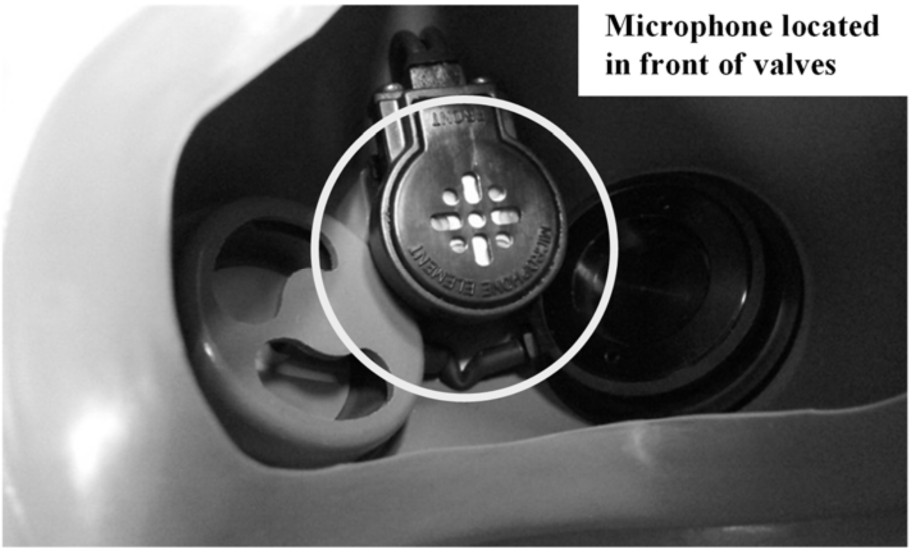

(a) Current location of microphone

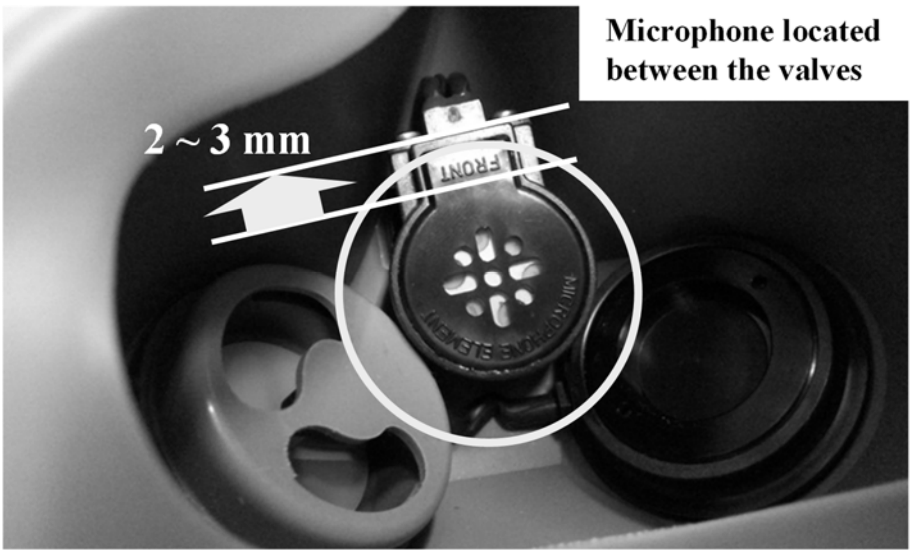

(b) Revised location of microphone

Figure 4.6. The existing and revised location of the microphone

4.2.4. Shape of Face-Mask Contact Area Based on Virtual Fit Assessment

Virtual Fit Assessment (VFA)

The VFA method which can virtually analyze oxygen mask fit by using 3D images of faces and oxygen masks was proposed by the present study (Figure 4.7). A VFA system coded by Matlab 2008a (The MathWorks, Inc., U.S.A.) was used to automatically align the 3D face scan images and the oxygen mask images (e.g., 3D scan image of the existing oxygen mask, or 3D CAD image of the revised oxygen mask) and quantitatively analyze their fit. The system aligns each 3D face image of the KAF pilots (*n* = 336) and corresponding sizes (SN, MN MW, LW) of the oxygen mask image, respectively, by determining the oxygen mask wearing characteristics (wearing position, wearing angle) as presented in Table 3.10 and Appendix C. In the case of the MN size, the oxygen mask wearing characteristics were examined by analyzing the photos of 23 pilots, and then were applied to the 3D face scan images of 121 pilots through the VFA method. Then, oxygen mask fit information (e.g., average and range) for the pilots were identified, and it was applied to an appropriateness evaluation for oxygen mask designs.

The VFA system aligns the 3D mask image to the 3D face image by a 5-step process (data loading, adjustment of vertical location, adjustment of horizontal location, adjustment of angle, evaluation of fit) as shown in Figure 5.2. First, the system loads the 3D face images of the KAF pilots and corresponding 3D mask images one by one. The 3D mask image is located 100 mm in front of the 3D face image. Supramentale landmark is defined as an origin, and supramentale-to-sellion is designated to Y axis for all the 3D face images. A simplified 3D mask image which consists of various points of a design profile of the facepiece and hardshell was used in the VFA. Second, the 3D mask image is vertically transferred based on mask-top-to-sellion distance (v) and mask-bottom-to-supramentale distance (v) shown in Table 3.10). Third, the 3D face image is horizontally transferred

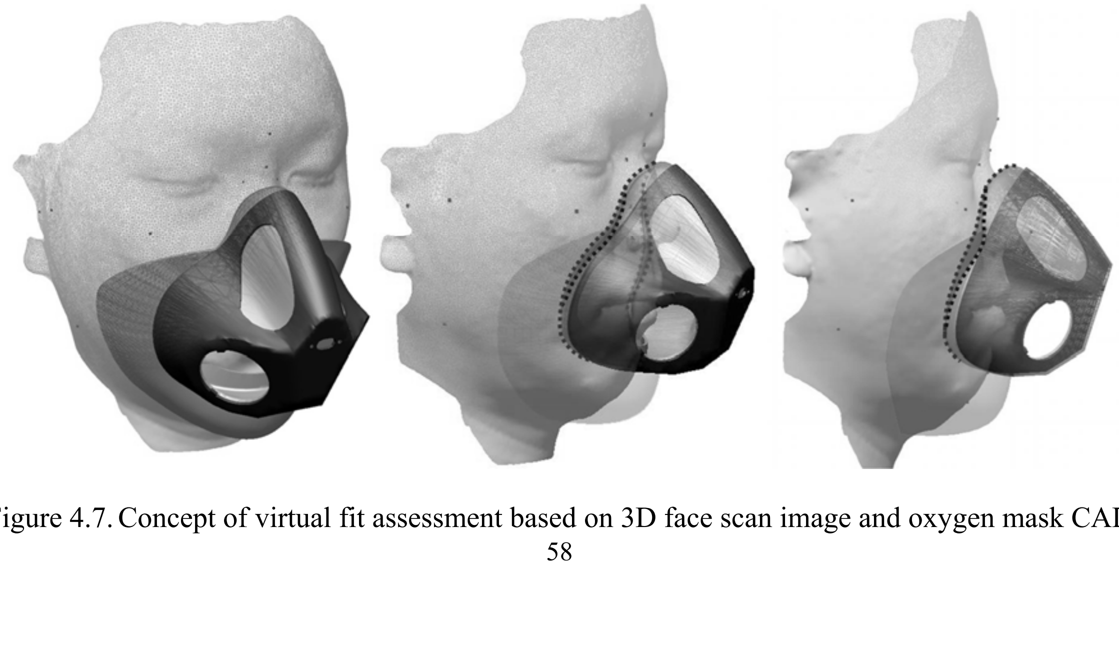

Figure 4.7. Concept of virtual fit assessment based on 3D face scan image and oxygen mask CAD

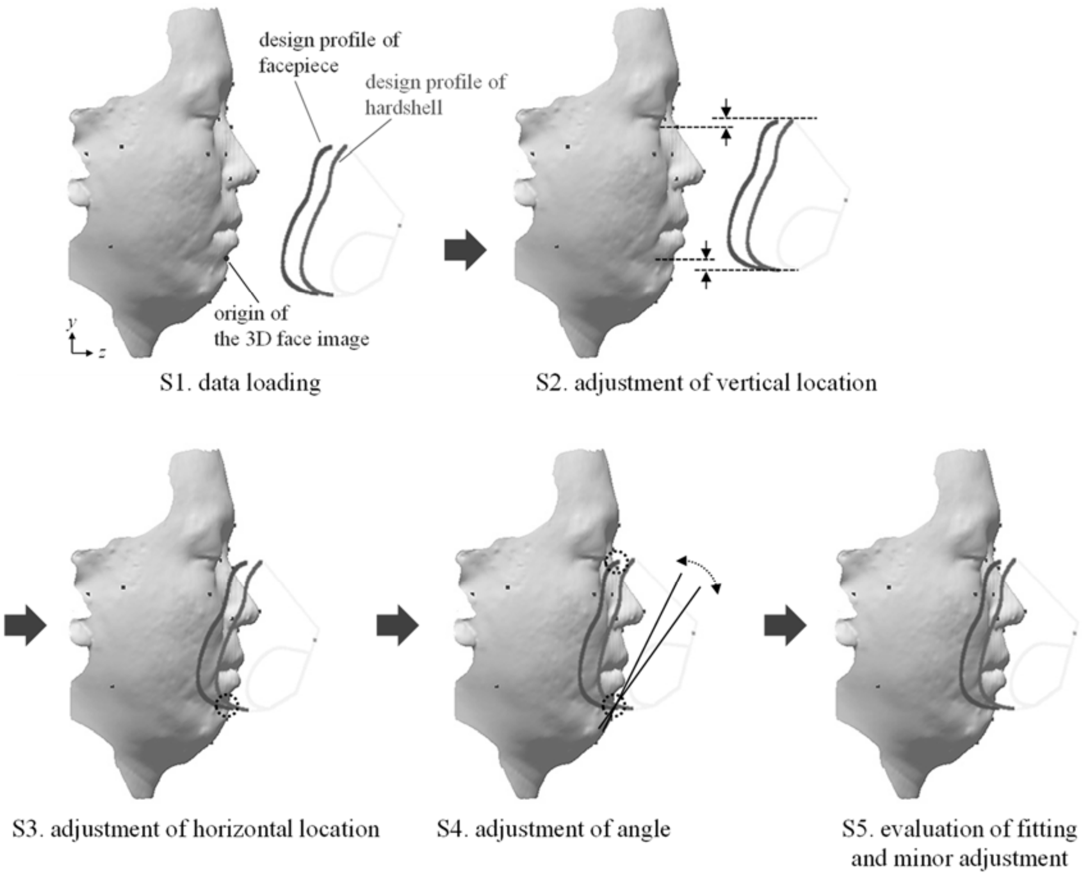

Figure 4.8. Process for virtual fit assessment

to locate the mask's bottom position to the chin according to mask-bottom-to-supramentale distance (h). Fourth, the 3D face image is rotated to locate the mask's top position to the nasal root according to mask-top-to-sellion distance (h) and wearing angle. Lastly, the 3D mask image is slightly adjusted (within ±5 mm and ±5˚) to be located to average value of the oxygen mask wearing characteristics as closely as possible.

Design of Initial Shape of the Revised Oxygen Mask

An initial shape of the revised oxygen mask was identified based on the existing design landmarks of the MBU-20/P. The design landmarks proposed by M. E. Gross et al. (1997) was projected to the RFM as shown in Figure 4.9. Then, the initial profile for the revised hardshell was found by cubic spline interpolation based on the projected landmarks as shown in Figure 4.10b. Facepiece design landmarks are not mentioned by M. E. Gross et al. (1997); therefore, the present study identified a design profile of the existing facepiece through 3D scanning (Figure 4.10a). An initial design profile for the revised facepiece was determined by defining facepiece design landmarks which were created based on the profile of the existing facepiece (Figure 4.10b). Therefore, the existing and the initially revised design profiles of the facepiece and hardshell look similar.

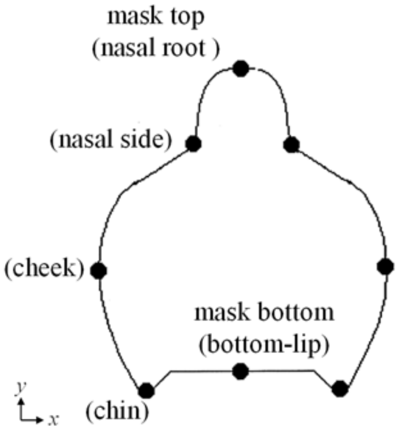

(a) Concepture illustration of 8 hardshell design landmarks proposed by M. E. Gross et al. (1997)

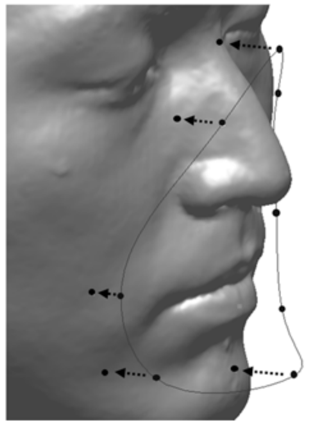

(b) New hardshell design landmarks which generated by projection of the existing design landmarks onto RFM's face (blue dots: existing design landmarks, black dots: projected points)

Figure 4.9. The existing and initially revised hardshell design landmarks

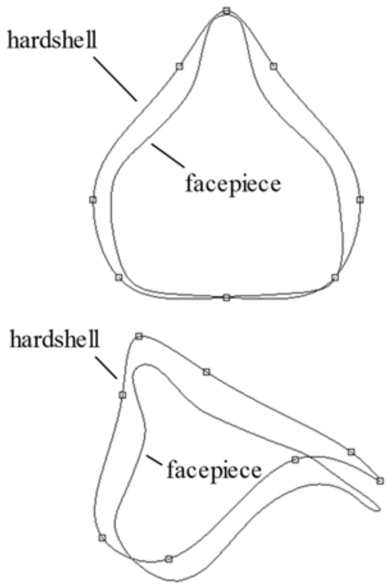

(a) Hardshell shape (outer line) of current mask generated based on design landmarks and facepiece shape (inner line) extracted by 3D scan

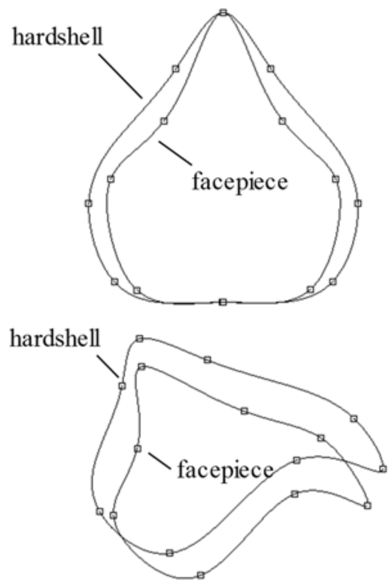

(b) Initial hardshell shape (outer line) generated by cubic spline interpolation based on new hardshell design landmarks and initial facepiece shape (inner line) generated based on hardshell shape

Figure 4.10. Shape of hardshell and facepiece (top view and perspective view)

Iterative Design Revision through Virtual Fit Assessment

The initial design profile for the revised oxygen mask was iteratively revised through the VFA method to find the best result for the KAF pilots. The VFA system aligned the initial design to the 3D face images, and then analyzed their fit as shown in Figure 4.11b. While the existing oxygen mask design

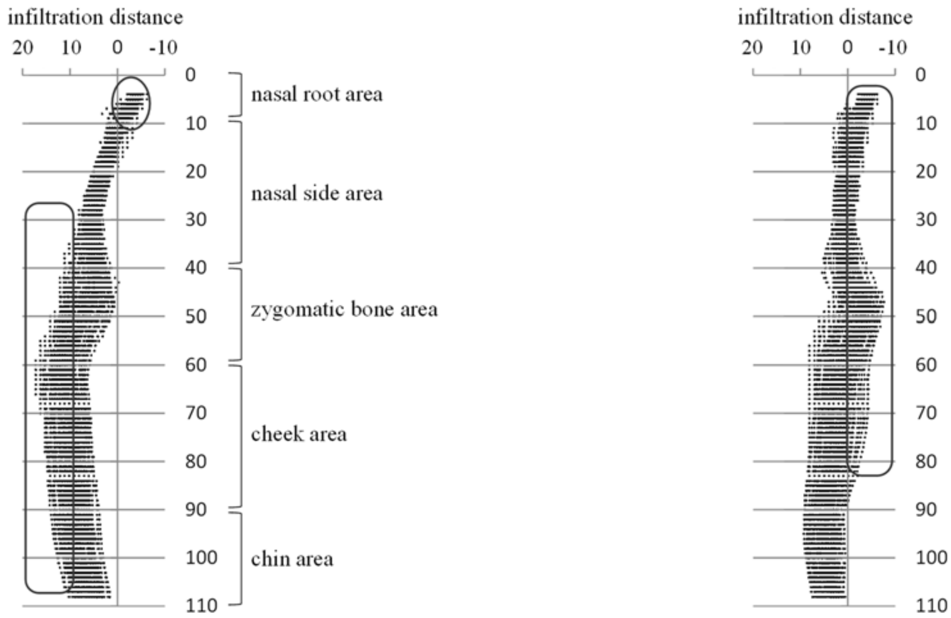

(a) Existing mask (b) Initial revision

Figure 4.11. Results of fit analysis for the existing and initially revised oxygen mask designs

showed excessive fit (infiltration distance > 10 mm) at the nasal side, zygomatic bone, and cheek area and lack of fit (infiltration distance < 0 mm) at the nasal root area to the face (Figure 4.11a), the initially revised design generated based on the RFM showed lack of fit (infiltration distance < 0 mm) at from the nasal root to the cheek area. Of course the mask design based on a facial shape of the RFM might not be fit to the other pilots' faces, therefore, the present study iteratively revised the design profile by referring to their result of fit analysis. An appropriate range of fit is important to avoid discomfort due to excessive pressure or oxygen leakage due to lack of fit (Dai et al., 2011). The present study tried to identify the appropriate fit range by analyzing the infiltration distance and the user preferences together; however, no statistical relationship was found between them at $\alpha = 0.05$. For this reason, the appropriate fit range (thick red lines in Figure 4.12) was defined by a panel of ergonomist based on comprehensive understanding among the infiltration distance, the user preferences, a flexible material of the facepiece, and the shape of the reflective seal in the facepiece. The reflective seal can prevent oxygen leakage at the nasal root area (vertical location = 1 ~ 10 mm) even at the infiltration distance < 0 mm. The final design profile for the revised oxygen (Figure 4.12c and 4.13c) mask was found by iteratively adjusting design landmarks and analyzing through the VFA system. Two design landmarks were added to design nose shape of the oxygen mask in detail. The design revision was conducted by using Rhino 3D 4.0 (McNeel, U.S.A.) CAD software. Table 4.1 and Figure 4.14 present a satisfactory percentage of the existing, initially revised, and finally revised oxygen mask designs. The satisfactory percentage of the final revision (82.3%) was increased 27% on average from that of the existing design (55.3%).

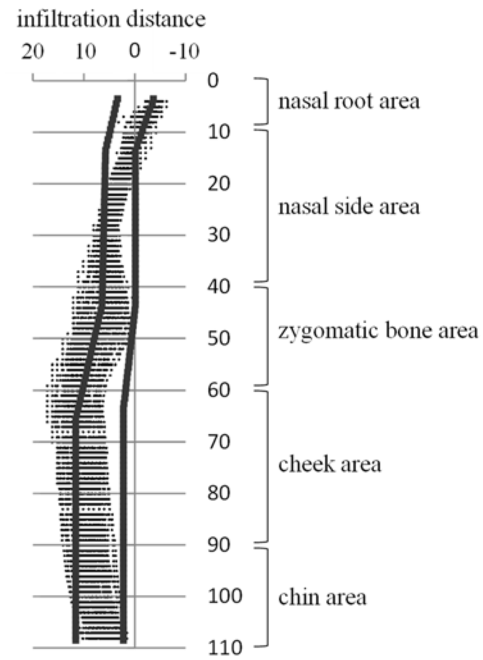

(a) Existing design (b) Initial revision (c) Final revision

Figure 4.12. Results of fit analysis according to the appropriate fit range

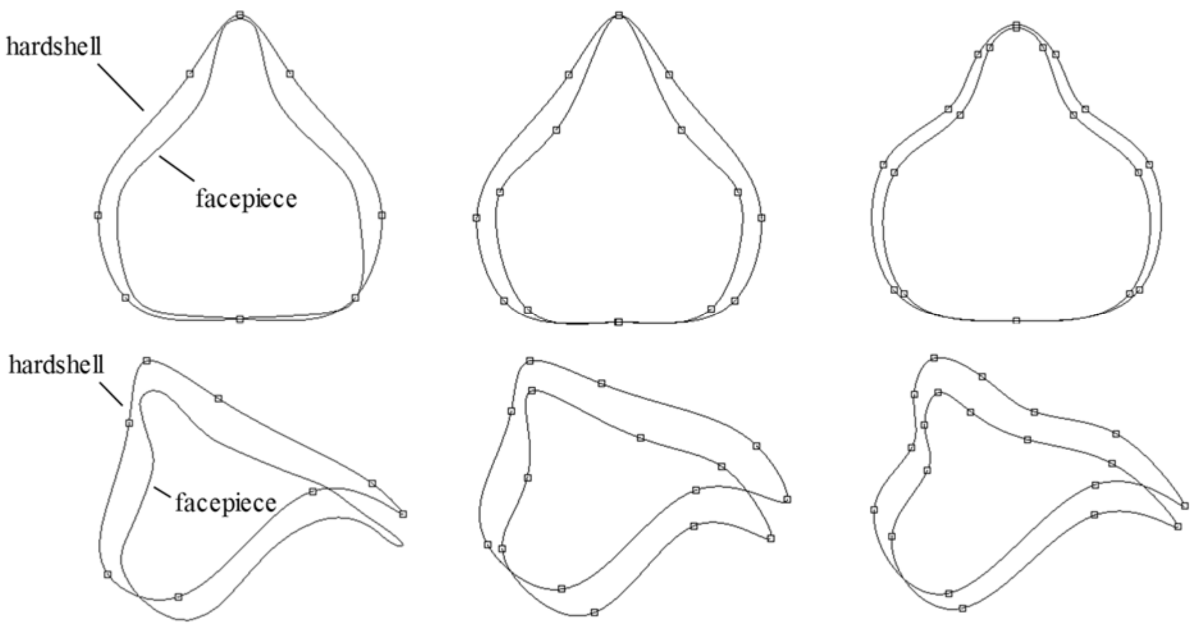

(a) Existing design (b) Initial revision (c) Final revision

Figure 4.13. Design profiles of the existing, initially revised, and finally revised oxygen masks

Table 4.1. The percentage of pilots whose virtual mask fit satisfy the design criteria (illustrated for the MN size)

No.	Facial area	Current mask design	Initial revision	Final revision
1	nasal root area	34% ~ 76%	13% ~ 33%	60% ~ 84%
2	nasal side area	47% ~ 100%	32% ~ 83%	75% ~ 100%
3	zygomatic bone area	11% ~ 44%	21% ~ 58%	50% ~ 78%
4	cheek area	27% ~ 74%	55% ~ 95%	79% ~ 90%
5	chin area	75% ~ 96%	94% ~ 96%	90% ~ 96%
	overall average (SD)	55.3% (26.0)	65.1% (23.9)	82.3% (10.5)

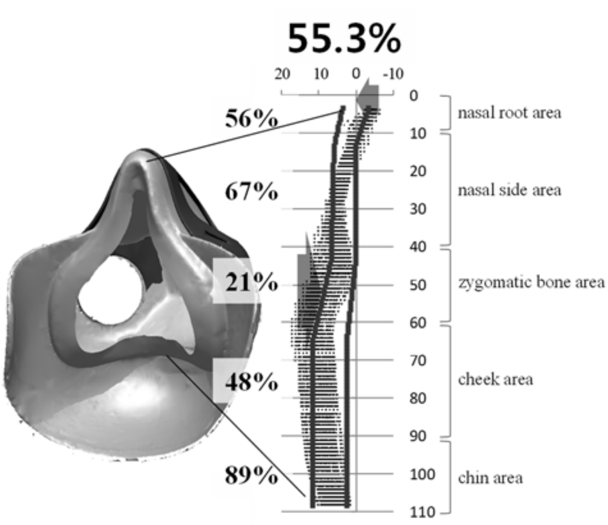

(a) Existing design

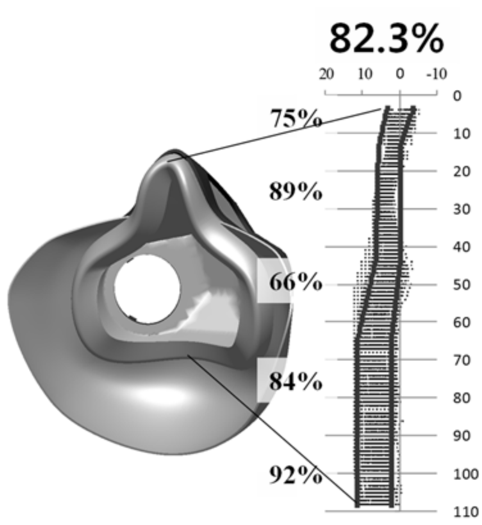

(c) Final revision

Figure 4.14. Results of the VFA: satisfactory percentages for the oxygen mask designs

4.3. Design Revision of MBU-20/P Oxygen Mask

The revised oxygen mask CAD was generated based on the revised design profile and the 3D scan image of the existing oxygen mask. First, the 3D scan image of the existing oxygen mask was redrawn to the CAD image. Then, the revised size, width of nose area, adjusted location of microphone base, and revised design profile were applied to the CAD image. A frontal area of the oxygen mask, reflective seal, and wing of facepiece were not modified by the present study. RapidForm™ 2006 (Inus Technology, Inc., South Korea) and Rhino 3D 4.0 (McNeel, U.S.A) software were used to create the CAD of the revised oxygen mask. Figure 4.14 comparatively presents the existing and revised oxygen masks designs.

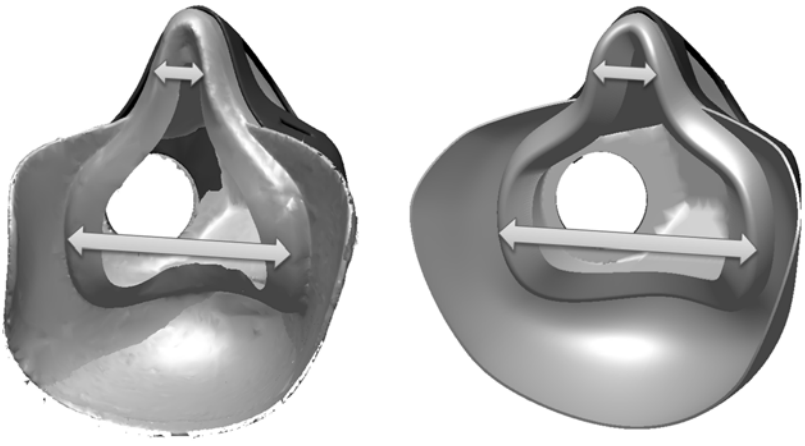

(a) Perspective view

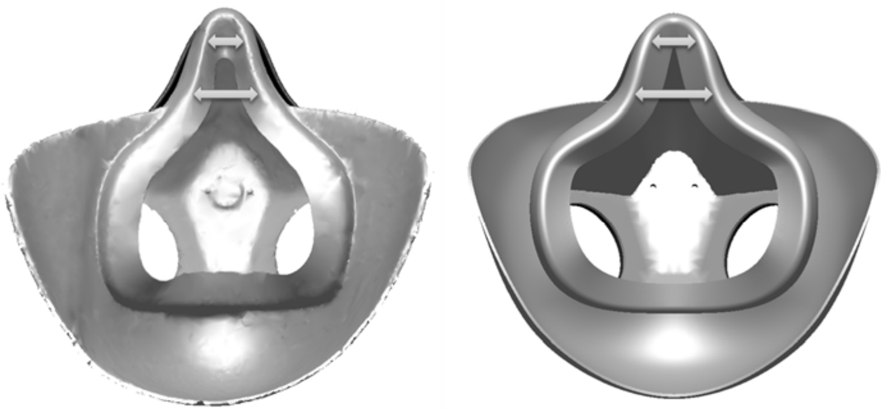

(b) Front view

(c) Side view

Figure 4.15. Comparison between the existing and revised mask designs

Chapter 5. OXYGEN MASK EVALUATION

An ergonomic usability evaluation between the existing and revised oxygen masks was conducted with the KAF pilots and the KAF Academy cadets in terms of discomfort, pressure, and suitability for military equipment (Figure 5.1). The prototype of the revised oxygen mask was manufactured and compared with the existing oxygen mask. The discomfort of the existing and revised oxygen masks was evaluated using a questionnaire developed by the present study. The pressure of the existing and revised oxygen masks was measured by *Prescale pressure indicating film* (Fujifilm, Japan) and was analyzed by a pressure analysis system developed by the present study. In addition, the revised mask's suitability for military equipment was evaluated in the situations of pressure breathing for gravity (PBG) mode, low atmospheric pressure, and high-G. Finally, design revision effects were analyzed and rationality and validity of the oxygen mask design process was evaluated.

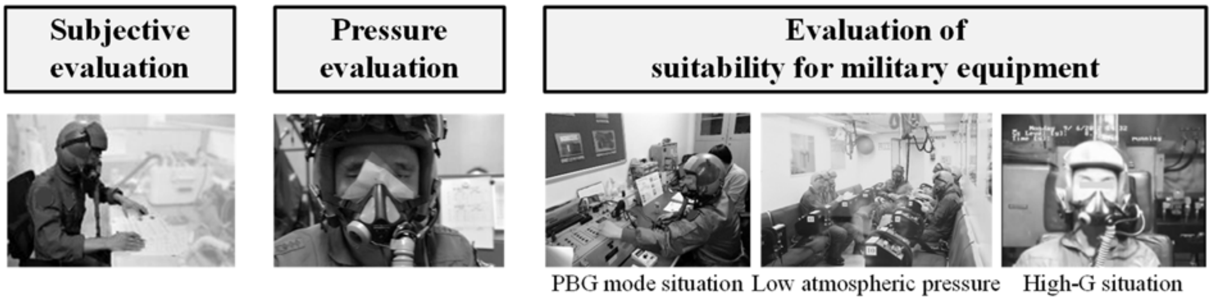

Figure 5.1. Evaluation methods for oxygen mask

5.1. Participants

The usability evaluation was conducted with 83 KAF pilots (81 males and 2 females) who currently use the MBU-20/P oxygen mask and 58 KAF Academy cadets (32 males and 26 females) who were potential users of the oxygen mask. 20 out of 83 pilots were randomly selected for test in PBG mode situation, and an additional 5 male pilots participated in the evaluation of suitability of the revised oxygen mask in high-G and low atmospheric pressure situations. The evaluation was conducted at three KAF bases, the KAF Academy, and the Aerospace Medical Center of KAF. Detailed information about participants is not presented in this dissertation at the request of the KAF.

5.2. Apparatus

The present study manufactured prototypes of the revised oxygen masks by sizes (SN, MN, MW, and LW). To evaluate the oxygen masks under similar conditions, the present study used similar materials as the MBU-20/P for the prototype of the revised oxygen mask (facepiece and hardshell). Material properties (e.g., hardness, toughness, tensile, and elasticity) were determined by a panel of materials experts. The existing components (e.g., valves, straps, and microphone) were used with the revised facepiece and hardshell.

A combined aircrew systems tester (CAST, Gentex Corp., U.S.A.), high-G training equipment, and an aviation physiology training chamber were used for the evaluation of suitability for military equipment. The pilot oxygen mask is used for a stable supply of oxygen to the pilot while a mission is conducted at high altitude where oxygen is lacking and in high gravity acceleration where the oxygen mask can slip to downward on the face. Therefore, the prototype of the revised oxygen mask was required to be tested in flight-like environments which simulate lack of oxygen and high-G. The CAST (Figure 5.2a) is equipped at each Air Force base to check defects of the oxygen mask (e.g., crack of hose or valves) by supplying air to the mask. The CAST can simulate the PBG mode which is

(a) Evaluation in the PBG mode

(a) Evaluation in high gravity

(b) Evaluation in low atmospheric pressure

Figure 5.2. Apparatus used for the oxygen mask evaluation

an excessive oxygen supplement mode automatically operated during high-G situations. The revised oxygen mask was evaluated in the PBG mode of the CAST system to identify its stability and suitability for military equipment. The aviation physiology training chamber and the high-G training equipment at the Aerospace Medical Center are part of a regular training facility for the KAF pilots. The aviation physiology training chamber (Figure 5.2b) can simulate various atmospheric pressure corresponding altitude (0 ~ ≥25,000 ft.), and the chamber supplies three types of air according to altitude (< 25,000 ft.: supplement of air with 20% oxygen, ≥ 25,000 ft. situation: supplement of 100% oxygen, emergency mode: excessive supplement of 100% oxygen at any altitude). The present study evaluated the stability of the revised oxygen mask according to the various types of air supply. Lastly, the high-G training equipment (Figure 5.2c) can simulate various gravity acceleration (1 ~ ≥ 9G), the present study evaluated the slippage of the existing and revised oxygen masks up to 9G with onset rate 0.2 G/s during 50 ~ 60 seconds. During the experiment, the pilot's face was recorded.

5.3. Methods

5.3.1. Evaluation Protocol for Oxygen Mask Comparison

The usability evaluation was conducted by a four-step protocol (introduction, mask selection and fitting, evaluation, debriefing) with the pilots and cadets. Figure 5.3 presents the protocol for the pilot participants. First, the study purpose and evaluation process were introduced to the participant and they signed an informed consent form. Second, the participant chose one of the revised oxygen masks among four sizes considering their size and fit. Then, the selected mask was fitted to the participant's

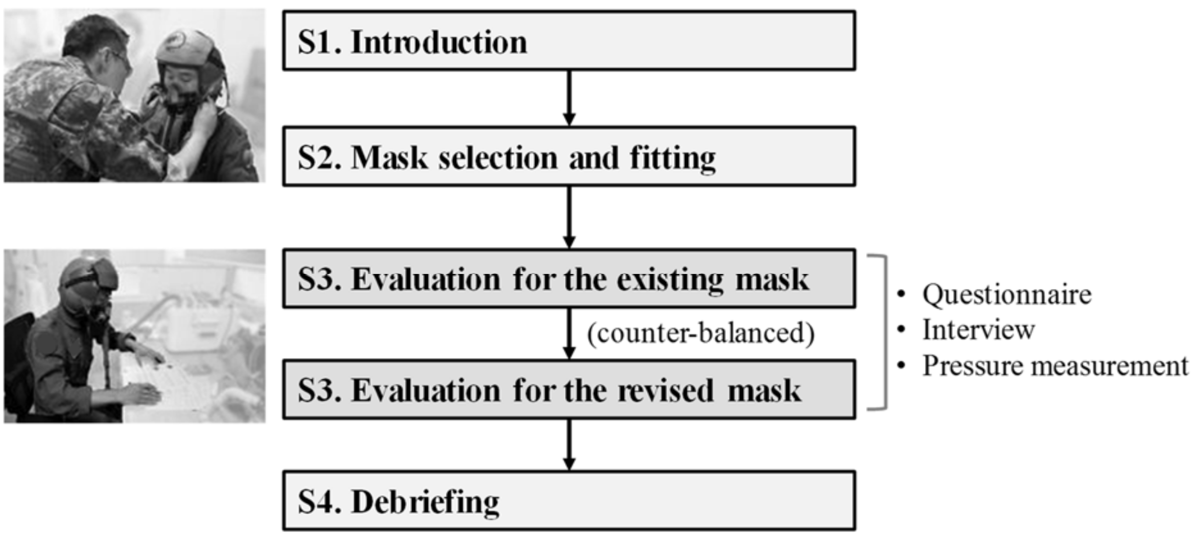

Figure 5.3. Oxygen mask evaluation protocol for the pilot

face by receiving assistance from noncommissioned officers according to a technical order about oxygen mask fitting. Third, their own MBU-20/P oxygen mask and the selected oxygen mask prototype were evaluated, respectively. Pilots wore the existing or revised oxygen masks and were interviewed about the oxygen mask for 10 minutes. Next, the discomfort was evaluated by a questionnaire and the pressure was measured using a pressure film. The evaluation order of the existing and revised oxygen masks was counterbalanced. Lastly, a debriefing about the experiment was verbally surveyed and their participation was compensated. On the other hand, a similar evaluation protocol was applied to the cadets. However, because the cadets do not have their own oxygen masks, they selected both the existing and revised oxygen masks and fit them to their faces, at the second step of the protocol. Also, the discomfort of the existing and revised oxygen masks was evaluated for three minutes, respectively. The pressure measurement was not applied for the cadets because the cadets do not exactly know how they wear the oxygen mask in flight situations. Therefore, the cadets evaluated only their preferences by comparing two masks.

Subjective Evaluation

The discomfort of the existing and revised oxygen masks was evaluated using the questionnaire (Figure 5.4 and Appendix D) prepared by the present study. The discomfort caused by pressure (0: no discomfort, 1: rare discomfort, 4: moderate discomfort, 7: extreme discomfort) and oxygen leakage (0: no leakage, 1: rare leakage, 4: moderate leakage, 7: extreme leakage) were evaluated by six (nasal root, nasal side, zygomatic bone, cheek, bottom lip, and chin) facial areas (Figure 5.5), respectively. The discomfort caused by slippage (0: no slippage, 1: rare slippage, 4: moderate slippage, 7: extreme slippage) and microphone-lip contact (0: no contact, 1: rare contact, 4: moderate contact, 7: extreme contact), and overall satisfaction (-3: very unsatisfied, 0: neutral, 3: very satisfied) were evaluated.

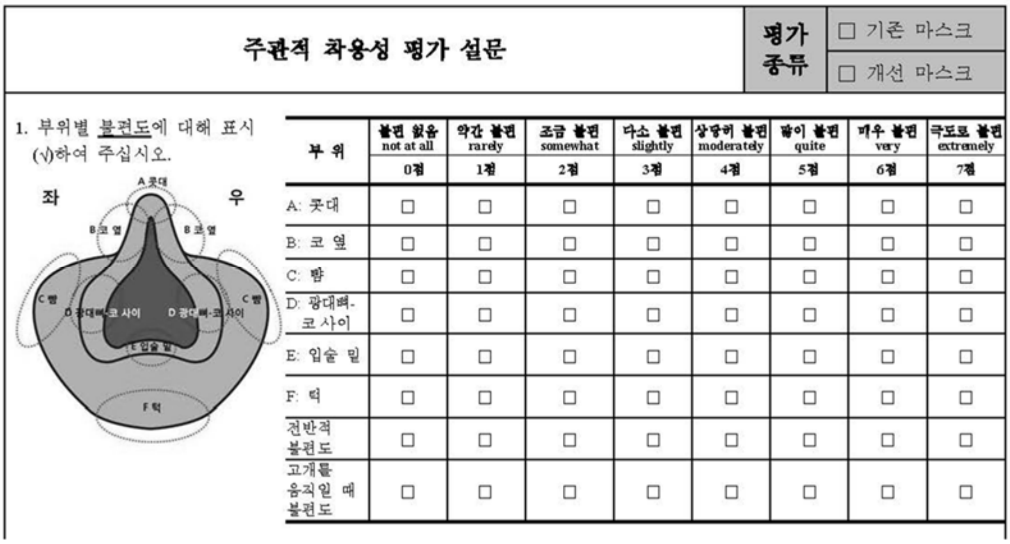
주관적 착용성 평가 설문

평가 종류: □ 기존 마스크 □ 개선 마스크

1. 부위별 불편도에 대해 표시(√)하여 주십시오.

부 위	불편 없음 not at all 0점	약간 불편 rarely 1점	조금 불편 somewhat 2점	다소 불편 slightly 3점	상당히 불편 moderately 4점	많이 불편 quite 5점	매우 불편 very 6점	극도로 불편 extremely 7점
A: 콧대	□	□	□	□	□	□	□	□
B: 코 옆	□	□	□	□	□	□	□	□
C: 뺨	□	□	□	□	□	□	□	□
D: 광대뼈-코 사이	□	□	□	□	□	□	□	□
E: 입술 밑	□	□	□	□	□	□	□	□
F: 턱	□	□	□	□	□	□	□	□
전반적 불편도	□	□	□	□	□	□	□	□
고개를 움직일 때 불편도	□	□	□	□	□	□	□	□

Figure 5.4. Questionnaire for subjective evaluation

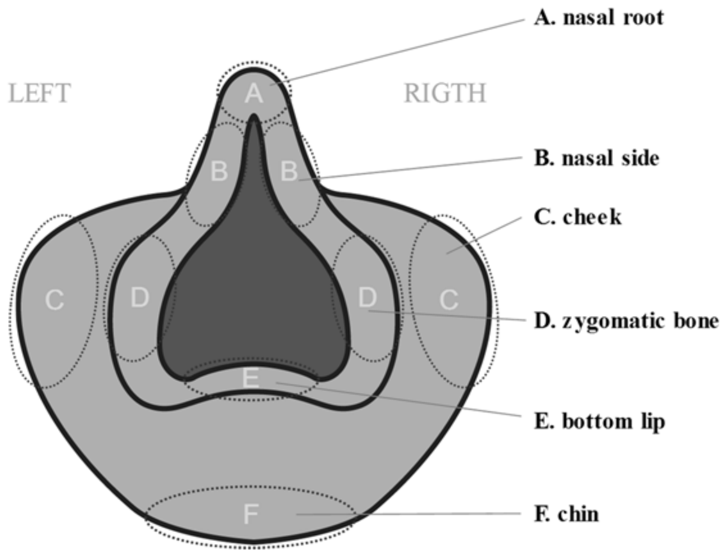

Figure 5.5. Facial areas for subjective evaluation

Pressure Evaluation

The pressure of the existing and revised oxygen masks was measured by the pressure film, and then evaluated by pressure analysis program coded with Matlab 2008a in the present study. The pressure evaluation was conducted by a five-step process (Figure 5.6) in the present study. The film was prepared considering the oxygen mask shape and used to measure amount of pressure between the

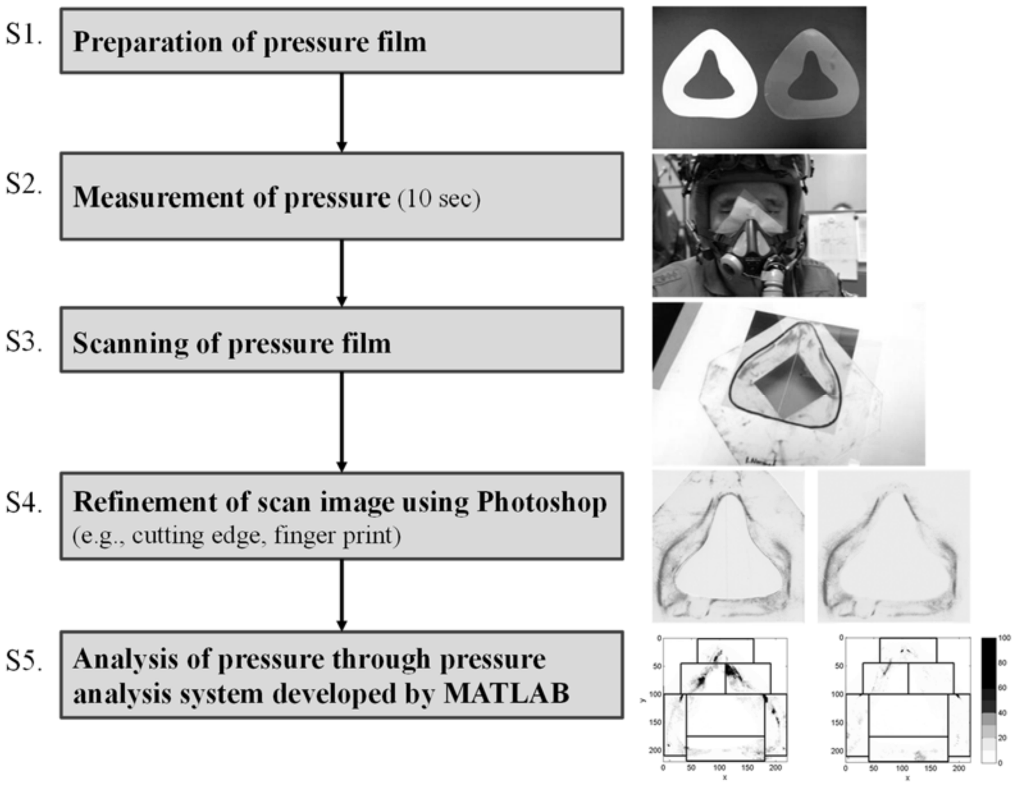

Figure 5.6. Protocol of pressure measurement and analysis

oxygen mask and face. The pressure is represented by darkness (white: no pressure; dark red: maximum pressure) according to the amount of pressure. After scanning the film (image size: 220 × 220 pixels), cut edges, finger prints, and unexpected marks pressed onto the film were eliminated using Photoshop (Adobe Systems Incorporated, U.S.A.). Then, the amount of pressure (pressure index, PI; no pressure: PI = 0, maximum pressure: PI = 100) was identified by the pressure analysis program according to four facial areas (nasal root, nasal side, cheek, and bottom lip) as shown in Figure 5.7. The pressure was classified into low pressure (PI < 40), moderate pressure (40 ≤ PI < 70), and high pressure (PI ≥ 70) by discussion of a panel of ergonomist in the present study. An actual pressure was identified as 40 PI ≒ 14 psi, 70 PI ≒ 25 psi, 100 PI = 29 psi. An average of PI (a mean pressure v

alue of PI > 0 area), a pixel size of moderately pressed area (PI ≥ 40; unit: number of pixels), and a pixel size of excessively pressed area (PI ≥ 70; unit: number of pixels) were analyzed according to the facial areas. Figure 5.8 presents an example of the pressure evaluation result analyzed by the program.

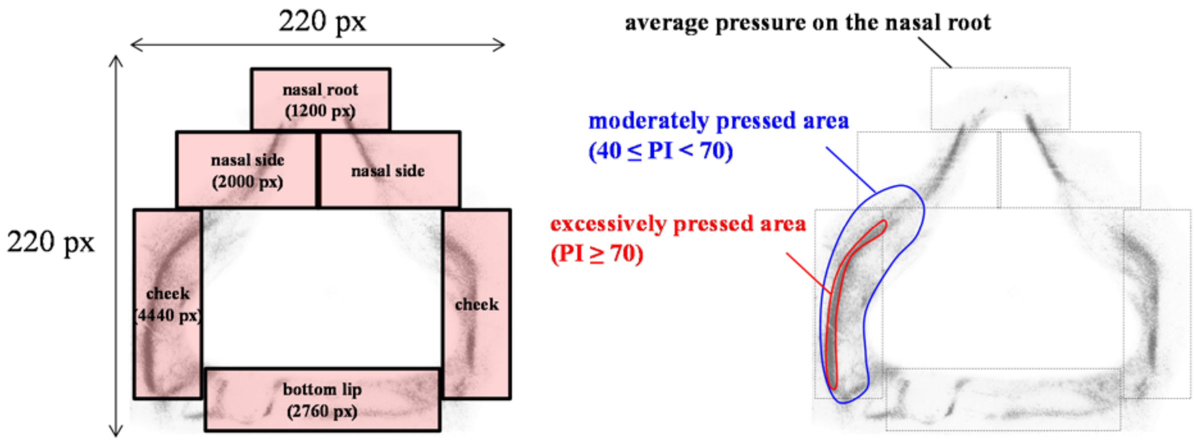

Figure 5.7. Facial areas and analysis criteria of pressure analysis

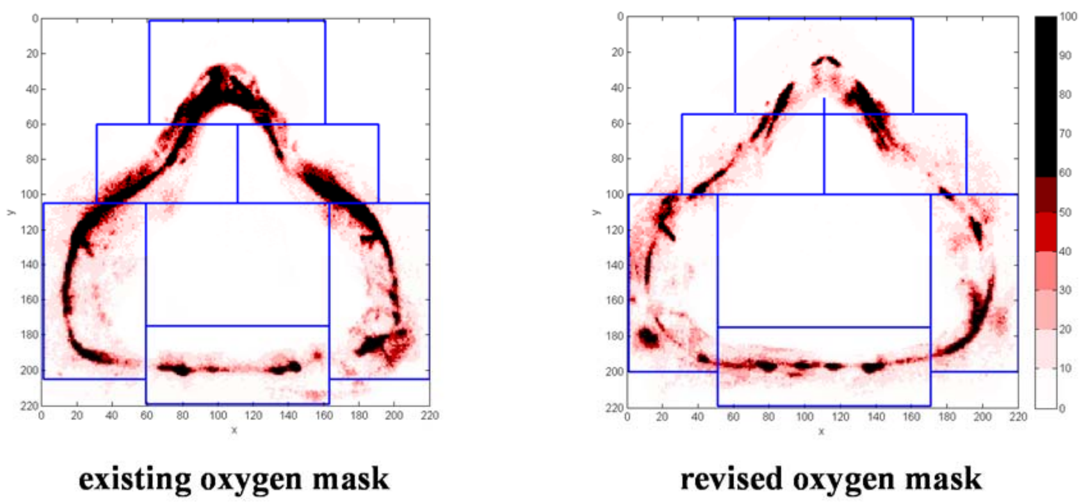

Figure 5.8. Example of pressure measurement result

5.3.2. Suitability Evaluation for Military Equipment

The suitability of the revised oxygen mask was evaluated in the PBG, low atmospheric pressure, and high-G situations. The randomly selected 20 pilots participated in the evaluation in the PBG situation right after the discomfort and pressure evaluation. The conditions of stability (stable or not stable) and problem (no problem or there is a problem) of the revised oxygen mask in the PBG situation was orally reported to the experimenter. The suitability in the low atmospheric pressure situation was evaluated with the revised oxygen mask by a four-step protocol (Figure 5.9): (1) introduction to the experiment and signing an informed consent form, (2) selection and fitting of the revised oxygen mask to the face, (3) administration of the main experiment, and (4) debriefing about the experiment. The conditions of stability and problem of the revised oxygen mask in the low atmospheric pressure situation was orally reported to the experimenter after the main experiment. Lastly, the suitability in the high-G situation was evaluated with the existing and revised oxygen mask by a four-step protocol as shown in Figure 5.10. Pilots' faces were recorded during the main experiment and a slippage of the

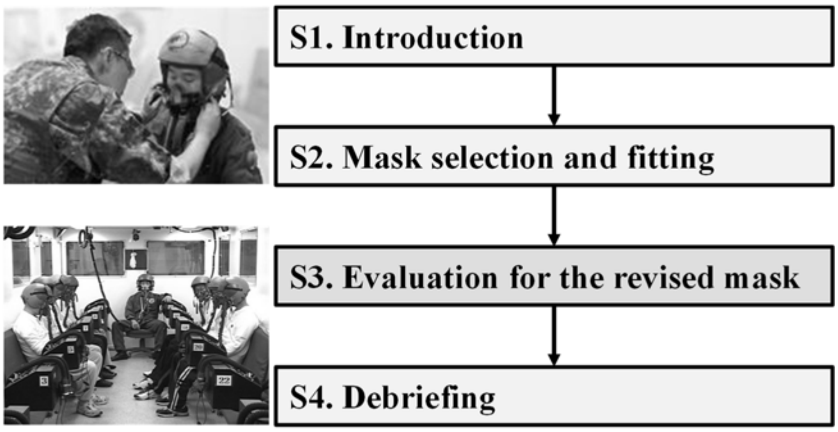

Figure 5.9. Protocol for evaluation in low atmospheric pressure situation

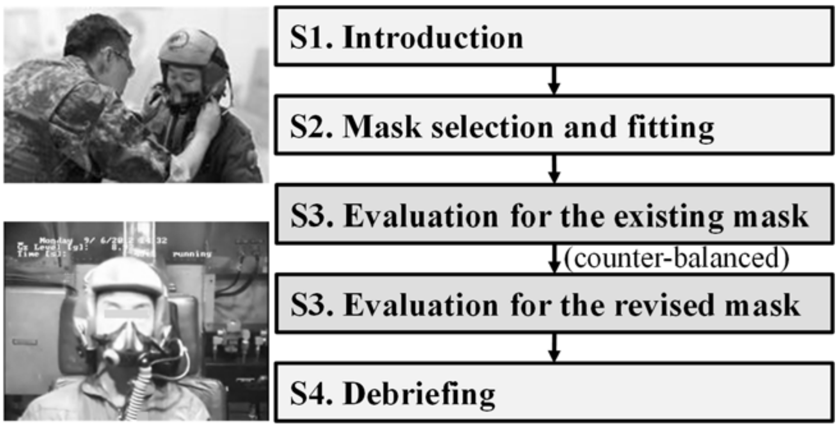

Figure 5.10. Protocol for evaluation in high-G situation

oxygen mask was evaluated using a questionnaire (0 = no slippage, 1 = rare slippage, 4 = moderate slippage, 7 = extreme slippage). The experiment order of the existing and revised oxygen masks was counterbalanced, and a 10-minute break was provided between the experiments.

5.4. Results

5.4.1. Subjective Evaluation

The discomfort of the revised oxygen mask was significantly lower than that of the existing oxygen mask. 32 out of 83 pilots and 24 out of 58 cadets whose discomfort score ≥ 3 (slightly discomfort) at the nasal root or nasal side areas in the existing oxygen mask were selected to identify a design revision effect for the nose area of oxygen mask. The discomfort of the revised oxygen mask was 56% ~ 81% lower on average for the pilots (Figure 5.11) and 33% ~ 60% for the cadets (Figure 5.12) than those of the existing oxygen mask by facial areas. The discomfort was analyzed by the paired *t*-test at $\alpha = 0.05$ (Table 5.1).

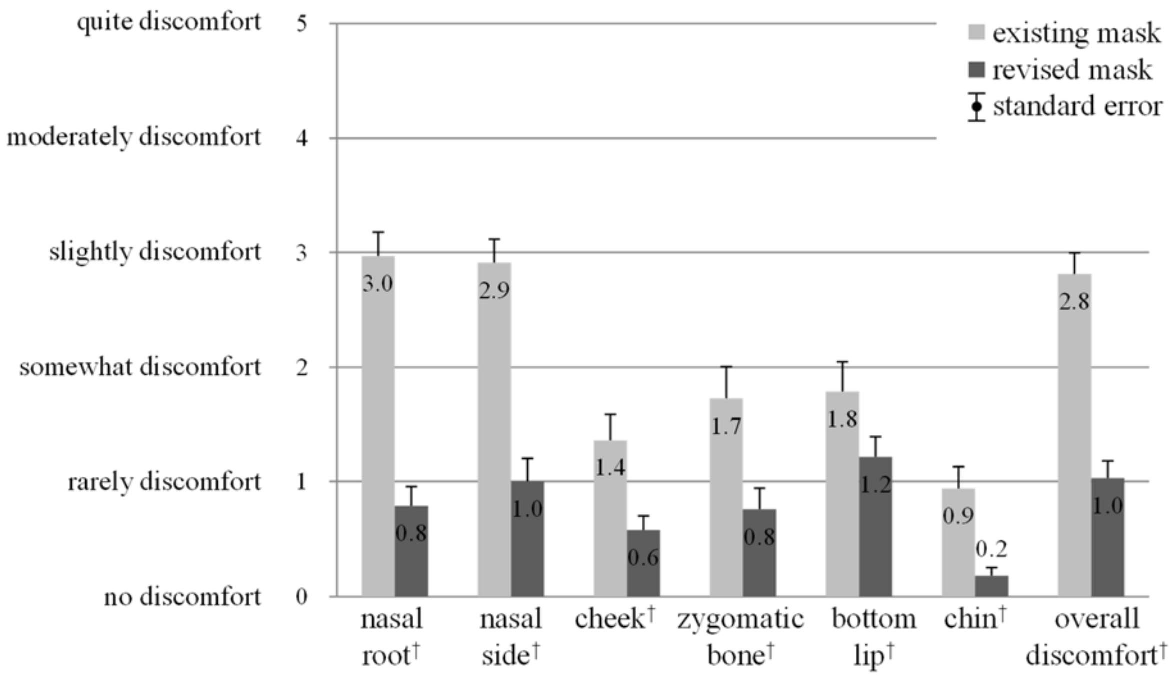

Figure 5.11. Discomfort of pilots ($n = 32$), † $p < 0.05$

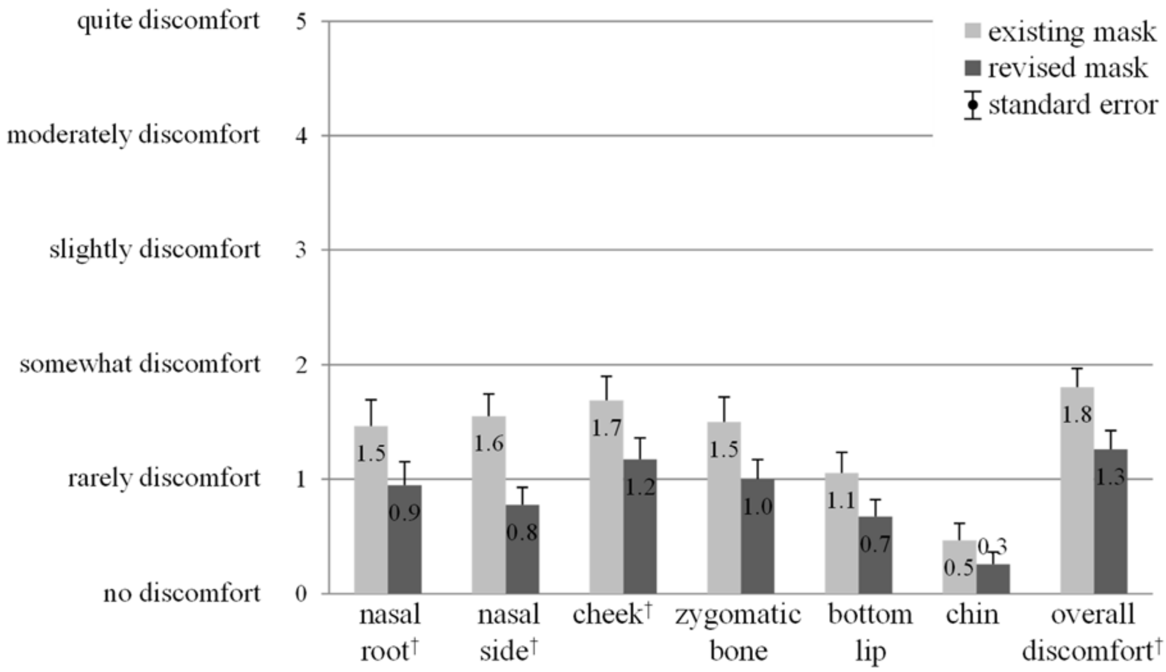

Figure 5.12. Discomfort of cadets ($n = 24$), † $p < 0.05$

Table 5.1. *t*-test result of discomfort analysis

Facial area	Pilots			Cadets		
	Improvement effect	***t*-value**	***p*-value**	**Improvement effect**	***t*-value**	***p*-value**
Nasal root	73%	9.40	**< 0.001**	42%	4.49	**< 0.001**
Nasal side	66%	7.83	**< 0.001**	60%	5.34	**< 0.001**
Cheek	58%	3.50	**0.001**	35%	4.16	**< 0.001**
Zygomatic bone	56%	4.81	**< 0.001**	40%	1.81	0.084
Bottom lip	32%	2.09	**0.045**	58%	1.81	0.083
Chin	81%	4.35	**< 0.001**	33%	0.49	0.627
Overall discomfort	63%	8.93	**< 0.001**	42%	3.46	**0.002**

The revised oxygen mask was preferred in terms of oxygen leakage, slippage, microphone-lip contact, overall satisfaction, and preference. The oxygen leakage of the revised oxygen mask was 50 ~ 87% lower on average than that of the existing oxygen mask by the facial areas. The slippage and microphone-lip contact of the revised oxygen mask showed 43% and 70% lower on average than those of the existing oxygen mask (slippage: $t(78) = 7.32$, $p < 0.001$; microphone-lip contact: $t(78) = 4.08$, $p < 0.001$), respectively. Lastly, the overall satisfaction of the revised oxygen mask was 80% higher than that of the existing oxygen mask ($t(76) = -8.48$, $p < 0.001$). A preference for the oxygen masks was surveyed during the debriefing session of the experiment, and 74% of pilots and 79% of cadets answered that the revised oxygen mask is preferred over the existing one (Figure 5.13).

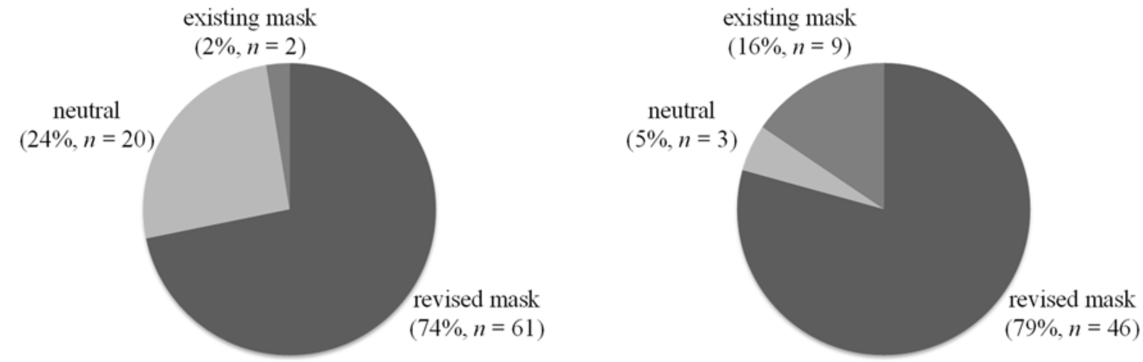

(a) Preference results of pilots (n = 83) (b) Preference results of cadets (n = 58)

Figure 5.13. Preference results

5.4.2. Pressure Evaluation

The revised oxygen mask showed less pressure than the existing mask, and evenly fitted to the pilots' face. According to the interview conducted during the experiment, 42 out of 83 pilots wear the oxygen mask tightly to the face and the other 31 pilots wear the oxygen mask loosely; therefore, the pressure was separately evaluated by oxygen mask wearing types. First, for the pilots who tightly wear the oxygen mask, the average of PI, the moderately pressed area, and the excessively pressed area of the revised oxygen mask were 11% ~ 25%, 24% ~ 33%, and 8% ~ 40% lower on average by facial areas than those of the existing oxygen mask, respectively, except the bottom lip (Figure 5.14a, 5.15a, and 5.16a). In terms of the bottom lip area, the average of PI and the moderately pressed area of the revised oxygen mask were 14% and 23% higher on average than those of the existing oxygen mask, respectively. However, this can be interpreted as a better fit instead of excessive pressure, because the

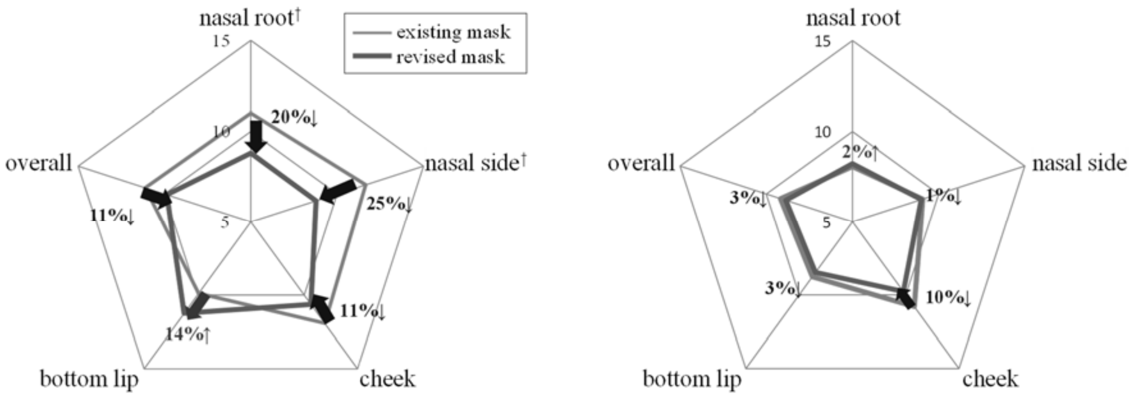

(a) Tightly wear pilots (n = 42) (b) Loosely wear pilots (n = 31)

Figure 5.14. Pressure analysis results for average of pressure, † $p < 0.05$

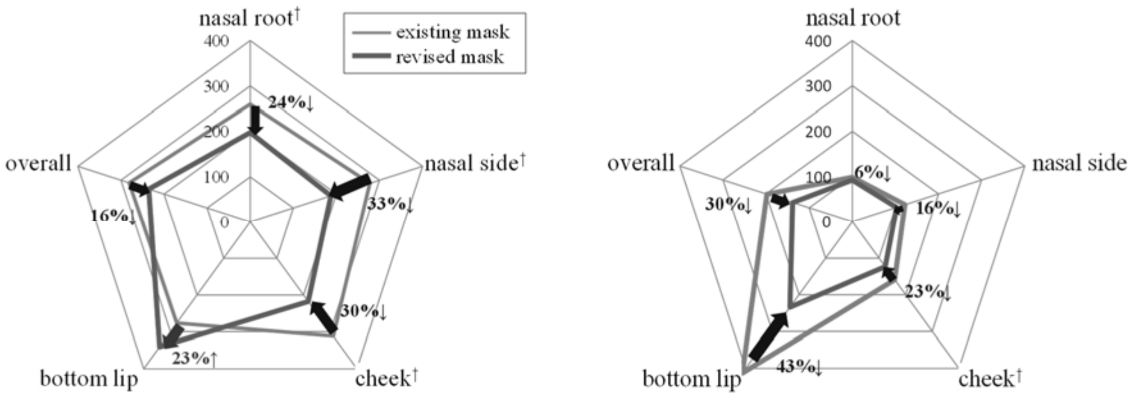

(a) Tightly wear pilots (n = 42) (b) Loosely wear pilots (n = 31)

Figure 5.15. Pressure analysis results for moderately pressed area, † $p < 0.05$

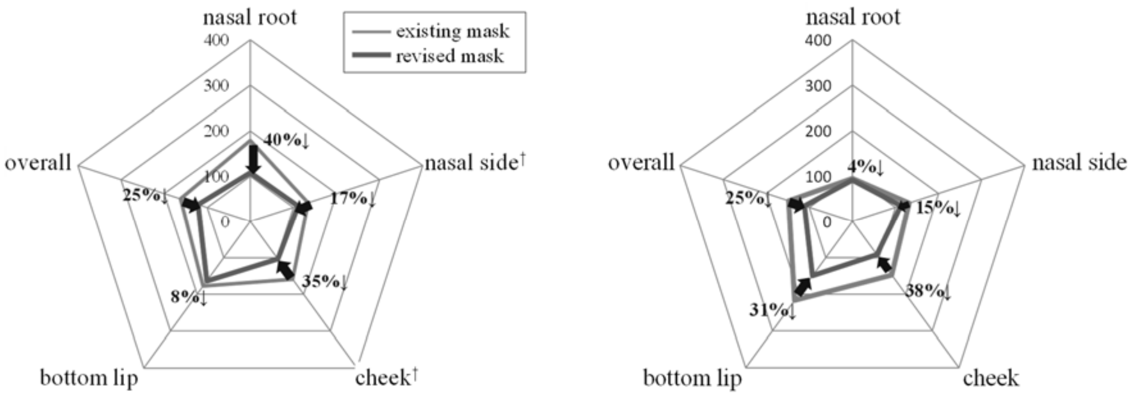

(a) Tightly wear pilots (n = 42) (b) Loosely wear pilots (n = 31)

Figure 5.16. Pressure analysis results for excessively pressed area, † $p < 0.05$

discomfort of the revised oxygen mask was lower than that of the existing oxygen mask at the bottom lip area. Nasal root, nasal side, and cheek partially showed significance; however, no significance was found at the bottom lip area (Table 5.2). On the other hand, for the pilots who wear the oxygen mask loosely, the average of PI of the revised oxygen mask was similar ($|\bar{d}| < 3\%$) to that of the existing oxygen mask except the cheek area. The revised oxygen mask exhibited 10% lower pressure than that of the existing oxygen mask (Figure 5.14b). The normally pressed area and the excessively pressed area of the revised oxygen mask were 6 ~ 43% and 4 ~ 38% lower on average by facial areas than those of the existing oxygen mask, respectively (Figure 5.15b, and 5.16b). Only the cheek showed significant difference ($t(30) = 2.02$, $p = 0.047$) for normally pressed area.

Table 5.2. *t*-test result of pressure analysis

Facial area		Tightly wear pilots			Loosely wear pilots		
		Improvement effect	***t*-value**	***p*-value**	**Improvement effect**	***t*-value**	***p*-value**
Average of pressure	Nasal root	**20%**	**2.03**	**0.048**	-2%	-0.18	0.859
	Nasal side	**25%**	**4.87**	**<0.001**	1%	0.13	0.893
	Cheek	11%	1.90	0.061	10%	1.85	0.070
	Bottom lip	-14%	-1.26	0.215	3%	0.36	0.719
Moderately pressed area	Nasal root	24%	1.78	0.081	6%	0.13	0.897
	Nasal side	**33%**	**4.75**	**<0.001**	16%	1.69	0.096
	Cheek	**30%**	**2.00**	**0.049**	**23%**	**2.02**	**0.047**
	Bottom lip	-23%	-1.41	0.215	43%	1.55	0.131
Excessively pressed area	Nasal root	40%	1.45	0.155	4%	0.42	0.678
	Nasal side	**17%**	**3.22**	**0.002**	15%	0.84	0.404
	Cheek	**35%**	**2.22**	**0.029**	38%	1.78	0.079
	Bottom lip	8%	-1.72	0.093	31%	0.65	0.518

5.4.3. Suitability Evaluation for Military Equipment

The revised oxygen mask showed suitability for military equipment in terms of PBG, low atmospheric pressure, and high-G situations. The revised oxygen mask was orally reported by the participants to have stability and no problems according to the oxygen supply types in the situations of PBG and low atmospheric pressure. Additionally, the revised oxygen mask showed less slippage in the high-G situation. According to the questionnaire, the slippage of the revised oxygen mask was 86% lower on average than that of the existing oxygen mask ($t(4) = 2.95$, $p = 0.042$). In addition to the questionnaire, the mask slippage was identified through video analysis as illustrated in Figure 5.17. Distances between sellion to the mask top at 1G and 9G situations were measured, and then the relative difference of the slippage distance between the existing and revised oxygen masks was compared by pilots ($n = 4$). The slippage distance of the revised oxygen mask was 31 ~ 83% shorter than that of the existing oxygen mask, but no significance was found ($t(3) = 1.71$, $p = 0.185$).

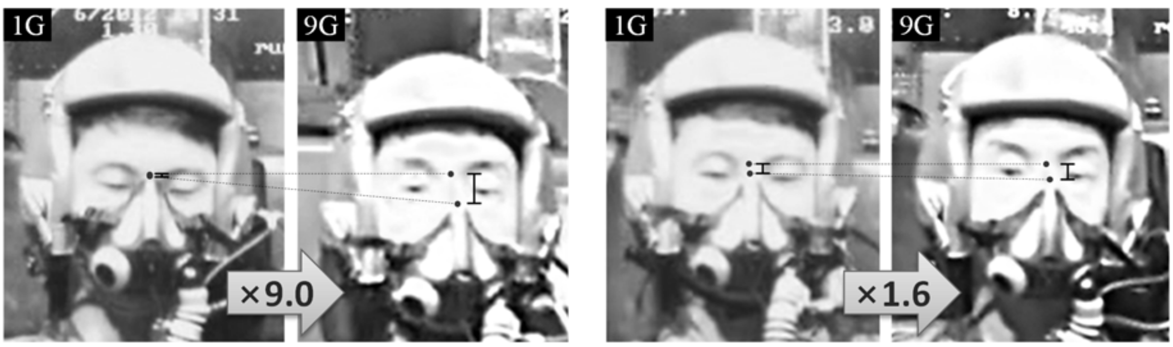

(a) Existing oxygen mask (b) Revised oxygen mask

Figure 5.17. Oxygen mask slippage distance identified by video analysis (illustrated)

Chapter 6. DISCUSSION

6.1. 3D Facial Anthropometry

The present study selected 22 facial dimensions as those required to design a pilot's oxygen mask by a comprehensive review of existing face anthropometric studies and the recommendations of a panel of experts. Of the 107 facial dimensions identified by reviewing 15 studies on face anthropometry and mask design, 22 dimensions (vertical length dimensions: 9; horizontal length dimensions: 2; width dimensions: 7; circumference or arc dimensions: 4) were systematically selected as those pertinent to half-face mask design. The facial measurements collected in the present study can be utilized effectively for the design of various types of masks.

The facial measurements were efficiently extracted from 3D face scan data using the semi-automatic facial measurement extraction program developed in the present study. Once landmarks on the face scan are confirmed by the analyst, the facial measurement program coded by Matlab automatically extracts measurements for facial dimensions. A Euclidian distance between landmarks was calculated for length and width dimensions and an arc intersecting the facial image and a plane passing three designated landmarks was measured for arc dimensions. Note that the 3D face measurement method is superior to the conventional method which uses a tape measure for arc-related facial dimensions.

Since the facial measurements of the KAF pilots are significantly different from those of the Korean civilians and USAF personnel, the shape and sizing system of the oxygen mask need to be custom designed for KAF pilots considering composite gender. The KMP had a significantly lager head and were less varied in all the facial dimensions than the KMC, and the KMP had a significantly longer, wider, but flatter head and a longer and wider nose than the UMP. Therefore, the sizing system and corresponding oxygen mask designs for the KAF pilots was custom designed based on the KAF facial anthropometric data and 3D face images. For example, the largest mean difference at the nasal root area between the KMP and UMP was found in nasal root breadth ($\bar{d}$ = 5.2, ratio of means = 1.34) which can be the main cause of excessive pressure being experienced by most of KAF pilots wearing MBU-20/P masks. Based on this significant difference at the nasal root area, the present study widened the corresponding area of the existing oxygen mask design about 5 mm on average for a better fit to KAF pilots. Furthermore, a composite population of KAF pilots was applied to be formed for oxygen mask design by reflecting an increasing rate of the KFP in the future because of their significant differences in mean and SD from the KMP.

The KMP were found significantly larger (ratio of means = 1.05 to 1.12) than the KMC in all head-related dimensions except head circumference (ratio of means = 0.99). Demographic factors such as occupation and age commonly affect the anthropometric characteristics of a population (W. Lee et al., 2013; Roebuck, 1995; Zhuang et al., 2007). It is likely that the face of the KMP is larger than that of the KMC because of physical requirements such as height, weight, and physical fitness for pilots. However, the opposite occurs in head circumference, which is likely caused by the relatively short hair of pilots.

The sizing system proposed by the present study was custom developed based on the facial anthropometric data of the KAF pilots, and then adjusted towards the increase of the accommodation percentage and design applicability. There are no SW and LN among the MBU-20/P sizes due to anecdotal recommendations from expert fitters of the USAF (M. E. Gross et al., 1997). The present study determined to follow the existing size categories but exclude the XSN by discussion with the KAF Logistics Command considering efficiency of economics and equipment management. The revised sizing system was adjusted to increase the accommodation percentage and appropriate application to the oxygen mask design. The accommodation percentage of the revised oxygen mask was 93% in the present study. However, considering the elasticity of material (silicon rubber) of the oxygen mask, four sizes of the revised oxygen masks will be suitable to more than 93% of the KAF.

6.2. Oxygen Mask Design Method

The proposed design method based on the analysis of the FMI model has systemicity and rationality for the oxygen mask design. A user-friendly product design requires various factors related to user (e.g., body size, posture, motion, force), product (e.g., product shape, components, functions, and material properties), and their interface (e.g., task, handling method, usage environment, comfort, and satisfaction) (W. Lee et al., 2009). Previous respirator design methods mostly considered just factors about user such as facial anthropometric measurements or 3D face images, but there was limited consideration about the relationship of a user-product interface. However, the FMI analysis could fully consider the important factors related to the oxygen mask design by considering characteristics of user (facial anthropometric measurements, 3D face images), product (oxygen mask design dimensions), and their interface (oxygen mask wearing position, oxygen mask fit, user preferences). In particular, the VFA could have practicality and rationality by applying the oxygen mask wearing characteristics to the fit analysis in the virtual environment. Therefore, the quantitative design guidelines could be identified through the FMI analysis, systematically, in the present study. Furthermore, to identify the oxygen mask wearing characteristics, the present study used photos of pilots who wear the oxygen mask; however, instead of the photo, 3D scan images will be better applicable for the accuracy and ease of analysis.

The VFA method proposed in the present study can quantitatively analyze the fit characteristics of the oxygen mask design in the early stage of the mask design process. The quantitative fit characteristics were identified by analyzing the infiltration distance of the facepiece from the 3D face image of various pilots (n = 336), and a better design of the oxygen mask was found by determining the fit characteristics of those pilots. To validate a new design, a physical prototype needs to be manufactured and empirically tested with users; however, the physical prototype mostly requires expensive cost and time due to molding, material usage, manufacturing, and post-processing (Ulrich & Eppinger, 2011). Therefore, sufficient examination is important to check a design's rationality before prototyping. The present study could quantitatively consider design improvement effects before prototype manufacturing. According to the VFA, the satisfactory percentage of the revised oxygen mask design was 82%, but the usability evaluation showed that the revised oxygen mask prototype was appropriate to 92% (120 out of 131 pilots and cadets) of the KAF pilots.

The revised oxygen mask design based on various 3D face images through the VFA is more suitable to the user population than those designs based on the RFMs. The RFMs (Ball & Molenbroek, 2008; Han & Choi, 2003; Luximon et al., 2012; Song & Yang, 2010; Zhuang, Benson, et al., 2010) generated based on the facial anthropometric data are representable in terms of sizes of user population. However, the RFMs might not represent face shape of the population, because the facial anthropometric data alone may not be appropriately applied to the respirator design due to the complex shape of the face (Cobb, 1972; Lovesey, 1974; Piccus et al., 1993; Seeler, 1961; Yatapanage & Post, 1992). For example, according to the VFA, the satisfactory percentage of the initially revised oxygen mask design based on the RFMs was 65%, while that of the finally revised design based on 3D face images of various pilots was 82% in the present study. Therefore, 3D scan images are more applicable to design wearable products than the RFMs.

The developed VFA system can be upgraded to efficiently find an optimal oxygen mask design. The VFA system analyzed the fit of a designed oxygen mask using design profiles of the hardshell and facepiece, and those profiles were manually adjusted by using CAD software. The adjustment of design profiles and then fit evaluation through the VFA system were iteratively conducted to find a better design of the oxygen mask in the present study. However, this iterative process was time consuming, complex, and inefficient. Therefore, the VFA system can be upgraded to efficiently find the best design of the oxygen mask by adjusting design profiles, automatically. A modified five-step approach of the VFA can be an option for the oxygen mask shape design: (1) initial design of the oxygen mask, (2) projection of the initial mask design onto the 3D face scan images of KAF pilots, (3) extraction of an oral-nasal part of 3D face image based on the projected oxygen mask shape, (4) alignment of the extracted facial parts of all 3D face images by referring to facial landmarks, and (5) design revision of the initial oxygen mask shape by analyzing a variation of extracted facial parts.

Further areas of study for the VFA include considerations about material properties of the oxygen mask and facial skin, like the FEM. For the accurate analysis of the VFA, further study requires considerations of craniofacial anatomy such as the structure of bone, and thickness and elasticity of tissue of the facial area. Previous research on the virtual fit evaluation based on the FEM (Butler, 2009; Dai et al., 2011; Lei et al., 2012) presented quantitative analysis of pressure on the facial area by considering the material properties using density, Young's modulus, and Poisson's ratio, while the present study considered the infiltration distance of the facepiece into the human skin. The VFA method has advantages compared to the FEM-based method in terms of consideration of mask wearing characteristics, application of various 3D face images, and pressure measurement using pressure film. Additionally, the VFA system can be improved to analyze the combination of fit characteristics based on the mask infiltration distance and the material properties.

6.3. Oxygen Mask Usability Evaluation

Through the oxygen mask usability evaluation, the validity and rationality of the revised design were determined, and the oxygen mask design method and process could be verified. Compared to previous research which did not conduct a usability evaluation, the present study identified the design improvement effects by testing the existing and revised oxygen masks. The subjective evaluation, pressure evaluation, and evaluation of suitability for military equipment were conducted based on the ergonomic evaluation protocols, testing materials (e.g., questionnaire, pressure film), analysis protocols, and analysis system developed by the present study. The revised oxygen mask was more appropriate to the KAF pilots (including cadets) than the existing oxygen mask, and 92% of them were satisfied with the revised design. These results can be interpreted as the proposed method demonstrated good rationality in oxygen mask design.

The present study's proposed quantitative pressure measurement and analysis methods found corresponding results with the discomfort evaluation and the virtual fit assessment. The present study, for the first time, introduced methods and protocols to measure and analyze a mask's pressure to the face using pressure film. The pressure evaluation program was developed to efficiently compare the existing and revised oxygen masks. The pressure of the revised oxygen mask was lower on average than that of the existing mask by facial area, and this corresponded to the results of the discomfort evaluation. The revised oxygen mask supports a comfortable fit to the pilot's face by fitting with appropriate pressure. Also, both the VFA and pressure measurement showed that the pressure of the revised oxygen mask was decreased at the nasal side, zygomatic bone, and cheek area;

however, an opposite result was found at the nasal root area. The VFA indicated that the existing oxygen mask had less fit than the revised one at the nasal root area, while the pressure measurements of the existing oxygen mask were higher than the revised one at the same facial area. This inconsistency can occur due to differences between virtual assessment and experimental evaluation with human participants.

Some KAF pilots who have narrower nasal root breadth preferred the existing oxygen mask. Two KMP and nine cadets (4 males and 5 females) out of 131 participants answered that the existing oxygen mask was more appropriate to their faces than the revised oxygen mask. The present study found their nasal root breadth (17.4 ± 2.2 mm) was 2.6 mm narrower than an average of the KAF male and female pilots (20.0 ± 2.8 mm) and more closer to the UMP (15.4 ± 1.9 mm). Their discomfort score on the nasal root area (1.1 ± 1.5) was lower on average than that of the KAF pilots (1.8 ± 1.4) and cadets (1.5 ± 1.7).

The revised oxygen mask was suitable to use as military equipment due to stable performance in the situations of PBG, low atmospheric pressure, and high-G. Because the pilot oxygen mask is used in extreme environments such as high altitude and high gravity acceleration, the usability evaluation in those situations is necessary to identify the suitability and stability of the design for the pilots. Of course, the fit of the revised oxygen mask was improved, and the slippage of the revised design was decreased in the high-G situation. Also, the revised oxygen mask was evaluated to have no functional problems in PBG and low atmospheric pressure situations. Furthermore, additional in-depth examinations, such as material properties evaluation, compatibility testing, or environmental assessment are required in order to provide the revised oxygen mask to the KAF pilots.

6.4. Applications

The proposed oxygen mask design and evaluation process can be applied to wearable product development. First, users' anthropometric characteristics including body dimensions and 3D body scan images which are related to design characteristics of the product are collected and analyzed. Second, characteristics of product-user interface are comprehensively and systematically considered in terms of user, product, task, usage environment, and preferences (W. Lee et al., 2011). Third, a revised shape is designed through the virtual fit analysis method. Fourth, a prototype of the revised product design is fabricated and usability of the revised product is compared to the existing product by considering usage environments and situations. Finally, the revised design is determined by referring to the results of the usability evaluation. The oxygen mask design and evaluation methodology can be applied to the design of various types of masks such as: military gas filter masks, industrial dust-proof masks, industrial gas filter masks, firefighter's full-face masks, and diver's masks. Also, the proposed design method is applicable to wearable products such as: goggles, helmets, backpacks, gloves, shoes, and clothing.

The facial differences between Korean, Chinese, and Japanese civilians were less distinct in all of the facial dimensions than the differences between those East Asians and U.S. civilians, so the revised oxygen mask might be more appropriate to Asian pilots compared to the existing oxygen mask. Du et al. (2008) identified that Chinese male civilians (CMCs) have shorter face length ($\bar{d}$ = -5.4), larger head breadth ($\bar{d}$ = 4.2), flatter face thickness ($\bar{d}$ = -11.6), smaller nose protrusion ($\bar{d}$ = -2.2), larger nose width ($\bar{d}$ = 2.6), and wider lip width ($\bar{d}$ = 1.1) when compared with the facial dimensions of U.S. male civilians (UMCs) surveyed by Zhuang and Bradtmiller (2005). This facial difference pattern between CMCs and UMCs is found more distinct in all the face dimensions except head breadth and lip width when KMCs are compared with UMCs: shorter face length ($\bar{d}$ = -11.4), slightly larger head breadth ($\bar{d}$ = 1.0), smaller face thickness ($\bar{d}$ = -20.3), smaller nose protrusion ($\bar{d}$ = -8.5), larger nose width ($\bar{d}$ = 3.0), and narrower lip width ($\bar{d}$ = -2.1). Furthermore, H. Lee and Park (2008) surveyed facial dimensions of 124 KMCs and 124 Japanese male civilians (JMCs), and identified that KMCs have shorter face length ($\bar{d}$ = -6.0), narrower head breadth ($\bar{d}$ = -4.4), flatter face thickness ($\bar{d}$ = -4.6), smaller nose length ($\bar{d}$ = -2.0), narrower nose width ($\bar{d}$ = -4.6), and narrower lip width ($\bar{d}$ = -8.9) than those of JMCs. Both CMCs and JMCs faces have small differences ($|\bar{d}|_{max}$ < 10.0) when compared with KMCs, while UMCs show distinct differences ($|\bar{d}|_{max}$ = 20.3) than KMCs; therefore, the revised oxygen mask can be suitable to CMCs' and JMCs' faces.

Chapter 7. CONCLUSION

The main objectives of the present study were design and evaluation of the pilot oxygen mask for the KAF pilots. First, the revised oxygen mask design was derived based on 3D face images scanned from various user populations. Since the facial measurements of the KAF pilots are significantly different from those of the Korean civilians and USAF personnel, the shape and sizing system of the oxygen mask need to be custom designed for KAF pilots considering composite gender. The methods, process, and programs were proposed to measure and analyze the various 3D scan face images, efficiently. The revised design based on various 3D face images more appropriately fit the user population compared to the oxygen mask design based on the RFMs.

Second, the oxygen mask design method based on the FMI analysis and the VFA was proposed and applied to the oxygen mask design improvement. The systematic method used to establish the oxygen mask design strategy was introduced based on the comprehensive understanding of the human face, oxygen mask, and face-mask interface. Through the correlation analysis of the FMI factors, design problems and design improvement directions of the existing MBU-20/P oxygen mask were quantitatively identified. Then, the oxygen mask design was iteratively revised to find the best design for the KAF pilots through the VFA system. The revised design was found to have better fit to the user population compared to the oxygen mask design based on the RFMs.

Lastly, the ergonomic usability evaluation protocols were introduced to examine the discomfort, pressure, and suitability for military equipment. The proposed protocols include: questionnaire, measurement and analysis method for pressure evaluation, pressure analysis system, and details about the evaluation process in low atmospheric pressure and high-G situations. According to the usability evaluation, the revised oxygen mask has a better fit to the KAF pilots and appropriate and balanced pressure by the facial areas.

The revised oxygen mask and related design methods are expected to contribute to the KAF pilots, and to be applicable to a mass-customized design for wearable products. The revised oxygen mask can support the safety and satisfaction of the KAF pilots and increasing military power of the KAF by reducing physical and mental workload due to discomforts caused from excessive pressure or oxygen leakage. Furthermore, the proposed methods, including the FMI analysis, the VFA, and the usability evaluation, can be applied to the mass-customized design and evaluation of wearable products which have importance in fit, comfort, performance, and safety.

요 약 문

공군 조종사들이 착용하는 MBU-20/P 산소마스크는 미국인의 안면 data를 기반으로 제작되었기 때문에 한국 공군 조종사 안면에 적합하지 않고 코 부위에 과도한 압박이나 산소누설 등의 불편을 초래하고 있다. 안면부 형상에 적합한 호흡구 설계를 위하여 기존 연구들은 3D 안면 scan data를 이용하는 디지털 설계 또는 평가 방법들을 개발 및 적용하고 있으나 현재까지는 객관적 설계 기준 및 평가 기준이 제시되지 못하고 있다. 또한, 개발된 호흡구의 형상이 안면에 적절한지의 여부는 설계 대상 인구를 대상으로 한 시제품의 착용감 평가를 통해 파악될 필요가 있으나, 기존 연구들은 개발된 호흡구에 대한 주관적 및 객관적 측면에서의 체계적인 착용성 평가가 미흡하였다. 본 연구는 한국 공군 조종사들의 안면 특성을 기반으로 산소마스크의 형상을 설계 개선하고 시제품으로 제작하여 개선 마스크의 착용성을 평가하였다.

본 연구는 안면-마스크 인터페이스 분석(face-mask interface analysis)을 통해 산소마스크 설계 특성, 조종사 안면 특성(안면 치수, 3차원 안면 형상), 산소마스크 착용 특성, 그리고 주관적 착용성 특성을 파악하였다. 먼저 산소마스크의 설계 문제를 파악하기 위하여 한국 공군 조종사 490명을 대상으로 한 설문 평가를 통해 콧대와 코 옆 부위에서 과도한 압박 또는 산소누설로 인한 불편도가 상대적으로 높은 것으로 파악되었다. 산소마스크 설계 특성은 MBU-20/P 산소마스크를 구성하는 구성 부품들에 대한 설계 제원들(예: 크기, 형상, 작동방식 등)을 benchmarking함으로써 파악되었으며, 산소마스크 설계 특성을 기반으로 관련된 안면 측정 항목들(길이: 9, 두께: 2, 너비: 7, 둘레: 4)이 선정되었다. 조종사 안면 특성은 한국 공군 조종사 284명(남 278명, 여 6명)과 공군사관학교 여자 생도 52명의 안면을 3차원 계측하고 한국 일반인 및 미공군 안면 특성과 비교함으로써 분석되었다. 한국인 조종사는 한국 일반인에 비해 전반적으로 크며(mean difference = 0.7 ~ 26.5 mm) 미공군에 비해서도 큰(mean difference = 1.0 ~ 14.7 mm) 것으로 파악되었는데, 이는 현 미공군 안면 특성 기반으로 설계된 산소마스크 형상 및 치수체계가 한국 공군 조종사들에게 적합하도록 개선될 필요가 있음을 의미한다. 마지막으로, 산소마스크 착용 특성은 한국 공군 조종사 85명의 마스크 착용 사진을 토대로 3차원 안면 scan data에 마스크 scan data를 alignment 함으로써 착용 위치, 착용 각도, 여유공간, 그리고 밀착도 측면에서 파악되었다.

파악된 안면-마스크 인터페이스 특성들을 기반으로 마스크 설계 개선 부위 및 설계 개선 전략이 수립되었으며, 본 연구에서 개발한 가상 착의 평가 방법(virtual fit

assessment method)을 기반으로 한국 공군 조종사들의 안면 형상에 적합한 산소마스크 형상이 설계되었다. 설계 개선 전략을 통해 산소마스크의 치수, 콧대 부위 너비, 그리고 안면에 밀착되는 형상의 개선 방법이 수립되었다. 개선 산소마스크 형상은 여러 3차원 안면 scan data에 산소마스크 CAD를 가상으로 착의하고 정량적인 착의성을 평가해가며 다양한 크기 및 형상의 안면에 가장 적합한 마스크 형상을 탐색하는 방법인 산소마스크 가상 착의 평가 방법을 통해 설계되었다. 가상 착의 평가 결과, 기존 마스크는 코 옆과 광대뼈 부위에서 마스크가 과도하게 압박되거나 콧대 부위에서 마스크의 밀착이 결여되는 현상을 보였으나, 개선 산소마스크는 본 연구에서 정한 적정 밀착/압박 기준에 적합하게 설계된 것으로 분석되었으며, 기존 마스크에 비해 27%의 설계 개선 효과가 파악되었다.

개선된 산소마스크의 착용성을 평가하기 위해 기존 마스크와 유사한 물성치를 가진 개선 마스크의 시제품이 제작되었으며, 개선 마스크 시제품은 착용성 및 군 적합성 평가를 통해 기존 마스크와 비교되었다. 기존 및 개선 마스크는 조종사 산소마스크 사용 집단인 공군조종사(83명)와 잠재적인 사용 집단인 공군사관학교 생도(58명)를 대상으로 주관적 불편도와 객관적 압박 특성 측면에서 비교되었다. 개선 마스크는 안면 부위에 따라 주관적 불편도가 56%~81% 감소한 것으로 파악되었으며, 평균 압박지수가 안면 부위별 11%~25%, 압박부위 면적이 안면 부위별 6%~43%, 그리고 고압박 면적이 안면 부위별 4%~40% 감소하는 설계 개선 효과를 보였다. 또한 군 적합성 평가를 통해 개선 마스크가 PBG (pressure breathing for gravity) 사용 환경 및 저압 환경에서 문제가 없이 사용되며, 고중력가속도 환경에서 기존 마스크에 비해 평균 47% 적게 흘러내리는 것으로 파악되었다. 공군조종사 및 공군사관학교 생도의 92%가 개선 산소마스크의 형상이 만족스러운 것으로 응답하였다.

본 연구를 통해 안면-마스크 인터페이스 분석과 가상 착의 평가 방법 기반의 체계적이고 합리적인 마스크 설계 방법이 제안되었다. 본 연구를 통해 한국인 조종사 안면에 적합하게 설계된 MBU-20/P 산소마스크는 한국 공군 조종사들의 안면 형상에 적합하여 과도한 압박감 및 산소누설 감소시키고 만족감과 착용감 향상시키는 효과를 나타냈다. 개선된 산소마스크는 한국 공군 조종사들의 비행 부하를 감소시켜 잠재적인 안전 사고를 예방하고 군 전투 능력을 향상시킬 수 있을 것으로 기대된다. 또한, 본 마스크 설계 방법은 다양한 종류의 마스크 및 인체 착용 제품들의 설계에 적용될 수 있을 것으로 기대된다.

REFERENCES

Ahn, Y., and Suh, M. (2004). A study on the head type of Korean women's for headgear pattern making. *The Research Journal of the Costume Culture, 12*(6), 1021-1030.

Alexander, M., McConville, J. T., and Tebbetts, I. (1979). *Anthropometric Sizing, Fit-Testing, and Evaluation of the MBU-12/P Oral-Nasal Oxygen Mask* (AMRL-TR-79-44). Wright-Patterson Air Force Base, OH: Aerospace Medical Research Laboratory.

Ashdown, S. P., Loker, S., Schoenfelder, K., and Lyman-Clarke, L. (2004). Using 3D scans for fit analysis. *Journal of Textile and Apparel, Technology and Management, 4*(1), 1-12.

Ball, R. M. (2009). 3-D design tools from the SizeChina project. *Ergonomics in Design, 17*(3), 8-13.

Ball, R. M., and Molenbroek, J. F. M. (2008). Measuring Chinese heads and faces. *Proceedings the 9th International Congress of Physiological Anthropology, Human Diversity: Design for Life*, Delft, The Netherlands.

Ball, R. M., Shu, C., Xi, P. C., Rioux, M., Luximon, Y., and Molenbroek, J. F. M. (2010). A comparison between Chinese and Caucasian head shapes. *Applied Ergonomics, 41*(6), 832-839.

Bitterman, B. H. (1991). *Application of Finite Element Modeling and Analysis to the Design of Positive Pressure Oxygen Masks* (ADA244045, AFTT/GAE/ENY/91D-22). Wright-Patterson Air Force Base, OH: The Air Force Institute of Technology.

Brazile, W. J., Buchan, R. M., Sandfort, D. R., Melvin, W., Johnson, J. A., and Charney, M. (1998). Respirator fit and facial dimensions of two minority groups. *Applied Occupational and Environmental Hygiene, 13*(4), 233-237.

Buikstra, J. E., and Ubelaker, D. H. (1994). *Standards for Data Collection from Human Skeletal Remains*. Fayetteville, NC: Arkansas Archaeological Survey.

Butler, K. M. (2009). Using 3D head and respirator shapes to analyze respirator fit. *Proceedings the 13th International Conference on Human-Computer Interaction (HCII 2009), LNCS 5620*, San Diego, CA.

Bye, E., and McKinney, E. (2010). Fit analysis using live and 3D scan models. *International Journal of Clothing Science and Technology, 22*(2/3), 88-100.

Churchill, E., Kikta, P., and Churchill, T. (1977). *The AMRL Anthropometric Data Bank Library: Volumes I-V* (AMRL-TR-77-1, ADA047314). Wright-Patterson Air Force Base, OH: Aerospace Medical Research Laboratory.

Clauser, C., Tebbetts, I., Bradtmiller, B., McConville, J. T., and Gordon, C. C. (1988). *Measurer's Handbook: U.S. Army Anthropometric Survey 1987-1988* (NATICK/TR-88/043). Natick, MA: U.S. Army Natick Research, Development and Engineering Center.

Cobb, J. (1972). *A Projected Grid Method for Recording the Shape of the Human Face* (AD0753864, TR71184). Farnborough, UK: Procurement Executive, Ministry of Defence, UK.

Coffey, C. C., Lawrence, R. B., and Myers, W. R. (2002). Comparison of five methods for fit testing N95 filtering-facepiece respirator. *Applied Occupational and Environmental Hygiene, 17*(10), 723-730.

Dai, J. C., Yang, J. Z., and Zhuang, Z. (2011). Sensitivity analysis of important parameters affecting contact pressure between a respirator and a headform. *International Journal of Industrial Ergonomics, 41*(3), 268-279.

Du, L. L., Zhuang, Z., Guan, H. Y., Xing, J. C., Tang, X. Z., Wang, L. M., Wang, Z. L., Wang, H. J., Liu, Y. W., Su, W. J., Benson, S., Gallagher, S., Viscusi, D., and Chen, W. H. (2008). Head-and-face anthropometric survey of Chinese workers. *Annals of Occupational Hygiene, 52*(8), 773-782.

Godil, A. (2009). Facial shape analysis and sizing system*. Proceedings the 13th International Conference on Human-Computer Interaction (HCII 2009), LNCS 5620*, San Diego, CA.

Gordon, C. C., Bradtmiller, B., Churchill, T., Clauser, C. E., McConville, J. T., Tebbetts, I. O., and Walker, R. A. (1988). *1978-1988 Anthropometric Survey of U.S. Army Personnel: Methods and Summary Statistics* (NATICK/TR-89/044, ADA225094). Natick, MA: U.S. Army Natick Research, Development and Engineering Center.

Gross, M. E., Taylor, S. E., Mountjoy, D. N., and Hoffmeister, J. (1997). *Antropometric Research on the Sizing of the MBU-20/P* (AFRL-HE-WP-TR-2002-0181). Wright-Patterson Air Force Base, OH: Human Effectiveness Directorate, Crew System Interface Division.

Gross, S. F., and Horstman, S. W. (1990). Half-mask respirator selection for a mixed worker group. *Applied Occupational and Environmental Hygiene, 5*(4), 229-235.

Hack, A. L., Hyatt, E. C., Held, B. J., Moore, T. O., Richards, C. P., and McConville, J. T. (1973). *Selection of Respirator Test Panels Representative of U.S. Adult Facial Sizes* (LA-5488). Los Alamos, NM: Los Alamos Scientific Lab.

Hack, A. L., and McConville, J. T. (1978). Respirator protection factors: Part I - Development of an anthropometric test panel. *American Industrial Hygiene Association Journal, 39*(12), 970-975.

Han, D. (1999). Fit testing for respirators and development of fit test panels for Koreans. *Korean Industrial Hygiene Association Journal, 9*(1), 1-13.

Han, D., and Choi, K. (2003). Facial dimensions and predictors of fit for half-mask respirators in Koreans. *American Industrial Hygiene Association Journal, 64*(6), 815-822.

Han, D., and Lee, J. (2005). Evaluation of particulate filtering respirators using inward leakage (IL) or total inward leakage (TIL) testing - Korean experience. *Annals of Occupational Hygiene, 49*(7), 569-574.

Han, D., Rhi, J., and Lee, J. (2004). Development of prototypes of half-mask facepieces for Koreans using the 3D digitizing design method: A pilot study. *Annals of Occupational Hygiene, 48*(8), 707-714.

Han, D., Willeke, K., and Colton, C. E. (1997). Quantitative fit testing techniques and regulations for tight-fitting respirators: Current methods measuring aerosol or air leakage, and new developments. *American Industrial Hygiene Association Journal, 58*, 219-228.

Harrison, C. R., and Robinette, K. M. (2002). *CAESAR: Summary Statistics for the Adult Population (Ages 18-65) of the United States of America* (AFRL-HE-WP-TR-2002-0170). Wright-Patterson Air Force Base, OH: Air Force Research Laboratory, Human Effectiveness Directorate, Crew System Interface Division, Air Force Materiel Command.

Hertzberg, H. T. E., Daniels, G. S., and Churchill, E. (1954). *Anthropometry of Flying Personnel-1950* (WADC TR 52-321, AD0047953). Wright-Patterson Air Force Base, OH: Wright Air Development Center, Air Research and Development Command.

Hotzman, J., Gordon, C. C., Bradtmiller, B., Corner, B. D., Mucher, M., Kristensen, S., Paquette, S., and Blackwell, C. L. (2011). *Measurer's Handbook: U.S. Army and Marine Corps Anthropometric Surveys, 2010-2011* (NATICK/TR-11/017). Natick, MA: U.S. Army Natic Soldier Research, Development and Engineering Center.

Hughes, J. G., and Lomaev, O. (1972). An anthropometric survey of Australian male facial sizes. *American Industrial Hygiene Association Journal, 33*(2), 71-78.

ISO. (2006). *General Requirements for Establishing Anthropometric Databases* (ISO 15535). Geneva, Switzerland: International Standards Organisation.

Jeon, E. (2011). *Designing of ergonomic flight suit through developing pattern and size systematization.* (Doctoral disseration), Kyungpook National University, Daegu, South Korea. Retrieved from http://www.riss.kr/link?id=T12342713

Jung, K., Kwon, O., and You, H. (2010). Evaluation of the multivariate accommodation performance of the grid method. *Applied Ergonomics, 42*, 156-161.

Kim, H., Han, D., Roh, Y., Kim, K., and Park, Y. (2003). Facial anthropometric dimensions of Koreans and their associations with fit of quarter-mask respirators. *Industrial Health, 41*(1), 8-18.

Kim, K., Kim, H., Lee, J., Lee, E., and Kim, D. (2003). Development of the new 3D test panel for half-mask respirators by 3D shape analysis for Korean faces. *Journal of Korean Society of Occupational and Environmental Hygiene, 13*(3), 1-9.

Kim, S. (2004). Analysis on the measurement and shape classification of the head and face for Korean female children aged 9~12 years. *The Research Journal of the Costume Culture, 12*(5), 757-768.

Kim, S. (2005). Analysis on the shape classification of the head of Korean female children for the headwear sizing system. *The Research Journal of the Costume Culture, 13*(2), 200-208.

Kim, S., Lee, H., and Choi, H. (2004). Analysis on the measurement and shape classification of the head and face for Korean male children aged 9~12 years. *The Research Journal of the Costume Culture, 12*(6), 933-944.

Kolear, E. S., Cosgrove, D. J., de la Barre, C. M., and Theis, C. F. (1982). Comparison of respirator protection factors measured by two quantitative fit test methods. *Aviation, Space, and Environmental Medicine, 53*(11), 1116-1122.

Korean Agency for Technology and Standards (KATS). (1998). *The Report on the 4th Size-Korea (Korean Body Measurement and Investigation)* Seoul, Korea: Size Korea, Ministry of Knowledge Economy.

Korean Agency for Technology and Standards (KATS). (2004). *The Report on the 5th Size-Korea (Korean Body Measurement and Investigation)* Seoul, Korea: Size Korea, Ministry of Knowledge Economy.

Korean Agency for Technology and Standards (KATS). (2010). *The Report on the 6th Size-Korea*

(Korean Body Measurement and Investigation) Seoul, Korea: Size Korea, Ministry of Knowledge Economy.

Lee, B., Jung, K., and You, H. (2011). Development of a distributed representative human model generation and analysis system for multiple-size product design. *Journal of the Ergonomics Society of Korea, 30*(5), 683-688.

Lee, H., and Park, S. (2008). Comparison of Korean and Japanese Head and Face Anthropometric Characteristics. *Human Biology, 80*(3), 313-330.

Lee, W., Jung, K., Jeong, J., Park, J., Cho, J., Kim, H., Park, S., and You, H. (2013). An anthropometric analysis of Korean male helicopter pilots for helicopter cockpit design. *Ergonomics, 56*(6), 879-887.

Lee, W., Jung, K., Lee, H., Song, H., Oh, J., and You, H. (2011). Development of a comprehensive usability testing and analysis framework for the physical interface between product and user. *Journal of the Ergonomic Society of Korea, 30*(2), 1-8.

Lee, W., Jung, K., Park, J., Kim, S., Yoon, S., Kim, M., and You, H. (2009). Development of a quantitative and comprehensive usability evaluation system based on user needs. *Proceedings the Human Factors and Ergonomics Society 53rd Annual Meeting*, San Antonio, TX.

Lee, W., Yoon, S., and You, H. (2010). Development of a 3D semi-automatic measurement protocol for hand anthropometric measurement. *Proceedings the Human Factors and Ergonomics Society 54th Annual Meeting*, San Francisco, CA.

Lei, Z., Yang, J., and Zhuang, Z. (2012). Headform and N95 filtering facepiece respirator interaction: Contact pressure simulation and validation. *Journal of Occupational and Environmental Hygiene, 9*, 46-58.

Liau, Y. H., Bhattacharya, A., Ayer, H., and Miller, C. (1982). Determinations of critical anthropometric parameters for design of respirators. *American Industrial Hygiene Association Journal, 43*, 897-899.

Lovesey, E. J. (1974). The development of a 3-dimensional anthropometric measuring technique. *Applied Ergonomics, 5*(1), 36-41.

Luximon, Y., Ball, R. M., and Justice, L. (2010). The Chinese face: A 3D anthropometric analysis. *Proceedings the 8th International Symposium on Tools and Methods of Competitive Engineering (TMCE)*, Anncona, Italy.

Luximon, Y., Ball, R. M., and Justice, L. (2012). The 3D Chinese head and face modeling. *Computer-Aided Design, 44*(1), 40-47.

Meunier, P., Tack, D., Ricci, A., Bossi, L., and Angel, H. (2000). Helmet accommodation analysis using 3D laser scanning. *Applied Ergonomics, 31*(4), 361-369.

Myers, W. R. (2000). *Respiratory protective equipment* (5th ed.). New York, NY: John Wiley & Sons.

National Institute for Occupational Safety and Health (NIOSH). (1987). *Guide to Industrial Respiratory Protection* (HDDS/NIOSH pub. no. 87-116). Washington, DC: Goverment Printing Office.

Oestenstad, R. K., Dillion, H. K., and Perkins, L. L. (1990). Distribution of faceseal leak sites on a half-mask respirator and their association with facial dimensions. *American Industrial Hygiene Association Journal, 51*(5), 285-290.

Oestenstad, R. K., and Perkins, L. L. (1992). An assessment of critical anthropometric dimensions for predicting the fit of a half-mask respirator. *American Industrial Hygiene Association Journal, 53*(10), 639-644.

Oh, Y., and Park, S. (2010). The facial anthropometry with 3D head scanner for designing Korean gas mask. *Proceedings the Society of CAD/CAM Engineers Conference*.

Ozsoy, U., Demirel, B. M., Yildirim, F. B., Tosun, O., and Sarikcioglu, L. (2009). Method selection in craniofacial measurements: Advantages and disadvantages of 3D digitization method. *Journal of Cranio-Maxillofacial Surgery, 37*(5), 285-290.

Piccione, D., and Moyer Jr., E. T. (1997). *Modeling the interface between a respirator and the human face* (ADA325547). Aberdeen Proving Ground, MD: U.S. Army Research Laboratory, Human Research and Engineering Directorate.

Piccus, M. E., Smith, G. A., Standley, B. K., Volk, T. L., and Wildes, L. B. (1993). *Creation of Prototype Aircrew Protection Equipment Based on Face Anthropometry* (ADA273865). Wright-Patterson Air Force Base, OH: The Air Force Institute of Technology.

Research Institute of Human Engineering for Quality Life (HQL). (2008). *Japanese Body Size Data Book 2004-2006*. Osaka, Japan: Research Institute of Human Engineering for Quality Life.

Robinette, K. M., and Annis, J. F. (1986). *A Nine-Size System for Chemical Defense Gloves* (AAMRL-TR-86-029, AD-A173 193). Wright-Patterson Air Force Base, OH: Armstrong Aerospace Medical Research Laboratory, Aerospace Medical Division, Air Force Systems Command.

Robinette, K. M., Blackwell, S., Daanen, H., Boehmer, M., Fleming, S., Brill, T., Hoeferlin, D., and Burnsides, D. (2002). *Civilian American and European Surface Anthropometry Resource (CAESAR) Final Report, Volume I: Summary* (AFRL-HE-WP-TR-2002-0169). Wright-Patterson Air Force Base, OH: Human Effectiveness Directorate, Crew System Interface Division.

Roebuck, J. A. (1995). *Anthropometric Methods: Designing to Fit the Human Body*. Santa Monica, CA: Human Factors and Ergonomics Society.

Sanders, M. S., and McCormick, E. J. (1998). *Human Factors in Engineering and Design* (7th ed.). New York, NY: McGraw-Hill.

Seeler, H. W. (1961). *Development of Oral-Nasal Masks, Oxygen, MC-1 and MBU-5/P* (ASD-TR-61-395, AD0267151). Wright-Patterson Air Force Base, OH: Aeronautical Systems Division, Air Force Systems Command.

Song, Y., and Yang, W. (2010). Half-mask interface prototype design using Korean face anthropometric data. *Journal of Korea Safety Management and Science, 12*(4), 87-92.

Ulrich, K. T., and Eppinger, S. D. (2011). *Product Design and Development* (5th ed.). Boston, MA: McGraw-Hill/Irwin.

Weinberg, S. M., Scott, N. M., Neiswanger, K., Brandon, C. A., and Marazita, M. L. (2004). Digital three-dimensional photogrammetry: Evaluation of anthropometric precision and accuracy using a genex 3D camera system. *Cleft Palate-Craniofacial Journal, 41*(5), 507-518.

Wikipedia. (2013). Mask. Retrieved April 11, 2013, from http://en.wikipedia.org/wiki/Mask

Yang, J., Dai, J., and Zhuang, Z. (2009). Human head modeling and personal head protective equipment: A literature review. *Proceedings the 13th International Conference on Human-Computer Interaction (HCII 2009), LNCS 5620*, San Diego, CA.

Yang, L., and Shen, H. G. (2008). A pilot study on facial anthropometric dimensions of the Chinese population for half-mask respirator design and sizing. *International Journal of Industrial Ergonomics, 38*(11-12), 921-926.

Yang, L., Shen, H. G., and Wu, G. (2007). Racial differences in respirator fit testing: A pilot study of whether American fit panels are representative of Chinese faces. *Annals of Occupational Hygiene, 51*(4), 415-421.

Yatapanage, K. G., and Post, K. (1992). Measurement of 3-D facial contours for the design of half-face respirators. *American Industrial Hygiene Association Journal, 53*(1), 19-26.

Yokota, M. (2005). Head and facial anthropometry of mixed-race U.S. Army male soldiers for military design and sizing: A pilot study. *Applied Ergonomics, 36*(3), 379-383.

Young, J. W. (1966). *Selected Facial Measurements of Children for Oxygen-Mask Design* (AM 66-9). Washington, DC: U.S. Department of Transportation, Federal Aviation Administration, Office of Aviation Medicine.

Young, J. W. (1993). *Head and Face Anthropometry of Adult U.S. Civilians* (DOT/FAA/AM-93/10). Washington, DC: U.S. Department of Transportation, Federal Aviation Administration, Office of Aviation Medicine.

Zhuang, Z., Benson, S., and Viscusi, D. J. (2010). Digital 3-D headforms with facial features representative of the current U.S. workforce. *Ergonomics, 53*(5), 661-671.

Zhuang, Z., and Bradtmiller, B. (2005). Head-and-face anthropometric survey of U.S. respirator users. *Journal of Occupational and Environmental Hygiene, 2*(11), 567-576.

Zhuang, Z., Bradtmiller, B., and Shaffer, R. E. (2007). New respirator fit test panels representing the current U.S. civilian work force. *Journal of Occupational and Environmental Hygiene, 4*(9), 647-659.

Zhuang, Z., Coffey, C. C., and Ann, R. B. (2005). The effects of subject characteristics and respirator features on respirator fit. *Journal of Occupational and Environmental Hygiene, 2*(12), 641-649.

Zhuang, Z., Guan, J., and Hsiao, H. (2002). Recapturing the sizing issues of respirator fit-test panels for emergency response. *Proceedings the International Society for Respiratory Protection (ISRP) Conference*, Edinburgh, UK.

Zhuang, Z., Slice, D. E., Benson, S., Lynch, S., and Viscusi, D. J. (2010). Shape analysis of 3D head scan data for U.S. respirator users. *Eurasip Journal on Advances in Signal Processing*.

APPENDICES

Appendix A. Questionnaire for oxygen mask preference evaluation

MBU-20/P 산소 Mask의 설계 적합성 평가 설문지

- 본 설문 평가는 **MBU-20/P 산소 mask 개선 설계**를 위한 기초자료로 사용될 예정입니다.
- 설문 평가 예상 **소요 시간은 약 5분** 입니다.
- 본 설문에 기재된 신상 정보 및 설문 결과는 본 연구의 분석을 위해서만 사용될 것입니다.
- 연구 수행 기관: 포항공과대학교 산업경영공학과
  공군사관학교 시스템공학과/기계공학과
  경북대학교 의류학과

Ⅰ. 기본 정보

1. 이름: ______________ 2. 생년월일: ________ 년 ____ 월 ____ 일

3. 본인 착용 산소 mask size (mask 하단부 표기 사항 참고)

☐ Extra Small Narrow ☐ Small Narrow ☐ Medium Narrow ☐ Medium Wide ☐ Large Wide

4. 현재 MBU-20/P 수령 이후 비행시간: _______ 시간

Ⅱ. 산소 Mask 적합성 평가

Ⅱ-1. 착용 안락감 (comfort)

1. 아래 그림을 참고하여 산소 mask 각 부위별 압박에 따른 불편감에 대해 표시해 주세요.

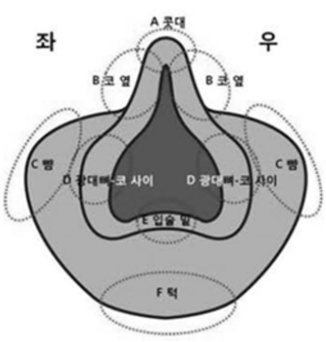

부 위	불편 없음 (comfortable)	조금 불편 (slightly uncomfortable)	불편 (moderately uncomfortable)	매우 불편 (very uncomfortable)	극히 불편 (hot spot)
A: 콧대	☐	☐	☐	☐	☐
B: 코 옆	☐	☐	☐	☐	☐
C: 뺨	☐	☐	☐	☐	☐
D: 광대뼈-코 사이	☐	☐	☐	☐	☐
E: 입술 밑	☐	☐	☐	☐	☐
F: 턱	☐	☐	☐	☐	☐

2. 산소 mask의 전반적인 착용 안락감에 대해 표시해 주세요.

불편 없음 (comfortable)	조금 불편 (slightly uncomfortable)	불편 (moderately uncomfortable)	매우 불편 (very uncomfortable)	극히 불편 (hot spot)
☐	☐	☐	☐	☐

3. 산소 mask 착용 중 말을 할 때, 산소 mask의 전반적인 착용 안락감에 대해 표시해 주세요.

불편 없음 (comfortable)	조금 불편 (slightly uncomfortable)	불편 (moderately uncomfortable)	매우 불편 (very uncomfortable)	극히 불편 (hot spot)
☐	☐	☐	☐	☐

1

4. High G 또는 highest G에서 산소 mask의 착용 안락감에 대해 표시해 주세요.

불편 없음 (comfortable)	조금 불편 (slightly uncomfortable)	불편 (moderately uncomfortable)	매우 불편 (very uncomfortable)	극히 불편 (hot spot)
☐	☐	☐	☐	☐

Ⅱ-2. 미끄러짐 (slippage)

1. 산소 mask의 미끄러짐 정도에 대해 표시해 주세요.

미끄러짐 없음 (no slippage)	조금 미끄러짐 (slight slippage)	미끄러짐 (moderate slippage)	과도하게 미끄러짐 (excessive slippage)
☐	☐	☐	☐

2. 산소 mask 착용 중 말을 할 때, 산소 mask의 미끄러짐 정도에 대해 표시해 주세요.

미끄러짐 없음 (no slippage)	조금 미끄러짐 (slight slippage)	미끄러짐 (moderate slippage)	과도하게 미끄러짐 (excessive slippage)
☐	☐	☐	☐

3. 산소 mask가 미끄러진다면, 어느 정도의 G부하에서 mask가 미끄러지기 시작합니까? ________ G

4. 산소 mask 미끄러짐의 원인이 무엇이라고 생각합니까?

☐ 땀 발생 ☐ 얼굴 피지 ☐ 밀착 결여 ☐ 통신을 위한 입술 움직임 ☐ 기타 __________

Ⅱ-3. 산소 밀폐 및 얼굴 밀착도

1. 아래 그림을 참고하여 산소 mask 각 부위별 산소 누설의 정도를 표시해 주세요.

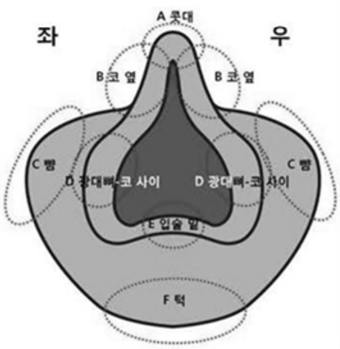

부 위	누설 없음 (no leaks)	조금 누설 (slight leakage)	누설 (moderate leakage)	과도하게 누설 (excessive leakage)
A: 콧대	☐	☐	☐	☐
B: 코 옆	☐	☐	☐	☐
C: 뺨	☐	☐	☐	☐
D: 광대뼈-코 사이	☐	☐	☐	☐
E: 입술 밑	☐	☐	☐	☐
F: 턱	☐	☐	☐	☐

2. 산소 mask의 전반적인 산소 밀폐 정도를 표시해 주세요.

매우 좋음 (excellent)	좋음 (good)	보통 (OK/average)	나쁨 (poor)	매우 나쁨 (very poor)
☐	☐	☐	☐	☐

2

3. 산소 mask 착용 중 말을 할 때, 산소 mask의 전반적인 산소 밀폐 정도를 표시해 주세요.

매우 좋음 (excellent)	좋음 (good)	보통 (OK/average)	나쁨 (poor)	매우 나쁨 (very poor)
☐	☐	☐	☐	☐

4. 산소 mask 밀착 결여가 조종 수행 능력을 어느 정도 감소시키는지 표시해 주세요.

감소 없음 (no degradation)	약간 감소 (slight degradation)	감소 (moderate degradation)	과도하게 감소 (excessive degradation)
☐	☐	☐	☐

5. 산소 mask의 착용 안락감, 미끄러짐, 산소 누설을 바로잡기 위해 조치를 취합니까 (예: 장비 조정)?

☐ 예 ☐ 아니오

조치를 취한다면, 각각의 문제점에 대해 어떠한 조치를 취합니까? 또한 당신이 취한 조치는 문제점을 해결할 수 있습니까?

구분	조치	문제해결 여부
착용 안락감 향상		☐ 예 ☐ 아니오
미끄러짐 방지		☐ 예 ☐ 아니오
산소 누설 방지		☐ 예 ☐ 아니오

Ⅱ-4. 통신 문제점 및 기타 사항

1. Microphone이 코를 건드리거나 방해합니까? ☐ 예 ☐ 아니오

2. Microphone이 입을 건드리거나 방해합니까? ☐ 예 ☐ 아니오

Ⅲ. 기타

1. Helmet을 포함한 기타 Combat Edge 장비에 문제점이 있는 경우 기술해 주시고 원인을 설명해 주세요.

____

____

____

____

____

설문에 응해 주셔서 감사합니다.

3

Appendix B. Head and face dimensions

B.1. Total 107 head and face dimensions

Dimension category	No.	Name of dimension		Related research
		English	Korean	
Length	1	menton to top of head (= head height)	턱끝점-머리마루점 수직길이 (= 머리수직길이)	1, 2, 7, 8, 9, 10, 13
	2	menton to metopion	턱끝점-이마돌출점 수직길이	7, 8, 9
	3	menton to crinion	턱끝점-이마시작점 수직길이	4, 7, 8, 9, 10
	4	menton to glabella	턱끝점-눈살점 수직길이	1, 4, 7, 8, 9
	5	menton to ectocanthus	턱끝점-눈초리점 수직길이	7, 9
	6	menton to sellion (= face length)	턱끝점-코뿌리점 수직길이 (= 얼굴수직길이)	1, 2, 3, 4, 5, 6, 7, 9, 10, 11, 12, 14, 15
	7	menton to subnasale (= lower-face length)	턱끝점-코밑점 수직길이	1, 2, 5, 6, 7, 9, 10, 11, 13
	8	menton to rhinion	턱끝점-코돌출뼈 수직길이	4, 7, 9
	9	menton to pronasale	턱끝점-콧끝점 수직길이	7, 9
	10	menton to superior auricle	턱끝점-귀바퀴위점 수직길이	7, 8, 9
	11	menton to otobasion superius	턱끝점-귀바퀴위뿌리점 수직길이	7, 8, 9
	12	menton to tragion	턱끝점-귀구슬점 수직길이	7, 8, 9
	13	menton to inferior auricle	턱끝점-귀바퀴아래점 수직길이	7, 8, 9
	14	menton to labiale superius	턱끝점-입술위점 수직길이	7, 9
	15	menton to stomion	턱끝점-입술중간점 수직길이	7, 9
	16	menton to labiale inferius	턱끝점-입술아래점 수직길이	7, 9
	17	menton to supramentale	턱끝점-입술밑함몰점 수직길이	7, 9
	18	menton to promentale	턱끝점-앞턱끝점 수직길이	7, 9
	19	top of head to occiput	머리마루점-뒤통수돌출점 수직길이	1
	20	top of head to inion	머리마루점-뒤통수점 수직길이	1
	21	top of head to glabella	머리마루점-눈살점 수직길이	1, 2, 10
	22	top of head to ectocanthus	머리마루점-눈초리 수직길이	1, 2, 10
	23	top of head to sellion	머리마루점-코뿌리점 수직길이	1, 2, 10, 13
	24	top of head to pronasale	머리마루점-코끝점 수직길이	1, 2, 10
	25	top of head to subnasale	머리마루점-코밑점 수직길이	1, 2, 10
	26	top of head to zygion	머리마루점-협골궁점 수직길이	1
	27	top of head to tragion	머리마루점-귀구슬점 수직길이	1, 2, 10
	28	top of head to superior auricle	머리마루점-귀바퀴위점 수직길이	1, 10
	29	top of head to inferior auricle	머리마루점-귀바퀴아래점 수직길이	1
	30	top of head to posterior auricle	머리마루점-귀바퀴뒤바깥점 수직길이	1
	31	top of head to stomion	머리마루점-입술중간점 수직길이	1, 2, 10
	32	top of head to gonion	머리마루점-턱모서리점 수직길이	1, 10
	33	top of head to submandibular	머리마루점-아래턱밑점 수직길이	2
	34	glabella to crinion	눈살점-이마시작점	1
	35	glabella to subnasale	눈살점-코밑점	1

(continued)

Dimension category	No.	Name of dimension		Related research
		English	Korean	
Vertical length	36	tragion to superior auricle	귀구슬-귀바퀴위점 길이	3
	37	tragion to stomion	귀구슬점-입술중간점 수직길이	10
	38	superior auricle to inferior auricle (= ear length)	귀길이	1, 3, 10
	39	sellion to subnasale (= nose length)	코길이	1, 2, 4, 5, 6, 10, 11, 13, 14, 15
	40	sellion to pronasale	코뿌리점-코끝점 사선길이	10
	41	sellion to stomion	코뿌리점-입술중간점 수직길이	14
	42	sellion to supramentale	코뿌리점-입술밑함몰점 수직길이	14
	43	sellion to promentale	코뿌리점-앞턱끝점 수직길이	4
	44	subnasale to labiale superius (= philtrum length)	코밑점-입술위점 수직길이 (= 인중 길이)	2
	45	labiale superius to labiale inferius	입술위점-입술아래점 수직길이	2
Horizontal length	46	occiput to glabella (= head length)	뒤통수돌출점-눈살점 수평길이 (= 머리두께)	1, 2, 3, 7, 8, 9, 10, 14, 15
	47	occiput to vertex	뒤통수돌출점-머리마루점 수평길이	1
	48	occiput to crinion	뒤통수돌출점-이마시작점 수평길이	1
	49	occiput to inion	뒤통수돌출점-뒤통수점 수평길이	1
	50	occiput to ectocanthus	뒤통수돌출점-눈초리점 수평길이	1, 2, 10
	51	occiput to zygion	뒤통수돌출점-협골궁수평거리	1
	52	occiput to sellion	뒤통수돌출점-코뿌리점 수평길이	1, 2, 10
	53	occiput to pronasale	뒤통수돌출점-코끝점 수평길이	1, 2, 10
	54	occiput to subnasale	뒤통수돌출점-코밑점 수평길이	1, 2
	55	occiput to tragion	뒤통수돌출점-귀구슬점 수평길이	1, 2, 10, 13
	56	occiput to superior auricle	뒤통수돌출점-귀바퀴위점 수평길이	1
	57	occiput to inferior auricle	뒤통수돌출점-귀바퀴아래점 수평길이	1
	58	occiput to posterior auricle	뒤통수돌출점-귀바퀴뒤바깥점 수평길이	1
	59	occiput to stomion	뒤통수돌출점-입술중간점 수평길이	1, 2
	60	occiput to cheilion	뒤통수돌출점-입술옆점 수평길이	1
	61	occiput to gonion	뒤통수돌출점-턱모서리점 수평길이	1
	62	occiput to promentale	뒤통수돌출점-앞턱끝점 수평길이	1, 2
	63	occiput to menton	뒤통수돌출점-턱끝점 수평길이	1, 10
	64	otobasion superius to sellion	귀바퀴위뿌리점-코뿌리점 수평길이	10
	65	otobasion superius to posterior auricle (= ear breadth)	귀너비	1, 3, 10
	66	subnasale to pronasale (= nose protrusion)	코 돌출 높이	4, 5, 6, 10, 12, 15
	67	ear protrusion	귀 돌출 높이	3
	68	tragion to glabella	눈살점-귀구슬점 수평길이	10
	69	tragion to ectocanthus	눈초리점-귀구슬점 수평길이	10

(continued)

Dimension category	No.	Name of dimension		Related research
		English	Korean	
Width	70	head breadth	머리 너비	1, 3, 7, 8, 9, 10, 12, 13, 14, 15
	71	bifrontotemporal breadth (= minimum frontal breadth)	이마 너비	2, 12, 14, 15
	72	bizygofrontal breadth (= maximum frontal breadth)	눈썹끝점 사이 너비	1, 2, 4, 15
	73	bizygomatic breadth (= face width)	얼굴 너비	2, 3, 4, 5, 6, 7, 8, 9, 11, 12, 13, 14, 15
	74	interpupillary breadth (= bipupil breadth)	눈동자 사이 너비 (= 동공 너비)	2, 3, 10, 12, 14, 15
	75	bientocanthus breadth (= interocular breadth)	눈구석 사이 너비	1, 2, 10, 14
	76	biectocanthus breadth (= biocular breadth)	눈초리 사이 너비	1, 2, 7, 9, 10, 13, 14
	77	bitragion breadth	귀구슬 사이 너비	1, 2, 10, 14
	78	inter-otobasion superius breadth	귀바퀴위뿌리점 사이 너비	10
	79	inter-mastoid tip breadth	유양돌기 사이 너비	1
	80	nasal root breadth	코뿌리 너비	2, 11, 12, 15
	81	maximum nasal-bridge breadth (= bimaxillonasal breadth)	코뼈 최대너비	4, 14
	82	minimum nasal-bridge breadth	코뼈 최소너비	4
	83	bialar breadth (= nose breadth)	코 너비	2, 4, 5, 7, 9, 10, 11, 12, 13, 14, 15
	84	bicheilion breadth (= lip width or lip length)	lip width	2, 4, 5, 6, 7, 9, 10, 11, 13, 14, 15
	85	bicheilion breadth (= lip width or lip length), smiling	lip width (웃을때)	4
	86	bigonial breadth	턱 너비	1, 2, 5, 11, 12, 13, 14, 15
	87	head circumference	머리둘레	1, 3, 7, 8, 9, 14, 15
Circumference and arc	88	crinion-vertex-occiput arc	이마시작점-머리마루점-뒤통수돌출점 둘레	1
	89	crinion-glabella arc	이마시작점-눈살점 둘레	1
	90	bitragion-vertex arc	귀구슬점-머리마루점 둘레	1, 2, 3, 7, 8, 9, 10, 15
	91	bitragion-vertex (adj)	귀구슬점-머리마루점 둘레 (보정)	10
	92	bitragion-crinion arc	귀구슬점-이마시작점 둘레	1, 3, 8
	93	bitragion-bizygofrontal arc (= bitragion-minimum frontal arc)	귀구슬점-이마돌출점 둘레	2, 3, 4, 8, 15
	94	bitragion-bizygofrontale arc	귀구슬점-눈섭끝점 둘레	1
	95	bitragion-glabella arc	귀구슬점-눈살점 둘레	1, 8
	96	bitragion-occiput arc	귀구슬점-뒤통수돌출점 둘레	1
	97	bitragion-supramentale arc	귀구슬점-앞턱끝점 둘레	15
	98	bitragion-menton arc	귀구슬점-턱끝점 둘레	1, 2, 3, 5, 11
	99	bitragion-submandibular arc	귀구슬점-아래턱점 둘레	1, 2, 3, 4, 13
	100	bitragion-subnasale arc	귀구슬점-코밑점 둘레	1, 2, 3, 5, 11, 15
	101	bizygomatic-crinion arc	협골-이마시작점 둘레	4
	102	bizygomatic-bizygofrontal arc (= bizygomatic-minimum frontal arc)	협골-이마돌출점 둘레	4
	103	bizygomatic-menton arc	협골-턱끝둘레	4
	104	bizygomatic-submandibular arc	협골-아래턱밑 둘레	4
	105	glabella-vertex-occiput arc	눈살점-머리마루점-뒤통수돌출점 둘레	1, 7, 8, 9, 10

(continued)

Dimension category	No.	Name of dimension		Related research
		English	Korean	
Circumference and arc	106	glabella-vertex-occiput arc (adj)	눈살점-머리마루점-뒤통수돌출점 둘레 (보정)	10
	107	glabella-vertex-inion arc	눈살점-머리마루점-뒤통수점 둘레	7, 8, 9

(References)

[1]Ahn and Suh (2004), [2]Alexander et al. (1979), [3]Clauser et al. (1988), [4]Hack and McConville (1978), [5]Han and Choi (2003), [6]Hughes and Lomaev (1972), [7]S. Kim (2004), [8]S. Kim (2005), [9]S. Kim et al. (2004),

[10]KATS (2004), [11]Oestenstad et al. (1990),

[12]Oh and Park (2010), [13]Yokota (2005), [14]Young (1993), [15]Zhuang and Bradtmiller (2005)

B.2. Definition of dimensions applied to this study

This appendix contains descriptions of all the measurement dimensions taken by this study. All definitions of dimensions are described as referred by previous studies (Alexander et al., 1979; Clauser et al., 1988; Hack & McConville, 1978; KATS, 2004; Young, 1966). The first 4 dimensions were measured with a measurement tape and caliper, and remains 18 dimensions were measured by 3D scan. The participant was instructed to sit with looking straight ahead and the teeth in occlusion.

1 Head height: The maximum vertical distance between VERTEX and MENTON landmarks.

2 Head breadth: The maximum bilateral distance between right and left sides of the head above the ears (no landmarks).

3 Head length: The maximum distance between GLABELLA and the posterior projection point on the back of the head

4 Head circumference: The maximum surface distance around the head with the tape placed above the eyebrow ridges and positioned over the greatest posterior projection at the back of the head (no landmarks).

5 Face length: The midsagittal distance between SELLION and MENTON landmarks.

6 Lower-face length: The midsagittal distance between SUBNASALE and MENTON landmarks.

7 Sellion-to-supramentale length: The midsagittal distance between SELLION and SUPRAMENTALE landmarks.

8 Supramentale-to-menton length: The midsagittal distance between SUPRAMENTALE and MENTON landmarks.

9 Rhinion-to-menton length: The midsagittal distance between RHINION and MENTON landmarks.

10 Rhinion-to-promentale length: The midsagittal distance between RHINION and PROMENTALE landmarks.

11 Promentale-to-menton length: The midsagittal distance between PROMENTALE and MENTON landmarks.

12 Nose length: The midsagittal distance between SELLION and SUBNASALE landmarks of the nose.

13 Nose protrusion: The horizontal distance between SUBNASALE and PRONASALE landmarks

14 Face width (= bizygomatic breadth): The maximum bilateral distance of the face between right and left ZYGION landmarks at the zygomatic arch.

15 Chin width (= bigonial breadth): The bilateral distance between right and left GONION landmarks at the gonial angles of the mandible.

16 Nasal root breadth: The distance across the nasal bridge at its greatest indentation between DACRYON landmarks at the level of eyes.

17 Maximum nasal bridge breadth: The widest bilateral distance of the nasal bridge structure taken by right and left ALARE landmarks.

18 Nose width: The bilateral distance between right and left NASAL ALA landmarks of the nose.

19 Lip width: The bilateral distance between right and left CHEILION landmarks without facial expression.

20 Bitragion-menton arc: The surface distance between right and left TRAGION across MENTON landmark.

21 Bitragion-subnasale arc: The surface distance between right and left TRAGION across SUBNASALE landmark.

22 Bizygomatic-menton arc: The surface distance between right and left ZYGION across MENTON landmark.

B.3. Definition of landmarks

This appendix contains descriptions of all the landmarks used by this study. All definitions of landmarks are described as referred by previous studies (Alexander et al., 1979; Buikstra & Ubelaker, 1994; Clauser et al., 1988; Hack & McConville, 1978; Young, 1966).

Alare (left/right): The most laterally positioned point on the nasal aperture in a transverse plane.

Cheilion (left/right): The lateral junction point of the upper and lower lips with the facial skin at the corner of the mouth with no facial expression.

Dacryon (left/right): The intersection point of the maxillary bone, lacrimal bone, and frontal bone on the side of the nasal root between SELLION and ENDOCANTHION.

Glabella: The most anterior midsagittal point on the frontal bone at the level of the eyebrow ridges.

Gonion (left/right): The most posterior-inferior midpoint of the rounded gonial angle between the mandibular body and ramus.

Menton: The most inferior midsagittal point of the mandible (bottom of the chin).

Nasal ala (left/right): The most lateral point on the surface of the nostil.

Promentale (= pogonion): The most anterior midsagittal point on the chin prominence.

Pronasale: The most anterior midsagittal point on the tip of the nose.

Rhinion: The most anterior midsagittal osseocartilaginous junction point at the nasal bone.

Sellion (= nasion): The most posterior midsagittal point of the nasal bone at the top of the nasal bridge.

Subnasale: The midsagittal point at the junction of the inferior surface of the nose and the superior aspect of the philtrum.

Supramentale (= sublabiale): The most posterior midsagittal point in the concavity between the lower lip and promentale.

Tragion (left/right): The most anterior of the ear notch just superior edge of the tragus flap.

Vertex: The top of head. The topmost point of the vault of the skull.

Zygion (left/right): The most lateral point on the zygomatic arch.

Appendix C. The oxygen mask wearing characteristics

SN size (n = 21; unit: °, mm)

No.	Wearing characteristics		Average	SD	Min	Max
1	wear position	mask-top-to-sellion distance (v)	17.8	6.6	5.3	31.4
2		mask-top-to-sellion distance (h)	5.3	3.2	0.6	12.9
3		mask-bottom-to-supramentale distance (v)	7.3	3.3	2.0	14.5
4		mask-bottom-to-supramentale distance (h)	-0.5	2.5	-4.1	3.5
5	wear angle		56.7	5.5	43.9	67.7
6	microphone to upper-lip clearance		37.6	3.6	32.1	46.5

MN size (n = 23; unit: °, mm)

No.	Wearing characteristics		Average	SD	Min	Max
1	wear position	mask-top-to-sellion distance (v)	16.4	6.3	5.2	29.7
2		mask-top-to-sellion distance (h)	5.8	2.3	1.9	10.6
3		mask-bottom-to-supramentale distance (v)	9.9	5.1	0.5	19.5
4		mask-bottom-to-supramentale distance (h)	-0.3	2.0	-2.9	2.9
5	wear angle		52.5	5.6	43.3	61.7
6	microphone to upper-lip clearance		36.0	2.4	32.5	41.5

MW size (n = 19; unit: °, mm)

No.	Wearing characteristics		Average	SD	Min	Max
1	wear position	mask-top-to-sellion distance (v)	17.8	5.1	4.1	25.3
2		mask-top-to-sellion distance (h)	4.0	2.2	0.5	7.9
3		mask-bottom-to-supramentale distance (v)	9.9	4.6	2.7	16.8
4		mask-bottom-to-supramentale distance (h)	-1.1	2.4	-4.5	3.5
5	wear angle		50.2	4.8	44.1	64.7
6	microphone to upper-lip clearance		35.2	2.5	29.4	39.2

LW size (n = 22; unit: °, mm)

No.	Wearing characteristics		Average	SD	Min	Max
1	wear position	mask-top-to-sellion distance (v)	11.5	6.2	4.3	13.2
2		mask-top-to-sellion distance (h)	6.6	2.4	3.0	11.7
3		mask-bottom-to-supramentale distance (v)	13.6	7.1	3.2	26.2
4		mask-bottom-to-supramentale distance (h)	-2.3	2.9	-9.9	3.1
5	wear angle		49.8	4.5	43.2	60.0
6	microphone to upper-lip clearance		37.1	2.8	33.0	41.8

Appendix D. Questionnaire for the existing and revised oxygen masks comparison

관리 번호: ______________

산소마스크 착용성 평가 참여 동의서

연구 주제: 공군 F-15, F-16/K 조종사 고성능 산소마스크 개선 및 착용성 평가

연구원: 이원섭, 유희천 교수 (포항공과대학교),
손동훈 중위, 정대한 중령, 박세권 대령 (공군사관학교), 방하연, 김희은 교수 (경북대학교)

1. **연구 목적**: 본 평가는 **한국 조종사의 얼굴에 적합하도록 형상 변경된** MBU-20/P의 **설계 개선 효과**를 파악하는데 목적을 두고 있습니다. 본 실험을 통해 파악된 착용 평가 결과는 한국형 고성능 산소마스크 최종 형상을 도출하는데 유용하게 활용될 예정입니다.

2. **실험 구성**: 본 실험은 현행 및 개선 산소마스크에 대하여 (1) 주관적 평가와 (2) pressure film을 사용한 압박도 평가, 그리고 (3) 착용 사진 촬영으로 구성됩니다. 각 평가에 대한 상세한 지시사항은 각 평가 진행 시 알려드리겠습니다.

3. **불편함 및 피로**: 실험 진행 중 **불편한 사항이나 신체적인 피로**가 발생할 수 있습니다. 만약, 실험 중 과도한 불편함이나 피로 등이 발생할 경우, 언제든지 실험 중지를 요구하실 수 있으며 실험진행자에게 자세한 사항을 알려주시기 바랍니다.

4. **소요 시간**: 본 실험은 **30분 이내**로 소요될 예정입니다.

5. **개인 정보 비밀 보장**: 본 실험에 사용되는 모든 개인 정보는 비밀이 보장됩니다. 실험 참여자의 동의 없이는 신상정보가 공개되지 않습니다.

6. **질문할 권리**: 실험 참여자는 실험 중 언제든지 질문을 할 수 있는 권리를 가지고 있습니다. 또한, 실험 참여자는 질문들에 대해 성실하고 만족스러운 답변을 들을 권리를 가지고 있습니다.

본인은 실험 참여자로서 상기 사항들을 이해하고 실험에 자발적으로 참여했음을 확인합니다.

2012 년 　　월 　　일

실험 참여자: ______________ 서명: ______________

연구 수행 기관
포항공과대학교 산업경영공학과
공군사관학교 시스템공학과/기계공학과
경북대학교 의류학과

1

관리 번호:_______________

주관적 착용성 평가 설문	평가 종류	□ 기존 마스크 □ 개선 마스크

1. 부위별 불편도에 대해 표시(√)하여 주십시오.

좌 우

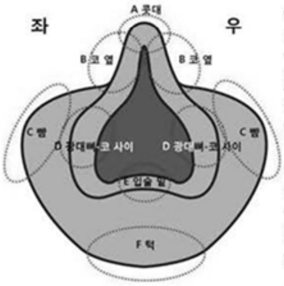

부 위	불편 없음 not at all	약간 불편 rarely	조금 불편 somewhat	다소 불편 slightly	상당히 불편 moderately	많이 불편 quite	매우 불편 very	극도로 불편 extremely
	0점	1점	2점	3점	4점	5점	6점	7점
A: 콧대	□	□	□	□	□	□	□	□
B: 코 옆	□	□	□	□	□	□	□	□
C: 뺨	□	□	□	□	□	□	□	□
D: 광대뼈-코 사이	□	□	□	□	□	□	□	□
E: 입술 밑	□	□	□	□	□	□	□	□
F: 턱	□	□	□	□	□	□	□	□
전반적 불편도	□	□	□	□	□	□	□	□
고개를 움직일 때 불편도	□	□	□	□	□	□	□	□

2. 부위별 산소누설 정도에 대해 표시(√)하여 주십시오.

좌 우

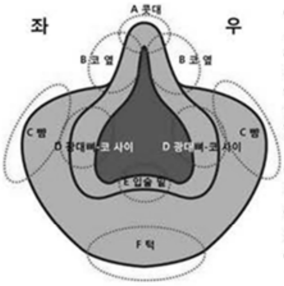

부 위	누설 없음 not at all	약간 누설 rarely	조금 누설 somewhat	다소 누설 slightly	상당히 누설 moderately	많이 누설 quite	매우 누설 very	극도로 누설 extremely
	0점	1점	2점	3점	4점	5점	6점	7점
A: 콧대	□	□	□	□	□	□	□	□
B: 코 옆	□	□	□	□	□	□	□	□
C: 뺨	□	□	□	□	□	□	□	□
D: 광대뼈-코 사이	□	□	□	□	□	□	□	□
E: 입술 밑	□	□	□	□	□	□	□	□
F: 턱	□	□	□	□	□	□	□	□

3. 가속도 환경 시 mask가 아래로 미끄러지는 정도에 대해 표시(√)하여 주십시오. (가속도 환경을 고려하여 아래로 잡아당겨보며 평가)

미끄러짐 없음 not at all	약간 미끄러짐 rarely	조금 미끄러짐 somewhat	다소 미끄러짐 slightly	상당히 미끄러짐 moderately	많이 미끄러짐 quite	매우 미끄러짐 very	극도로 미끄러짐 extremely
0점	1점	2점	3점	4점	5점	6점	7점
□	□	□	□	□	□	□	□

4. Microphone이 입술에 접촉되는 정도에 대해 표시(√)하여 주십시오.

접촉 없음 not at all	약간 접촉 rarely	조금 접촉 somewhat	다소 접촉 slightly	상당히 접촉 moderately	많이 접촉 quite	매우 접촉 very	극도로 접촉 extremely
0점	1점	2점	3점	4점	5점	6점	7점
□	□	□	□	□	□	□	□

5. 전반적 만족도에 대해 표시(√)하여 주십시오.

매우 만족 very	상당히 만족 slightly	조금 만족 somewhat	중립 neutral	조금 불만족 somewhat	상당히 불만족 slightly	매우 불만족 very
1점	2점	3점	4점	5점	6점	7점
□	□	□	□	□	□	□

2

관리 번호: ________________

평가 중 질문지

<현 착용 mask에 대한 질문>

1. 현 착용 mask의 size: □ XSN □ SN □ MN □ MW □ LW
2. 현 mask의 사용 기간: ____________년
3. Mask fitting 시 특이 사항 (예: grinding, reflective seal cutting): ________________
4. 평소 mask 착용 유형: □ 항상 압박 착용 □ 항상 느슨하게 착용 □ 고기동시만 압박 착용

<현 착용 mask의 불편 사항>

5. 평소 가장 불편하다고 생각한 부위: ( )
6. 평소 비행 후 가장 통증이 심하게 남아 있는 부위: ( )
7. Valsalva 방법: □ 자연스럽게 valsalva 됨 □ valsalva hole 이용 □ mask를 풀고 valsalva □ ____________
   (배기 valve를 이용한 valsalva 방법에 대한 안내)
8. Mic나 valve의 입술 접촉 여부: □ 접촉하지 않음 □ 항상 접촉함 □ ____________
9. PBG 모드 사용 여부: □ 사용 □ 미사용. / PBG 모드 사용 시 불편 사항: ____________

<기존 mask와 개선 mask 간 비교 >

10. 개선 mask의 선택한 size: □ SN □ MN □ MW □ LW
11. 압박도 또는 밀착도 측면에서 새로운 mask에 대한 의견: ( )
12. Reflective seal의 모서리로 인해 불편한 부위에 대한 의견: ( )
13. Wing의 모서리로 인해 불편한 부위에 대한 의견: ( )
14. 고기동 시라고 간주하고 아래로 당겼을 때 미끄러짐 정도에 대한 의견: ( )
15. 목 움직임(상방, 하방, 측방, 후방 주시)에 따른 불편도에 대한 의견: ( )
16. 기존 mask와 개선 mask 중 본인 얼굴에 더 잘 맞다고 생각되는 것: □ 현재 mask □ 개선 mask □ 중립
17. 향후, 개선 mask로의 변경 의사: □ 변경함 □ 변경하지 않음 □ 조건적 변경 ( )

<기타 조종사 의견>

18. 그 외의 mask 관련 또는 mask 외 기타 장구 (helmet 등) 관련 언급할 사항, 특이 사항, 기타 문제점?

8